Renewed diversification following Miocene landscape turnover in a Neotropical butterfly radiation

Nicolas Chazot, Keith R Willmott, Gerardo Lamas, André Freitas, Florence Piron-Prunier, Carlos F Arias, James Mallet, Donna Lisa De-silva, Marianne Elias

This manuscript is published in Global Ecology and Biodiversity as:
Chazot N, Willmott KR, Lamas G, Freitas AVL, Piron-Prunier F, Arias CF, Mallet J, De-Silva DL & M Elias. 2019. Renewed diversification following Miocene landscape turnover in a Neotropical butterfly radiation. Global Ecology and Biogeography. https://doi.org/10.1111/geb.12919. A previous version has been recommended by PCI Evolutionary Biology (http://dx.doi.org/10.24072/pci.evolbiol.100032)

Title

Renewed diversification following Miocene landscape turnover in a Neotropical butterfly radiation

Authors

Nicolas Chazot[1,2,3*], Keith R. Willmott[4], Gerardo Lamas[5], André V.L. Freitas[6], Florence Piron-Prunier[2], Carlos F. Arias[7], Jim Mallet[8], Donna Lisa De-Silva[2], Marianne Elias[2].

Affiliations

1. Department of Biological and Environmental Sciences, University of Gothenburg, Box 461, 405 30 Gothenburg, Sweden.
2. Institut de Systématique, Évolution, Biodiversité, ISYEB, CNRS MNHN UPMC EPHE, Sorbonne Université, Université des Antilles, 45 rue Buffon CP50 F-75005, Paris, France.
3. Gothenburg Global Biodiversity Centre, Box 461, 405 30 Gothenburg, Sweden.
4. McGuire Center for Lepidoptera and Biodiversity, Florida Museum of Natural History, University of Florida, Gainesville, Florida 32611, USA.
5. Museo de Historia Natural, Universidad Nacional Mayor de San Marcos, Lima, Peru.
6. Departamento de Biologia Animal and Museu de Zoologia, Instituto de Biologia, Universidade Estadual de Campinas, Campinas, São Paulo, Brazil.
7. Smithsonian Tropical Research Institute, Panamá, Panama.
8. Department of Organismic and Population Biology, Harvard University, USA

Corresponding author (*):
Nicolas Chazot

Acknowledgements

This project was funded by an ATIP (CNRS, France) grant awarded to ME, with LDS as a postdoc. NC was funded by a doctoral fellowship from Ecole Doctorale 227 (France) and BECC (Biodiversity and Ecosystem services in a Changing Climate). ME acknowledges additional funding by the ANR grant SPECREP (ANR-14-CE02-0011-01). JM acknowledges funding from NERC and BBSRC. We thank the authorities of Peru, Ecuador and Brazil (SISBIO n° 10438-1) for providing research and collection permits, as well as many assistants and colleagues for their help in the field and with databasing museum specimens. Molecular work was performed at the GenePool (University of Edinburgh, UK), CBMEG-Unicamp (Brazil) and the Service de Systématique Moléculaire UMS2700 (2AD) of the MNHN

(France). We are grateful to Niklas Wahlberg for providing unpublished sequences of *Greta diaphanus*. We thank Fabien Condamine and Hélène Morlon for constructive discussions about time-dependent diversification analyses. AVLF thanks CNPq (grant 303834/2015-3), RedeLep-SISBIOTA-Brasil/CNPq (563332/2010-7), National Science Foundation (DEB-1256742), FAPESP (grants 2011/50225-3, 2012/50260-6 and 2013/50297-0) and USAID and the U.S. National Academy of Sciences (NAS) under the PEER program (Sponsor Grant Award Number: AID-OAA-A-11-00012) (Mapping and Conserving Butterfly Biodiversity in the Brazilian Amazon). KRW thanks the National Geographic Society, the Leverhulme Trust, the Darwin Initiative, the National Science Foundation (DEB-0103746, DEB-0639861), the Florida Museum of Natural History and the University of Florida. Finally, we thank four anonymous reviewers for their constructive comments on previous versions of the manuscript.

Author contributions:

NC and ME conceived the study, with contribution from KRW, GL and AVLF. All co-authors provided specimens and sequence data. NC, ME, FPP, CFA, DLDS performed the labwork. NC performed the analyses. NC wrote the paper with major contributions from ME, and contributions from all co-authors.

Biosketch

All authors on this paper have a longstanding interest in Ithomiini 'clearwing' butterflies, spanning systematics, the role of host-plants and mimetic interaction from micro- to macroevolutionary scale, community ecology, and/or historical biogeography. This paper is the result of 15 years of collaborative efforts to collect, describe, sequence and classify Ithomiini butterflies to unravel the evolutionary patterns of the diversification of this clade.

Abstract

Aim: The landscape of the Neotropical region has undergone dynamic evolution throughout the Miocene, with the extensive Pebas wetland occupying western Amazonia between 23 and ~10 My ago and the continuous uplift of the Andes mountains. The complex interaction between the Andes and Amazonia likely influenced the trajectory of Neotropical biodiversity, but evidence from time-calibrated phylogenies of groups that diversified during this period are lacking. We investigate the role of these landscape transformations on the dynamics of diversification in the Neotropical region using a 26 My-old endemic butterfly radiation.

Location: Neotropics

Time period: Oligocene to present

Major taxa studied: Ithomiini butterflies

Methods: We generated one of the most comprehensive time-calibrated molecular phylogenies of a large clade of Neotropical insects, the butterfly tribe Ithomiini, comprising 340 species (87% of extant species) and spanning 26 My of diversification. We applied a large array of birth-death models and historical biogeography estimations to assess the dynamics of diversification and biotic interchanges, especially at the Amazonia/Andes interface.

Results: Our results suggest that the Amazonian Pebas wetland system played a major role in the timing and geography of diversification of Ithomiini, by constraining dispersal and diversification in the Amazon basin until ~10 My ago. During the Pebas wetland period Ithomiini diversification mostly took place in the Andes, where terrestrial habitats where not affected. An explosion of interchanges with Amazonia and with the Northern Andes accompanied the demise of the Pebas system (11-8 My ago), and was followed by local diversification in those areas, which led to a substantial renewal of diversification.

Main conclusions: While many studies on Neotropical diversity have focused only on the Andes, we show that it is the waxing and waning of the Pebas mega-wetland, interacting with Andean uplift, that have determined the timing and patterns of regional interchanges and diversification in Ithomiini.

Keywords

Neotropics, phylogeny, diversification, biogeography, Andes, Pebas system, Western-Andean Portal, Ithomiini, butterflies

INTRODUCTION

There has been a long fascination among biologists for the Neotropics and the origin of its intriguingly high biodiversity. Nevertheless, the timing of Neotropical diversification, and therefore its major driving processes, are still controversial despite the large amount of publications that have addressed these questions (e.g., Hoorn et al. 2010, Rull et al. 2008, Smith et al. 2014).

Notwithstanding uncertainty about the precise timing and magnitude of surface uplift, the formation of the Andean cordilleras during the Cenozoic broadly shaped Neotropical landscapes and affected diversification in the Neotropics. As the Andes arose they created new biotic and abiotic conditions along their slopes, modified the climate of the Neotropical region and deeply affected the formation of the Amazonian basin by introducing large amounts of sediment and modifying water drainage (Hoorn et al. 2010). There is increasing evidence that the Andes influenced the diversification of Neotropical lineages, primarily by driving increased speciation rates, perhaps most spectacularly in the high altitude páramo habitat (e.g., Madriñán et al. 2013). In parallel, the western part of the Amazon basin, which is connected to the Andes, experienced major turnovers of ecological conditions. During the Oligocene, western Amazonia was occupied by a fluvial system flowing northward (the paleo-Orinoco basin), which transformed ~23 million years (My) ago into an aquatic system of shallow lakes and swamps episodically invaded by marine conditions, known as the Pebas system (Wesselingh et al. 2001, Antonelli et al. 2009, Wesselingh et al. 2010, Hoorn et al. 2010, Antonelli & Sanmartín 2011). The Pebas was connected northward with the Caribbean Sea and likely also with the Pacific Ocean through the Western-Andean portal ("WAP", Antonelli et al. 2009), a low-elevation gap that separated the Central Andes and the Northern Andes until 13-11 My ago. During the late Miocene and during the Andean uplift, the accumulation of sediments combined with a sea level decrease initiated the eastward drainage of the Pebas, and by 10-8 My ago the region had changed into a fluvial system, which then evolved into the modern configuration of the Amazon. More recently, climatic fluctuations during the Peistocene (2.5-0 My ago) may have led to episodic dryness affecting Amazonian forest habitats and have been proposed as a driver of diversification of the Neotropical biota (Haffer 1969). The extent of the influence of Pleistocene events and their effects on Neotropical diversification, and even the importance of dryness episodes, are controversial (e.g, Colinvaux et al. 2000, Rull et al. 2008, Garzón-Orduña et al. 2014, Matos-Maraví 2016).

In this study we focus our attention mostly on the Miocene and Pliocene and how the interaction between the rise of the Andes and coincident large landscape modifications in western Amazonia determined diversification and dispersal over 30 million years. The Pebas ecosystem covered up to 1.1 million km^2 at its maximum extent (Wesselingh et al. 2001) and was probably unsuitable for terrestrial fauna dependent on *terra firme* forest habitats. Therefore, between ca. 23 and 10 My ago, diversification of terrestrial lineages may have been impeded in western Amazonia or restricted to its

edge (Wesselingh et al. 2001). By contrast, the uplift of the Central and the Northern Andes, also occurring throughout the Miocene and the Pliocene, and the ecological gradients present along this mountain chain, probably constituted an important driver of diversification. In the last 10-8 My, the retreat of the Pebas potentially provided new opportunities for terrestrial lineages to radiate in lowland western Amazonia. The Pebas may also have constrained dispersal, acting as a barrier between the Andes and Amazonia.

Paleontological studies have shown that the Pebas greatly contributed to the diversification of the aquatic fauna, including molluscs (Wesselingh 2006), ostracods (Muñoz-Torres et al. 2006) and crocodilians (Salas-Gismondi et al. 2015). However, the fossil record also suggests a negative effect of the Pebas system on the terrestrial fauna (Antoine et al. 2016, Antoine et al. 2017). The hypothesis that the Pebas has shaped patterns of terrestrial diversification and dispersal in western Amazonia has grown over the years (e.g., Wesselingh & Salo 2006, Antonelli et al. 2009, Wesselingh et al. 2001, Antonelli & Sanmartín 2011, Antoine et al. 2016), but support from molecular phylogenies mostly stems from the observation that many western Amazonian clades have diversified during the last 10-8 My and not before (Antonelli & Sanmartín 2011, Chazot et al. 2016b, and references therein). Yet, there is very little information on what happened before, when the Pebas was occupying western Amazonia, particularly on whether the presence of Pebas constrained diversification and interchange patterns in this region. A thorough assessment of the role of the Pebas ecosystem on diversification and dispersal requires phylogenies of large Neotropical clades that originated before the formation of the Pebas, i.e. clades older than 23 My. Phylogenies of Neotropical clades meeting these conditions are surprisingly rare. In insects – which are among the most diverse terrestrial organisms – attempts to build phylogenies of Neotropical groups to test different drivers of Neotropical diversification have either suffered from a small size or a low sampling fraction (e.g. Hall & Harvey 2002, Elias et al. 2009, Penz et al. 2012, Condamine et al. 2012, Price et al. 2014, Chazot et al. 2016a,b), and therefore from low statistical power and reliability.

Among the most emblematic Neotropical insects is the butterfly tribe Ithomiini (Nymphalidae: Danainae, 393 species), also referred to as ‘clearwing’ butterflies because of the transparent wings of the majority of species. Ithomiini are forest-dwellers distributed throughout the Neotropics, from sea level up into montane cloud forests (to 3000 m), where their larvae feed on plants of the families Solanaceae, Gesneriaceae and Apocynaceae (Drummond & Brown 1987, Willmott & Freitas 2006). Species richness is primarily concentrated in the Andes, where about half the species occur (mostly on the eastern slopes), and in western Amazonia. Ithomiini are chemically-defended and engage in Müllerian mimicry, whereby co-occurring species exhibit convergent wing colour patterns that advertise their toxicity to predators (Müller 1879). Ithomiini butterflies represent a keystone group in Neotropical forests by numerically dominating mimetic butterfly communities and sharing wing colour patterns with a large number of other palatable and unpalatable Lepidoptera, such as the iconic

Heliconius butterflies (Brown & Benson 1974). For this reason, Ithomiini were used by both Bates (Bates 1862) and Müller (Müller 1879) in their original descriptions of deceptive (Batesian) and mutualistic (Müllerian) mimicry, respectively.

The diversity and the intriguing ecology of Ithomiini has generated a great interest among researchers and a broad and diverse literature on topics including life history (Bolaños Martinez et al. 2011, Hill et al. 2012, McClure & Elias 2016, McClure & Elias 2017), chemical ecology (Brown 1984, Trigo & Brown 1990, Schulz et al. 2004, McClure et al. accepted), systematics (Brown & Freitas 1994, Mallarino et al. 2005, Willmott & Freitas 2006, Brower et al. 2006, Elias et al. 2009, De-Silva et al. 2010, Brower et al. 2014, Chazot et al. 2016b, De-Silva et al. 2017), cytogenetics (Brown et al. 2004, McClure et al. 2018), population ecology (Freitas 1993, 1996), community ecology (Beccaloni 1997, DeVries et al. 1999, Elias et al. 2008, Hill 2010, Chazot et al. 2014, Willmott et al. 2017), wing colour pattern evolution (Jiggins et al. 2006), and biogeography (Elias et al. 2009, Dasmahapatra et al. 2010, De-Silva et al. 2016, 2017, Chazot et al. 2016b, Chazot et al. 2018).

In this study, we generate the first species-level molecular phylogeny of the entire tribe, providing a large and densely sampled (340 species included out of 393 currently recognized) phylogenetic dataset for a Neotropical insect clade that underwent diversification during the last ~30 million years (Wahlberg et al. 2009, De-Silva et al. 2017). We investigate the dynamics of diversification and dispersal rates in Ithomiini, focusing on the turnover of ecological conditions in Western Amazonia and the concomitant Andean uplift during the Miocene. Specifically, an important role for Andean uplift and the Pebas wetland would be supported if: (1) *During the Pebas period*: (a) Andean diversification largely exceeded Amazonian diversification, due to increased diversification in the Andes driven by the evolving ecological gradient and uplift dynamics and/or a reduced diversification rate in Amazonia accompanying the loss of terrestrial habitats; (b) interchanges between the Andes and Amazonia were reduced; (c) interchanges between the Central and the Northern Andes were reduced, because of the existence of the WAP. (2) *During the retreat of the Pebas*: interchanges between the Andes and Amazonia and between the Central and the Northern Andes increased, as a result of new terrestrial habitats and the disappearance of the WAP, respectively. (3) *After the Pebas period*: Diversification rates in Amazonia increased and biotic interchanges became newly unconstrained. In addition, decreasing speciation rates would suggest the existence of post-Pebas radiations in Amazonia, while a scenario of increasing speciation rates would be consistent with speciation driven by climatic fluctuations during the last 2.5 My.

MATERIAL AND METHODS

Time-calibrated phylogeny

Molecular data

We compiled sequences of 1474 Ithomiini individuals (see Appendix S1.1 in Supporting Information) that included 718 sequences newly generated for this study and 3147 previously published sequences (Whinnett et al. 2005, Mallarino et al. 2005, Brower et al. 2006, Elias et al. 2009, De-Silva et al. 2010, Chazot et al. 2014, De-Silva et al. 2016, Chazot et al. 2016b, De-Silva et al. 2017, Chazot et al. 2018). We used a concatenation of nine gene fragments, a mitochondrial fragment spanning genes COI-tRNA-COII, and fragments of nuclear genes EFIα, Tektin, CAD, RPS2, MDH, GAPDH, representing a total of 7083 bp (Wahlberg & Wheat 2008). Primers and PCR conditions followed Mallarino et al. (2005) and Wahlberg & Wheat (2008). We obtained at least one gene fragment for 340 species out of 393 currently known in the group, which represents 87% of the known species richness of the tribe. For each species we produced the consensus sequence of all sequences belonging to individuals of that species to obtain the longest sequence possible. We added 41 outgroups, which spanned all Danainae genera as well as representatives of the main Nymphalidae clades. In total, nine concatenated genes from 381 taxa were used to generate the time-calibrated phylogeny of the Ithomiini.

Tree topology and time calibrations

We used PartitionFinder v.1.1 (Lanfear et al. 2012) to find the best gene partitioning and substitution models (Appendix S2.1, Table S2.1). Then we generated a phylogeny under maximum likelihood inference (ML), using IQ-Tree software as implemented in the W-ID-TREE server (Trifinopoulos et al. 2016, Nguyen et al. 2014) in order to obtain a tree topology (Appendix S2.2). Finally, this topology was time-calibrated using BEAST v1.8.2 (Drummond et al. 2012). We used four secondary calibrations from Wahlberg et al. (2009)'s phylogeny of Nymphalidae that were placed outside of Ithomiini, and six secondary calibrations consisting of maximum ages of hostplant (Solanaceae) lineages from De-Silva et al. (2017), and placed on Ithomiini lineages (Appendix S2.3, Table S2.2). We used a birth-death tree prior and we set an uncorrelated lognormal relaxed clock for each gene partition. We performed two independent runs of BEAST v.1.8.2, which were combined after applying a 15% burnin. Median branch lengths and credibility intervals were recovered using TreeAnnotator v.1.8.3 (Drummond et al. 2012) (Appendix S2.3), and outgroups were pruned to generate an Ithomiini tree with median branch lengths (hereafter, median tree). Full details are given in Appendix S2.

Diversification rates

Time

We investigated the dynamics of diversification rates through time and across the phylogeny using two different birth-death models: (1) Morlon et al.'s (2011) method allowing both speciation and

extinction rates to vary as a function of time, and allowing extinction to be higher than speciation, (2) TreePar (Stadler 2011) which accommodates models where diversification rates can vary at points in time but are constant between these points. Because none of these methods can automatically detect the number and position of different diversification processes, we first ran MEDUSA (Alfaro et al. 2009, Appendix S3.1.1) on the whole tree in order to partition the tree into different diversification processes. MEDUSA detected two shifts from the background diversification rates (see Results and Table S3.3, and additional analyses using BAMM v.2.5.0 (Rabosky 2014, Appendix S3.1.4, Figure S3.3): 1) one shift at the root of a large clade, hereafter referred to as the core-group, and 2) one shift at the root of a subclade of the genus *Melinaea* that, for simplicity, is referred to as the *Melinaea*-group. The remaining lineages are collectively referred to as the backbone.

Six models from Morlon et al. (2011) were fitted on the core-group, the *Melinaea*-group and the backbone including time-constant and time-dependent functions of speciation and extinction rates (Appendix S3.1.2). We also explored the effect of potential residual diversification rate heterogeneity in the backbone on the results from Morlon et al. (2011) method (Appendix S3.1.5). TreePar (Stadler 2011) analyses were performed on the core-group and the backbone, and diversification rate estimated in bins of 4 My (Appendix S3.1.3). We did not fit TreePar on the *Melinaea*-group since it is only 1 My old. We allowed diversification rate to be negative but we did not allow mass-extinction events. For both methods the models were fitted on 100 trees randomly sampled from BEAST's posterior distribution for each partition.

Diversification in the Andes

To investigate the pattern of diversification in the Andes with respect to the rest of the Neotropical region, we classified species as Andean or non-Andean, based on a combination of published and unpublished (i.e., databases generated from museum collections and our own field collections) georeferenced distribution data and elevation ranges of species (Appendix S1.2). We used models of trait-dependent diversification implemented in ClaSSE (Goldberg & Igić 2012), to compare the rates of speciation, of extinction and of transition between the Andean area and the non-Andean regions (Chazot et al. 2016b, Beckman & Witt 2015, Appendix S3.2). Ten models were fitted on the full tree and the core-group alone to account for the major diversification shift at the root of the core-group. In both cases all models were fitted on the 100 trees randomly sampled from BEAST's posterior distribution. We also performed additional analyses with the model HiSSE (Beaulieu & O'Meara 2016) to test the hypothesis that a hidden character explained the pattern of trait-dependent diversification estimated with ClaSSE (Appendix S3.2). Finally, we also conducted ancestral state estimations based on the two best models of trait-dependent diversification, which were compared to the ancestral areas estimated by the historical biogeography analyses outlined below.

Diversification in Amazonia

We further investigated the pattern of diversification in Amazonia during the post-Pebas period, where speciation in some taxa may have been driven by climatic fluctuations during the Quaternary (Haffer 1969). To test whether speciation rates had increased in the last 2.5 My, we identified seven major Amazonian diversification events from the BioGeoBEARS ancestral state reconstruction (see below) and we fitted a model of time-dependent speciation rate (no extinction) to see whether speciation rates increased through time (supporting a recent diversification potentially caused by Pleistocene climatic fluctuations) or decreased through time (supporting radiations accompanying the post-Pebas recolonizations) (Appendix S3.3). Analyses were performed on 100 trees randomly sampled from BEAST's posterior distribution.

Historical biogeography

We inferred the historical biogeography of Ithomiini with BioGeoBEARS v.0.2.1 (Matzke 2014) using the model DEC. We divided the Neotropics into nine distinct biogeographic regions (Figure S4.7): 1) Central America, 2) Caribbean Islands, 3) lowlands on the Western part of the Andes, including the Magdalena valley, 4) Northern Andes that comprise the Western and eastern Ecuadorian and Colombian cordilleras and the Venezuelan cordillera, 5) Central Andes, 6) Western Amazonia, 7) eastern Amazonia, 8) Guiana Shield and 9) Atlantic Forest. We proceeded in three steps. First, we performed an estimation of ancestral ranges using a model with refined area adjacency (unrealistic distributions, such as disjunct distributions, were avoided) but uniform dispersal multipliers (null-model, Appendix S4.1). Second, we performed 1000 biogeographic stochastic mapping replicates to compute rates of dispersal between specific regions per million years (Appendix S4.2). We computed rates of dispersal in the core-group between Andean and non-Andean regions, between the Andes and Amazonia, between the Central and the Northern Andes, between the Atlantic Forest and the other regions, and between Central America and the rest of the Neotropics (Figure S4.8). This allowed us to test some biogeographic hypotheses but also to identify relevant time frames among which dispersal probabilities between areas might vary. Third, we implemented a time-stratified model designed from the previous information to refine our biogeographic reconstruction. (Appendix S4.3). We created four time frames: i) 0-4, ii) 4-8, iii) 8-13, and iv) 13-30 My ago, where dispersal multipliers between areas reflected the colonization rate variations identified previously (Table S4.6). All these analyses were performed on the median tree.

RESULTS

Time-calibrated phylogeny

Tree topology and time-calibration

The topology of Ithomiini phylogeny was generally well supported, including deep nodes (Figure S2.1). The inferred crown age of Ithomiini was 26.4 My ago (95% credibility interval CI=22.75-30.99) (Figure 1, Figure S2.2), and the divergence time from its sister clade Tellervini was 42.1 My ago (CI=39.50-48.44). All subtribes (10 in total) diverged during the first 10 My (Figure 1). Node ages in our phylogeny were generally slightly younger than those inferred in Wahlberg et al. (2009), but older than those inferred in Garzón-Orduña et al. (2015) (see De-Silva et al. 2017 for further discussion of such differences).

Diversification rates

Time-dependent diversification

We partitioned the dynamics of diversification into 1) the core-group, which accounts for ~85% of present-day diversity of Ithomiini; 2) the *Melinaea*-group (i. e., the high-diversity clade in the genus *Melinaea*) and 3) the backbone (i. e., the remaining lineages) (Figure 1, Appendix S3).

When fitting Morlon *et al.* (2011)'s models on the core-group, no model of time-dependent diversification had a significantly better fit than the null model of constant speciation rate without extinction (average of 0.257 $lineage^{-1}My^{-1}$, Figure 2, Table 1, Table S3.4). For the *Melinaea*-group, which radiated into eight species during a time lapse of only one million years, the best fitting model was an exponentially decreasing speciation rate without extinction, with a very high initial speciation rate (average of 14.54 $lineage^{-1}My^{-1}$ at the root, average of 0.31 $lineage^{-1}My^{-1}$ at present, Figure 2, Table 1, Table S3.4). On the remaining backbone, the best fitting model involved a time-dependency of both speciation and extinction rates. The resulting net diversification rate was initially high (average of 0.78 at the root), but decreased rapidly and became negative around 19 My ago, before starting a slow recovery, while remaining negative (average of -0.04 $lineage^{-1}My^{-1}$ at present, Figure 2, Table 1, Table S3.4). This signal of high relative extinction rate was not affected by initial parameters for maximum likelihood search or by diversification rate heterogeneity potentially remaining in the backbone (Figure S3.4). Several clades within the backbone show positive net diversification rates during the last 5 My, which further supports the recovery trend described above.

We obtained congruent results with TreePar (Figure 2), with a fairly constant diversification through time for the core-group, and an initially high diversification rate for the backbone lineages, followed by a general decline during the last 15 My, leading to a negative net diversification rate between 12 and 4 My ago.

Diversification in the Andes

For the whole Ithomiini, five ClaSSE models were within an AIC interval of two. There was no clear consensus across those models, since three of them supported higher speciation rate in the Andes,

while the others had equal speciation rates. Two models found inferred different dispersal rates but in two opposite ways (Table 2, Table S3.5). This lack of consensus probably reflects the heterogeneity of diversification processes across the Ithomiini. Non-zero extinction rate was inferred in all cases. In the core-group, three out of four models within an AIC interval of two had identical speciation rates, and the fourth model had a slightly higher speciation rate in the Andes (Table 2, Table S3.5). Three of those models have identical transition rates between Andean and non-Andean regions, and the fourth one has a higher transition rate towards the Andes. All have very low extinction rate. Overall, the results for the core group converge on similar speciation and transition rates between Andean and on-Andean regions, and low extinction. This interpretation was confirmed by additional analyses in which we tested the presence of a hidden character using the model HiSSE (Box S3.1, Table S3.5, Figure S3.5).

The most likely state of the root of Ithomiini was non-Andean but with high uncertainty (probability of 0.508 with different speciation rates [model 1] and 0.543 with different speciation and transition rates [model 2], Figure S3.6) and there was high uncertainty at the nodes leading to the core-group (Figure 1, Figure S3.6). The most recent common ancestor (hereafter MRCA) of the core-group was inferred as most likely Andean (probability of 0.558 for model 1 and 0.625 for model 2). The MRCAs of backbone subtribes were always inferred to be non-Andean with a strong support, except for Athesitina (Figure 1, Figure S3.6). Within the core-group, an Andean origin for subtribes Napeogenina, Dircennina and Godyridina was inferred with model 1, whereas an Andean origin for all five subtribes was inferred with model 2 (Figure S3.6).

Diversification in Amazonia

Only two Amazonian diversification events in the backbone, *Mechanitis* + *Forbestra* and *Melinaea* (the whole genus), and one core-group event (*Brevioleria*-group), showed a pattern of increasing speciation rate through time (Figure 3), consistent with a potential effect of Pleistocene climatic fluctuations in driving diversification. The other four Amazonian diversification events (*onega*-group, *Hypothyris*-group, *agnosia*-group and *Methona*) showed decreasing speciation rates through time (Figure 3), suggesting an early diversification.

Historical biogeography

Biogeographic null model and diversification of the core-group

Under the null model (no dispersal multiplier) the ancestral area of the Ithomiini MRCA was unclear (Central Andes + Western Amazonia for the highest probability), and all subtribes except Melinaeina

and Mechanitina originated and started diversifying in the Central Andes (Figure 1, Figure S4.9). However, all estimations at the basal nodes of the backbone were highly uncertain.

While an absence of dispersal events out of the Central Andes characterized the initial Andean phase of diversification in the core-group (Figure 3), we found a major peak of interchanges between the Andes and Amazonia 12-8 My ago, entirely driven by colonization from the Andes towards Amazonia (Figure 3, Figure S4.8). After this peak, the rate of dispersal towards Amazonia rapidly decreased through time until around 4 My ago, when a second peak of interchanges, involving reverse colonizations towards the Andes, occurred (Figure 3). We also recorded a large increase of interchanges between the Central and the Northern Andes after around 12 My, i.e. simultaneously with the increase of dispersal rate towards Amazonia (Figure 3, Figures S4.2 and S4.3). Rates of interchanges between the Central and Northern Andes then remained relatively constant through time, although they increased during the last 3 My, due to dispersal from the Northern Andes towards the Central Andes. Colonization of Central America likely started around 8 My ago, but interchanges increased mainly during the last 4 My (Figure S4.8). Colonizations of the Atlantic Forest also started early (around 9-10 Mya), but the rate of interchanges between the Atlantic Forest and the remaining Neotropical regions remained relatively constant during the last 10 My (Figures S4.2 and S4.3).

Until ~10 My ago speciation events occurring in the Central Andes fully accounted for the core-group diversification (no dispersal events). During the last ~10 My, however, speciation slowed down in the Central Andes (Figure 3). At the same time, following the peaks of dispersal identified above, Northern Andean and Amazonian lineages started diversifying, although the latter diversified at a slower pace than the former. A large number of dispersal events into the Northern Andes were followed by important local diversification, for example in the genera *Hypomenitis* (17/20 species in the phylogeny occur in the Northern Andes) and *Pteronymia* (30/45 species in the phylogeny occur in the Northern Andes), or in subclades of the genera *Oleria* or *Napeogenes*. We also identified some important transitions to lowland Amazonia, for example at the origin of the *Brevioleria*-clade, during early divergence in the genus *Oleria* and in the genus *Hypothyris*.

Time-stratified biogeographic model

The time-stratified model designed from rates of colonization computed above led to a significant improvement of the model (likelihoods: DECnull: -1335.802, DECstrat: -1321.805). Both ancestral state reconstructions were very congruent but the time-stratified model increased the resolution of several nodes throughout the tree (Figure S4.9). Notably, the time-stratified model greatly increased the resolution of deep nodes in the backbone, estimating that both Mechanitina and Melinaeina originated in Western Amazonia, in agreement with the ancestral state estimations performed with trait-dependent diversification models. The Andean origin for the core-group was strongly supported.

DISCUSSION

We generated one of the largest species-level phylogenies to date for a tropical insect group, the emblematic Neotropical butterfly tribe Ithomiini, to investigate the temporal and spatial patterns of diversification of this group. Here, we propose that the multiple landscape transformations during the Miocene, and more specifically the interactions between the Andes and the Pebas wetland system, strongly affected the dynamics of diversification and biotic interchanges of Ithomiini butterflies in the Neotropical region.

Early diversification at the interface of the Pebas and Central Andes

Ithomiini probably started diversifying along the early Andean foothills at the transition with Western Amazonia. The onset of the uplift of the eastern cordillera of the Central Andes during late Oligocene coincides with the origin of Ithomiini (Eude et al. 2015). The backbone underwent a rapid early diversification, likely following the colonization of South America during the pre-Pebas period – the sister clade of Ithomiini, Tellervini, is found in Australia and Papua New Guinea (Wahlberg et al. 2009). Diversification was perhaps facilitated by an early shift to a new and diverse hostplant family, the Solanaceae, which originated in the Neotropics during the Paleogene and is particularly diverse in this region (Dupin et al. 2017).

From ca. 23 to 10 My ago the Pebas ecosystem replaced the previous Western Amazonian terrestrial ecosystem. Wesselingh et al. (2001) described the Pebas as an ecosystem "which was permanently aquatic with minor swamps and fluvial influence, and was connected to marine environments", and may have reached a maximum size of 1.1 million km^2. The presence of fossil marine fishes (Monsch 1998) and molluscs (Wesselingh 2006) testifies to the presence of saline waters. More recently, Boonstra et al. (2015) found evidence from foraminifera and dinoflagellate cysts that marine incursions reached 2000 km inland from the Caribbean Sea during the early to middle Miocene during periods of high sea levels. The extent and duration of these marine influences is controversial (see Jaramillo et al. 2017 and references therein). Yet, it is undeniable that the Pebas system was unsuitable for the late Oligocene terrestrial fauna and flora occupying Western Amazonia, and therefore was likely to affect the timing of diversification and dispersal of Neotropical biodiversity. This scenario is congruent with recent historical biogeography analyses of vertebrates (e. g., Hutter et al. 2017) and plant lineages belonging to multiple families (e. g., Schneider and Zizka 2017, Machado et al. 2018) and by a recent evaluation of the Amazonian fossil record, which pointed at a major decline of terrestrial diversity in western Amazonia during the early and middle Miocene (Antoine et al. 2016): mammalian diversity dropped from 11 orders, 29 families and 38 species during late Oligocene down to 1 order, 2 families and 2 species during middle Miocene (see also Antoine et al. 2017). Our results

with Ithomiini butterflies strongly support such a scenario. Although the ancestral area of Ithomiini is ambiguous, at least the two earliest diverging Ithomiini lineages (Melinaeina and Mechanitina) were clearly endemic to Western Amazonia. We found that the diversification rate of Ithomiini rapidly decreased through time and even became negative for backbone lineages during a period corresponding to the replacement of terrestrial habitats by the Pebas system, leading to a decline of diversity in those lineages. Estimations of extinction rates from molecular phylogenies, however, are still controversial and we remain cautious in our interpretation of the role of extinction during the Pebas period. The progressive recovery of backbone lineages towards the present, including positive diversification rates in some recent lineages, also concurs with the idea that the retreat of the Pebas released constraints on diversification during the last 10 My.

Ithomiini are tightly linked to their larval host-plants and forest habitats. As such, early Ithomiini lineages, which are largely Amazonian, may have been strongly impacted by habitat turnover in Western Amazonia and local extinctions of larval host-plant during the Pebas period, while the core-group lineages remained unaffected and diversified fast. Yet, uncertainties surrounding the range estimations at other deep nodes and also the time of first colonization of the Andes challenges a scenario where colonization of the Andes occurred at the root of the core group. If colonization of the Andes occurred earlier than the root of the core group, the shift of diversity dynamics may be explained by other factor(s), unknown at the moment. However, biogeographic inferences in the backbone should be taken with caution. Indeed, extinction events in the backbone (potentially higher in Western Amazonian lineages, as indicated by negative net diversification rates) may bias our biogeographic ancestral state estimations. Notably, asymmetrical extinction across different geographical regions may lead to inaccurate inferences of past geographic ranges (Lieberman 2002, Sanmartín & Meseguer 2016). Such a scenario, where backbone lineages were ancestrally Western Amazonian, would be consistent with the diversification shift observed at the root of the core-group being driven by colonization of the Andes, where ecosystems were unaffected by the Pebas.

The strongly supported origin of the core-group in the Central-Andes (19.1-22.1 My) parallel to the events occurring in Western Amazonia during the Pebas period had profound consequences on the pattern of diversification of Ithomiini. First, this early Andean lineage diversified to produced 85% of the current Ithomiini diversity. Second, until ~10 My ago, diversification in the core-group occurred exclusively in the Central Andes, and from 19.1-22.1 to ~10 My ago we do not detect a single dispersal event out of the Central Andes. Third, the core-group corresponds to a shift of diversification dynamics, characterized by a constant and relatively high diversification rate, which greatly contrasts with the slow and even negative diversification dynamics of the backbone during the same period.

Drivers of diversification in the core group probably include radiation on Solanaceae (Willmott & Freitas 2006), which were already diverse in the Neotropics during the Miocene (Dupin et al. 2017), in

conjunction with a diversity of habitats along the slopes of the Andes. Speciation was also potentially mediated by shifts in mimicry patterns (Chazot et al. 2014, Willmott & Mallet 2004), which can generate reproductive isolation in mimetic butterflies (Jiggins et al. 2001), including Ithomiini (Jiggins et al. 2006, McClure et al. accepted). Those ecological drivers of diversification were probably at play both in the Andes and in non-Andean areas, after the Pebas retreat. Indeed, in the core-group, Andean and non-Andean lineages had similar diversification rates. The lack of support for a general increase in diversification rate in the Andes within the core-group is also supported by analyses performed independently on different core-group subtribes. For example, in both Oleriina (Chazot et al. 2018) and Godyridina (Chazot et al. 2016b), radiations occurred in both Andean and Amazonian genera.

Dispersal out of the Central Andes at the demise of the Pebas

Gentry (1982) pointed out a dichotomy observed in the geographic distribution of Neotropical plant diversity, showing that groups could be divided into Andean-centred *versus* Amazonian-centred patterns. Clades tend to be species-rich in one of these centres and relatively species-poor in the other. Antonelli & Sanmartín (2011) coined this observation the "Gentry-pattern". They also suggested that in the absence of a barrier between the Andes and the Amazon basin we should observe continuous interchanges between these regions. Antonelli & Sanmartín (2011) proposed that the Pebas could be this "missing long-lasting barrier needed for creating the disjunction between Andean-centred and Amazonian-centred groups". Therefore, in addition to the constraints on diversification discussed above, we predicted that the Pebas ecosystem should have influenced interchanges towards or across Western Amazonia.

Our results conform remarkably well to the scenario proposed by Antonelli & Sanmartín (2011). Ithomiini are Andean-centered with more than half of their current diversity occurring in the Andes (see also Chazot et al. 2016b,c). Here we show that interchanges have been virtually absent during the Pebas period, with a period as long as 9-12 My without interchanges. However, rates of interchanges from the Central Andes towards the Northern Andes and Amazonia suddenly peaked ~10 My ago (between 13-8 My ago) and more recently (4-0 My ago). Regarding connections between Central Andes and the Northern Andes, the closure of the Western Andean Portal (Antonelli & Sanmartín 2011) may have allowed multiple colonizations of the Northern Andes facilitated by the presence of connecting higher altitude habitats. In parallel, between 10-8 My ago the Pebas system was progressively drained eastward, leading to the formation of the present-day configuration of the Amazonian basin and the expansion of terrestrial forest habitats in Western Amazonia (Leite et al. 2017). This corresponds precisely to the timing at which core-group lineages colonized Western Amazonia - perhaps again because this region was concomitantly recolonized by Solanaceae - and then diversified.

Diversification across the whole Neotropics following the demise of the Pebas

We found a strong dampening of local speciation in the Central Andes during the last 10 My. By contrast, colonizations following the retreat of the Pebas were followed by large local bursts of diversification within the Northern Andes and Amazonia. As an illustration, from our biogeographic reconstruction, 69 divergence events occurred strictly in the Central Andes in the core-group in the last 20 My. Multiple independent dispersal events followed by local diversification lead to the exact same number of divergences occurring strictly in the Northern Andes during the last 9 My only. The genera *Hypomenitis* and *Pteronymia*, for example, which comprise 23 and 53 species, respectively, diversified extensively within the Northern Andes (Chazot et al. 2016b; De-Silva et al. 2017). Lineages that dispersed into the Northern Andes and Amazonia after the demise of the Pebas probably accessed a large range of new ecological niches, including a diversity of host-plants that had already diversified or that radiated concomitantly. We detected a second peak of interchanges between the Central Andes and Amazonia or the Northern Andes. In both cases, these recent peaks of interchanges are clearly driven by reverse dispersal events. Three Amazonian radiations, the genus *Melinaea* (which comprises the rapidly-diversifying *Melinaea*-group) and the clade *Mechanitis* + *Forbestra* in the backbone and the *Brevioleria*-group in the core-group, showed increasing speciation rates towards the present. Those radiations may be interpreted as supporting an effect of recent climatic fluctuations during the Pleistocene on the diversification of the *Melinaea*-group (as well as the *Mechanitis* + *Forbestra* clade), although ecological drivers of speciation classically invoked in mimetic butterfly diversification, such as colour pattern and hostplant shifts, cannot be ruled out (Jiggins et al. 2006, Hill et al. 2012, McClure & Elias 2016, McClure & Elias 2017, McClure et al. accepted). Contrasting with those clades, four other Amazonian radiations showed diversification rates decreasing through time, meaning that diversification was highest just after the retreat of the Pebas. Recent radiations in Western Amazonia that post-date the Pebas period have repeatedly been reported. For example, in the palm genus *Astrocaryum* (Arecaceae), the upper Amazonian clade started diversifying only ~6 My ago (Roncal et al. 2013). In *Taygetis* butterflies, Amazonian lineages show rapid diversification during the last 7-8 My (Matos-Maraví et al. 2013). Such convergent timing of diversification in Western Amazonia strongly supports the scenario of a post-Pebas recovery of terrestrial habitats, which triggered dispersal followed by local diversification.

Taken together, our results point at a robust scenario for Neotropical diversification, which highlights the role of Miocene ecosystem turnover in determining the timing of interchanges, speciation and potentially extinction in the world's most biologically diverse region.

List of supporting information:

Appendix S1: List of all individuals and species used in this study (S1.1), and biogeographic distribution of species (S1.2).

Appendix S2: Detailed methods and supplementary results for phylogenetic inferences

Appendix S3: Detailed methods and supplementary results for diversification analyses

Appendix S4: Detailed methods and supplementary results for historical biogeography analyses

REFERENCES

Alfaro ME, Santini F, Brock C, Alamillo H, Dornburg A, Rabosky DL, Carnevale G, & Harmon LJ. (2009). Nine exceptional radiations plus high turnover explain species diversity in jawed vertebrates. *Proceedings of the National Academy of Sciences*, 106(32), 13410-13414.

Antoine PO, Abello MA, Adnet S, Sierra AJA, Baby P, Billet G, Boivin M, Calderón Y, Candela A, Chabain J, & Corfu F. (2016). A 60-million-year Cenozoic history of western Amazonian ecosystems in Contamana, eastern Peru. *Gondwana Research*, 31, 30-59.

Antoine P-O, Salas-Gismondi R, Pujos F, Ganerød M, & Marivaux L. (2017). Western Amazonia as a Hotspot of Mammalian Biodiversity Throughout the Cenozoic. *Journal of Mammalian Evolution*, 24, 5-17.

Antonelli A, Nylander JA, Persson C, & Sanmartín I. (2009). Tracing the impact of the Andean uplift on Neotropical plant evolution. *Proceedings of the National Academy of Sciences*, 106, 9749-9754.

Antonelli A, & Sanmartín I. (2011). Why are there so many plant species in the Neotropics? *Taxon*, 60, 403-414.

Bates HW. (1862). Contributions to an insect fauna of the Amazon valley (Lepidoptera: Heliconidae). *Transactions of the Linnean Society of London*, 23(3), 495-566.

Beaulieu JM, & O'Meara BC. (2016). Detecting hidden diversification shifts in models of trait-dependent speciation and extinction. *Systematic Biology*, 65, 583-601.

Beccaloni GW. (1997). Vertical stratification of ithomiine butterfly (Nymphalidae: Ithomiinae) mimicry complexes: the relationship between adult flight height and larval host-plant height. *Biological Journal of the Linnean Society*, 62(3), 313-341.

Beckman EJ, & Witt CC. (2015). Phylogeny and biogeography of the New World siskins and goldfinches: Rapid, recent diversification in the Central Andes. *Molecular Phylogenetics and Evolution*, 87, 28-45.

Bolaños Martinez I, Zambrano Gonzalez G, & Willmott K. (2011). Descripción de los estados inmaduros de Pteronymia zerlina zerlina, P. zerlina machay, P. veia florea y P. medellina de Colombia y del Ecuador (Lepidoptera: Nymphalidae: Ithomiini) de Colombia y del Ecuador. *Tropical Lepidoptera Research*, 21, 27-33.

Boonstra M, Ramos M, Lammertsma E, Antoine P-O, & Hoorn C. (2015). Marine connections of Amazonia: Evidence from foraminifera and dinoflagellate cysts (early to middle Miocene, Colombia/Peru). *Palaeogeography, Palaeoclimatology, Palaeoecology*, 417, 176-194.

Brower AV, Freitas AV, Lee MM, Silva-Brandão KL, Whinnett A, & Willmott KR. (2006). Phylogenetic relationships among the Ithomiini (Lepidoptera: Nymphalidae) inferred from one mitochondrial and two nuclear gene regions. *Systematic Entomology*, 31, 288-301.

514 Brower AV, Willmott KR, Silva-Brandão KL, Garzón-Orduña IJ, & Freitas AV. (2014). Phylogenetic
515 relationships of ithomiine butterflies (Lepidoptera: Nymphalidae: Danainae) as implied by
516 combined morphological and molecular data. *Systematics and Biodiversity,* 12(2), 133-147.

517 Brown Jr KS. (1984). Adult-obtained pyrrolizidine alkaloids defend ithomiine butterflies against a
518 spider predator. *Nature*, 309(5970), 707-709.
519 Brown Jr KS, & Benson WW. (1974). Adaptive polymorphism associated with multiple Müllerian
520 mimicry in Heliconius numata (Lepid. Nymph.). *Biotropica* 6(4), 205-228.
521 Brown Jr KS, & Freitas AVL. (1994). Juvenile stages of Ithomiinae: Overview and systematics
522 (Lepidoptera: Nymphalidae). *Tropical Lepidoptera* 5(1): 9-20.
523 Brown Jr KS, Von Schoultz, B, & Suomalainen E. (2004). Chromosome evolution in neotropical
524 Danainae and Ithomiinae (Lepidoptera). *Hereditas*, 141(3), 216-236.
525 Chazot N, Willmott KR, Santacruz Endara PG, Toporov A, Hill RI, Jiggins CD, & Elias M. (2014).
526 Mutualistic mimicry and filtering by altitude shape the structure of Andean butterfly
527 communities. *The American Naturalist*, 183(1), 26-39.
528 Chazot N, Panara S, Zilbermann N, Blandin P, Le Poul Y, Cornette R, Elias M, & Debat V. (2016a).
529 Morpho morphometrics: shared ancestry and selection drive the evolution of wing size and
530 shape in Morpho butterflies. *Evolution*, 70(1), 181-194.
531 Chazot N, Willmott KR, Condamine FL, De-Silva DL, Freitas AV, Lamas G, Morlon H, Giraldo, CE,
532 Jiggins CD, Joron M, Mallet J, & Elias M. (2016b). Into the Andes: multiple independent
533 colonizations drive montane diversity in the Neotropical clearwing butterflies Godyridina.
534 *Molecular Ecology*, 25(22), 5765-5784.
535 Chazot N, Willmott KR, Freitas AVL, de Silva DL, Pellens R, & Elias M. (2016c). Patterns of Species,
536 Phylogenetic and Mimicry Diversity of Clearwing Butterflies in the Neotropics. In:
537 Biodiversity Conservation and Phylogenetic Systematics: Preserving our evolutionary
538 heritage in an extinction crisis (eds Pellens R, Grandcolas P). Springer International
539 Publishing.
540 Chazot N, De-Silva DL, Willmott KR, Freitas AVL, Lamas G, Mallet J, Giraldo CE, Uribe S, & Elias
541 M. (2018). Contrasting patterns of Andean diversification among three diverse clades of
542 Neotropical clearwing butterflies. *Ecology & Evolution*, 8(8), 3965-3982.
543 Colinvaux PA, De Oliveira P, & Bush M. (2000). Amazonian and neotropical plant communities on
544 glacial time-scales: the failure of the aridity and refuge hypotheses. *Quaternary Science*
545 *Reviews,* 19, 141-169.
546 Condamine FL, Silva-Brandão KL, Kergoat GJ, & Sperling FA. (2012). Biogeographic and
547 diversification patterns of Neotropical Troidini butterflies (Papilionidae) support a museum
548 model of diversity dynamics for Amazonia. *BMC Evolutionary Biology*, 12(82), 1-16.

549 Elias M, Joron M, Willmott K, Silva-Brandão KL, Kaiser V, Arias CF, Gomez-Piñerez LM, Uribe S,
550 Brower AVZ, Freitas AVL, & Jiggins, CD. (2009). Out of the Andes: patterns of
551 diversification in clearwing butterflies. *Molecular Ecology*, 18(8), 1716-1729.
552 Dasmahapatra KK, Lamas G, Simpson F, & Mallet J. (2010). The anatomy of a 'suture zone' in
553 Amazonian butterflies: a coalescent-based test for vicariant geographic divergence and
554 speciation. *Molecular Ecology*, 19,4283-4301.
555 De-Silva DL, Day JJ, Elias M, Willmott K, Whinnett A, & Mallet J. (2010). Molecular phylogenetics
556 of the neotropical butterfly subtribe Oleriina (Nymphalidae: Danainae: Ithomiini). *Molecular*
557 *Phylogenetics and Evolution*, 55(3), 1032-1041.
558 De-Silva DL, Elias M, Willmott K, Mallet J, & Day JJ. (2016). Diversification of clearwing butterflies
559 with the rise of the Andes. *Journal of Biogeography*, 43(1), 44-58.
560 De-Silva DL, Mota LL, Chazot N, Mallarino R, Silva-Brandão KL, Piñerez LMG, Freitas AVL, Lamas
561 G, Joron M, Mallet J, Giraldo CE, & Elias M. (2017). North Andean origin and diversification
562 of the largest ithomiine butterfly genus. *Scientific Reports*, 7(45966), 1-17.
563 Drummond BA, & Brown KS. (1987). Ithomiinae (Lepidoptera: Nymphalidae): summary of known
564 larval food plants. *Annals of the Missouri Botanical Garden*, 74, 341-358.
565 DeVries P, Lande R, & Murray D. (1999). Associations of co-mimetic ithomiine butterflies on small
566 spatial and temporal scales in a neotropical rainforest. *Biological Journal of the Linnean*
567 *Society*, 67(1), 73-85.
568 Drummond AJ, Suchard MA, Xie D, & Rambaut A. (2012) Bayesian phylogenetics with BEAUti and
569 the BEAST 1.7. *Molecular Biology and Evolution*, 29, 1969-1973.
570 Dupin J, Matzke NJ, Särkinen T, Knapp S, Olmstead RG, Bohs L, & Smith SD. (2017), Bayesian
571 estimation of the global biogeographical history of the Solanaceae. *Journal of Biogeography*,
572 44, 887-899.
573 Elias M, Gompert Z, Jiggins C, & Willmott K. (2008). Mutualistic interactions drive ecological niche
574 convergence in a diverse butterfly community. *PLoS Biology*, 6(12)(e300),2642-2649.
575 Eude A, Roddaz M, Brichau S, Brusset S, Calderon Y, Baby P, & Soula JC. (2015). Controls on timing
576 of exhumation and deformation in the northern Peruvian eastern Andean wedge as inferred
577 from low-temperature thermochronology and balanced cross section. *Tectonics*, 34(4), 715-
578 730.
579 Freitas AVL. (1993). Biology and Population dynamics of Placidula euryanassa, a relict ithomiine
580 butterfly (Lepidoptera: Ithomiinae). *Journal of the Lepidopterists' Society*, 47, 87-105.
581 Freitas AVL. (1996). Population biology of Heterosais edessa (Nymphalidae) and its associated Atlantic
582 Forest Ithomiinae community. *Journal of the Lepidopterists' Society*, 50, 273-289.
583 Garzón-Orduña IJ, Benetti-Longhini JE, & Brower AV. (2014). Timing the diversification of the
584 Amazonian biota: butterfly divergences are consistent with Pleistocene refugia. *Journal of*
585 *Biogeography*, 41(9), 1631-1638.

586 Garzón-Orduña IJ, Silva-Brandão KL, Willmott KR, Freitas AV, & Brower AV. (2015). Incompatible
587 ages for clearwing butterflies based on alternative secondary calibrations. *Systematic Biology*,
588 64(5),752-767.
589 Gentry AH. (1982). Neotropical floristic diversity: phytogeographical connections between Central and
590 South America, Pleistocene climatic fluctuations, or an accident of the Andean orogeny?
591 *Annals of the Missouri Botanical Garden*, 69, 557-593.
592 Goldberg EE, & Igić B. (2012). Tempo and mode in plant breeding system evolution. *Evolution*, 66,
593 3701-3709.
594 Haffer J. (1969). Speciation in Amazonian forest birds. *Science*, 165, 131-137.
595 Hall JPW, & Harvey DJ. (2002). The phylogeography of Amazonia revisited: new evidence from
596 riodinid butterflies. *Evolution*, 56,1489-1497.
597 Hill RI. (2010). Habitat segregation among mimetic ithomiine butterflies (Nymphalidae). *Evolutionary*
598 *Ecology,* 24(2), 273-285.
599 Hill RI, Elias M, Dasmahapatra KK, Jiggins CD, Koong V, Willmott KR, & Mallet J. (2012).
600 Ecologically relevant cryptic species in the highly polymorphic Amazonian butterfly
601 *Mechanitis mazaeus s.l.* (Lepidoptera: Nymphalidae; Ithomiini). *Biological Journal of the*
602 *Linnean Society*, 106(3), 540-560.
603 Hoorn C, Wesselingh FP, Ter Steege H, Bermudez MA, Mora A, Sevink J, Sanmartín I, Sanchez-
604 Meseguer A, Anderson CL, Figueiredo JP & Jaramillo C. (2010). Amazonia through time:
605 Andean uplift, climate change, landscape evolution, and biodiversity. *Science*, 330(6006),
606 927-931.
607 Hutter CR, Lambert SM, & Wiens JJ. (2017). Rapid diversification and time explain amphibian species
608 richness at different scales in the Tropical Andes, Earth's most biodiverse hotspot. *The*
609 *American Naturalist*, 190, 828-843
610 Jaramillo C, Romero I, D'Apolito C, Bayona G, Duarte E, Louwye S, Escobar J, Luque J, Carrillo-
611 Briceño JD, Zapata V, Mora A, Schouten S, Zavada M, Harrington G, Ortiz J, and Frank P.
612 Wesselingh (2017). Miocene flooding events of western Amazonia. *Science Advances*, 3(5),
613 e1601693.
614 Jiggins CD, Naisbit RE, Coe RL, & Mallet J. (2001) Reproductive isolation caused by colour pattern
615 mimicry. *Nature*, 411(6835), 302-305.
616 Jiggins CD, Mallarino R, Willmott KR, Bermingham E, Funk D. (2006). The phylogenetic pattern of
617 speciation and wing pattern change in neotropical Ithomia butterflies (Lepidoptera:
618 Nymphalidae). *Evolution*, 60(7), 1454-1466.
619 Lanfear R, Calcott B, Ho SY, & Guindon S. (2012). PartitionFinder: combined selection of partitioning
620 schemes and substitution models for phylogenetic analyses. *Molecular Biology and Evolution*
621 29, 1695-1701.

Leite FPR, Paz J, do Carmo DA, & Silva-Caminha SA. (2017). The Effects of the Inception of Amazonian Transcontinental Drainage During the Neogene on the Landscape and Vegetation of the Solimões Basin, Brazil. *Palynology*, 41, 412-422.

Lieberman BS. (2002). Phylogenetic biogeography with and without the fossil record: gauging the effects of extinction and paleontological incompleteness. *Palaeogeography, Palaeoclimatology, Palaeoecology,* 178, 39-52.

Machado AFP, Rønsted N, Bruun-Lund S, Pereira RAS, & Paganucci de Queiroz L. (2018) Atlantic forests to the all Americas: Biogeographical history and divergence times of Neotropical *Ficus* (Moraceae). *Molecular Phylogenetics and Evolution*, 122, 46-58.

Madriñán S, Cortés AJ, & Richardson JE (2013). Páramo is the world's fastest evolving and coolest biodiversity hotspot. *Frontiers in Genetics*, 4, 192.

Mallarino R, Bermingham E, Willmott KR, Whinnett A, & Jiggins CD. (2005). Molecular systematics of the butterfly genus *Ithomia* (Lepidoptera: Ithomiinae): a composite phylogenetic hypothesis based on seven genes. *Molecular Phylogenetics and Evolution*, 34(3), 625-644.

Matos-Maraví PF, Peña C, Willmott KR, Freitas AVL, & Wahlberg N. (2013). Systematics and evolutionary history of butterflies in the "*Taygetis* clade" (Nymphalidae: Satyrinae: Euptychiina): towards a better understanding of Neotropical biogeography. *Molecular Phylogenetics and Evolution*, 66(1), 54-68.

Matos-Maraví P. (2016). Investigating the timing of origin and evolutionary processes shaping regional species diversity: Insights from simulated data and neotropical butterfly diversification rates. *Evolution*, 70(7), 1638-1650.

Matzke NJ. (2014). Model selection in historical biogeography reveals that founder-event speciation is a crucial process in island clades. *Systematic Biology*, 63(6), 951-970.

McClure M, & Elias M. (2016). Unravelling the role of host plant expansion in the diversification of a Neotropical butterfly genus. *BMC Evolutionary Biology*, 16, 1471-2148.

McClure M, & Elias M. (2017). Ecology, life history, and genetic differentiation in Neotropical *Melinaea* (Nymphalidae: Ithomiini) butterflies from north-eastern Peru. *Zoological Journal of the Linnean Society*, 179(1), 110-124.

McClure M, Dutrillaux B, Dutrillaux AM, Lukhtanov V, & Elias M. (2018). Heterozygosity and chain multivalents during meiosis illustrate ongoing evolution as a result of multiple holokinetic chromosome fusions in the genus *Melinaea* (Lepidoptera, Nymphalidae). *Cytogenetic and Genome Research*, 153(4), 213-222.

McClure M, Mahrouche L, Houssin C, Monllor M, Le Poul Y, Frérot B, Furtos A & Elias M (Accepted) Does divergent selection predict the evolution of mate preference and reproductive isolation in the tropical butterfly genus Melinaea (Nymphalidae: Ithomiini)? *Journal of Animal Ecology*.

Monsch KA. (1998). Miocene fish faunas from the northwestern Amazonia basin (Colombia, Peru, Brazil) with evidence of marine incursions. *Palaeogeography, Palaeoclimatology, Palaeoecology,* 143(1-3), 31-50.

Morlon H, Parsons TL, & Plotkin JB. (2011). Reconciling molecular phylogenies with the fossil record. *Proceedings of the National Academy of Sciences*, 108(39), 16327-16332.

Müller F. (1879). *Ituna* and *Thyridia*: a remarkable case of mimicry in butterflies. *Proceedings of the Entomological Society of London*, 1879, xx-xxix.

Muñoz-Torres FA, Whatley RC, & Van Harten D. (2006). Miocene ostracod (Crustacea) biostratigraphy of the upper Amazon Basin and evolution of the genus *Cyprideis*. *Journal of South American Earth Sciences*, 21(1-2), 75-86.

Nguyen LT, Schmidt HA, von Haeseler A, & Minh BQ. (2014). IQ-TREE: a fast and effective stochastic algorithm for estimating maximum-likelihood phylogenies. *Molecular Biology and Evolution*, 32(1), 268-274.

Penz CM, Devries PJ, & Wahlberg N. (2012). Diversification of *Morpho* butterflies (Lepidoptera, Nymphalidae): a re-evaluation of morphological characters and new insight from DNA sequence data. *Systematic Entomology*, 37(4), 670-685.

Price SL, Powell S, Kronauer DJ, Tran LA, Pierce NE, & Wayne RK (2014). Renewed diversification is associated with new ecological opportunity in the Neotropical turtle ants. *Journal of Evolutionary Biology*, 27(2), 242-258.

Rabosky DL (2014). Automatic detection of key innovations, rate shifts, and diversity-dependence on phylogenetic trees. *PloS one*, 9(2), e89543.

Roncal J, Kahn F, Millán B, Couvreur T, Pintaud J-C. (2013). Cenozoic colonization and diversification patterns of tropical American palms: Evidence from *Astrocaryum* (Arecaceae). *Botanical Journal of the Linnean Society*. 171. 120-139. 10.1111/j.1095-8339.2012.01297.x.

Rull V. (2008). Speciation timing and neotropical biodiversity: the Tertiary–Quaternary debate in the light of molecular phylogenetic evidence. *Molecular Ecology*, 17(11), 2722-2729.

Sanmartín I, & Meseguer AS. (2016). Extinction in phylogenetics and biogeography: from timetrees to patterns of biotic assemblage. *Frontiers in Genetics*, 7.

Salas-Gismondi R, Flynn JJ, Baby P, Tejada-Lara JV, Wesselingh FP, & Antoine P-O. (2015). A Miocene hyperdiverse crocodylian community reveals peculiar trophic dynamics in proto-Amazonian mega-wetlands. *Proceedings of the Royal Society of London B: Biological Sciences*, 282, 20142490.

Schneider JV, & Zizka G. (2017). Phylogeny, taxonomy and biogeography of Neotropical Quiinoideae (Ochnaceae s.l.). *Taxon*, 4, 855-867.

Schulz S, Beccaloni G, Brown Jr KS, Boppré M, Freitas AVL, Ockenfels P, & Trigo JR. (2004). Semiochemicals derived from pyrrolizidine alkaloids in male ithomiine butterflies

(Lepidoptera: Nymphalidae: Ithomiinae). *Biochemical Systematics and Ecology*, 32(8), 699-713.

Smith BT, McCormack JE, Cuervo AM, Hickerson MJ, Aleixo A, Cadena CD, Pérez-Emán J, Burney CW, Xie X, Harvey MG, Faircloth BC, Glenn TC, Derryberry EP, Prejean J, Fields S, & Brumfield RT. (2014). The drivers of tropical speciation. *Nature*, 515, 406-409.

Stadler T. (2011). Mammalian phylogeny reveals recent diversification rate shifts. *Proceedings of the National Academy of Sciences*, 108, 6187-6192.

Trifinopoulos J, Nguyen L-T, von Haeseler A, & Minh BQ. (2016). W-IQ-TREE: a fast online phylogenetic tool for maximum likelihood analysis. *Nucleic Acids Research*, 44(W1):W232-5.

Trigo JR, & Brown KS. (1990). Variation of pyrrolizidine alkaloids in Ithomiinae: a comparative study between species feeding on Apocynaceae and Solanaceae. *Chemoecology*, 1(1), 22-29.

Wahlberg N, Leneveu J, Kodandaramaiah U, Peña C, Nylin S, Freitas AVL, & Brower AV. (2009). Nymphalid butterflies diversify following near demise at the Cretaceous/Tertiary boundary. *Proceedings of the Royal Society of London B: Biological Sciences*, 276(1677), 4295-4302.

Wahlberg N, & Wheat CW. (2008). Genomic outposts serve the phylogenomic pioneers: designing novel nuclear markers for genomic DNA extractions of Lepidoptera. Systematic Biology, 57(2), 231-242.Wesselingh FP, Räsänen ME, Irion G, Vonhof HB, Kaandorp R, Renema W, Pittman LR, & Gingras M. (2001). Lake Pebas: a palaeoecological reconstruction of a Miocene, long-lived lake complex in western Amazonia. *Cainozoic Research*, 1(1-2), 35-68.

Wesselingh F. (2006). Molluscs from the Miocene Pebas Formation of Peruvian and Colombian Amazonia. *Scripta Geologica*, 133(1), 19-290.

Wesselingh F, & Salo J. (2006). A Miocene perspective on the evolution of the Amazonian biota. *Scripta Geologica*, 133, 439-458.

Wesselingh FP, Hoorn C, Kroonenberg SB, Antonelli A, Lundberg JG, Vonhof HB, & Hooghiemstra H. (2010). On the origin of Amazonian landscapes and biodiversity: a synthesis. In: Amazonia: Landscape and Species Evolution: A look into the past, 419-431.

Willmott KR, & Freitas AV. (2006). Higher-level phylogeny of the Ithomiinae (Lepidoptera: Nymphalidae): classification, patterns of larval hostplant colonization and diversification. *Cladistics*, 22(4), 297-368.

Willmott KR, & Mallet J. (2004). Correlations between adult mimicry and larval host plants in ithomiine butterflies. *Proceedings of the Royal Society of London B: Biological Sciences*, 271(suppl.5), 266-269.

Willmott KR, Willmott JCR, Elias M, & Jiggins CD. (2017). Maintaining mimicry diversity: optimal warning colour patterns differ among microhabitats in Amazonian clearwing butterflies. *Proceedings of the Royal Society of London B: Biological Sciences*, 284(1855)(20170744), 1-9.

731 Whinnett A, Brower AV, Lee M-M, Willmott KR, & Mallet J. (2005). Phylogenetic utility of Tektin, a
732 novel region for inferring systematic relationships among Lepidoptera. *Annals of the*
733 *Entomological Society of America*, 98(6), 873-886.

734

DATA ACCESSIBILITY

All sequences are publicly available on Genbank (accession numbers are given in Appendix S1). Phylogenetic trees are available on TreeBase (http://purl.org/phylo/treebase/phylows/study/TB2:S23995?x-access-code=85eb5792b9ef59452b163c39eb80ae47&format=html).

Table 1. Results of time-dependent models of diversification fitted on 100 posterior trees partitioned into the backbone, the core-group and the *Melinaea*-group. For each subclade or the backbone, only the best fitting model is shown (Appendix 3.1.2). BCST = constant speciation, BVAR = time-dependent speciation, DCST = constant extinction, DVAR time-dependent extinction. λ = speciation rate at present, α = coefficient of time variation of the speciation rate, μ = extinction rate at present, ß = coefficient of time variation of the extinction rate. Values given are the mean estimated for 100 posterior trees.

	model	par	logL	AIC	λ	α	μ	ß
backbone	BVARDVAR	4	-129.75	267.50	0.153	0.160	0.193	0.148
Melinaea-group	BVAR	2	-1.58	7.17	0.311	3.772		
core-group	BCST	1	-702.25	1406.50	0.257			
Joint model		**7**	**-835.032**	**1684.065**				

Table 2. Results of ClaSSE models fitted on 100 posterior trees for whole Ithomiini tree (a.) and the core-group (b.) sorted by increasing mean AIC. Constraints of each model are indicated in the four first columns. 1=non-Andean, 2=Andean, λ111 and λ222 are within-region speciation rates (non-Andean and Andean, respectively), λ112 and λ212 are cladogenetic transition rates (non-Andean towards Andean, and Andean towards non-Andean, respectively) , μ = extinction rates, df =number of parameters, logL=log-likelihood, AIC= Akaike information criterion score, ΔAIC = AIC difference with the best fitting model. Values given are the mean estimated for 100 posterior trees (Appendix S3.2).

a. Whole tree

λ111/λ222		λ112/λ212	μ	df	logL	AIC	ΔAIC	λ111	λ222	λ112	λ212	μ1	μ2
λ111≠λ222	**≠**	**λ112=λ212**	**μ1=μ2**	**4**	**-1064.82**	**2137.63**	**0.00**	**0.154**	**0.186**	**0.052**	**0.052**	**0.003**	**0.003**
λ111=λ222	**≠**	**λ112=λ212**	**μ1=μ2**	**3**	**-1065.89**	**2137.79**	**0.16**	**0.171**	**0.171**	**0.052**	**0.052**	**0.004**	**0.004**
λ111≠λ222	**≠**	**λ112≠λ212**	**μ1=μ2**	**5**	**-1064.66**	**2139.31**	**1.68**	**0.151**	**0.188**	**0.046**	**0.058**	**0.002**	**0.002**
λ111=λ222	**≠**	**λ112=λ212**	**μ1≠μ2**	**4**	**-1065.70**	**2139.39**	**1.76**	**0.174**	**0.174**	**0.052**	**0.052**	**0.020**	**0.001**
λ111≠λ222	**≠**	**λ112=λ212**	**μ1≠μ2**	**5**	**-1064.73**	**2139.46**	**1.83**	**0.153**	**0.192**	**0.052**	**0.052**	**0.001**	**0.015**
λ111=λ222	≠	λ112≠λ212	μ1=μ2	4	-1065.88	2139.76	2.13	0.172	0.172	0.053	0.051	0.004	0.004
λ111=λ222	≠	λ112≠λ212	μ1≠μ2	5	-1065.65	2141.29	3.66	0.175	0.175	0.049	0.056	0.024	7E-05
λ111≠λ222	≠	λ112≠λ212	μ1≠μ2	6	-1064.65	2141.29	3.66	0.151	0.190	0.047	0.057	0.001	0.006
λ111=λ222	=	λ112=λ212	μ1=μ2	2	-1102.44	2208.88	71.25	0.111	0.111	0.111	0.111	6E-06	6E-06
λ111=λ222	=	λ112=λ212	μ1≠μ2	3	-1102.42	2210.84	73.21	0.151	0.151	0.151	0.151	0.001	0.006

b. Core-group

λ111/λ222		λ112/λ212	μ	df	logL	AIC	ΔAIC	λ111	λ222	λ112	λ212	μ1	μ2
λ111=λ222	**≠**	**λ112=λ212**	**μ1=μ2**	**3**	**-877.96**	1757.74	**0.00**	**0.190**	**0.190**	**0.059**	**0.059**	**4.26E-07**	**4.26E-07**
λ111≠λ222	**≠**	**λ112=λ212**	**μ1=μ2**	**4**	**-877.00**	1757.80	**0.08**	**0.168**	**0.205**	**0.060**	**0.060**	**8.15E-07**	**8.15E E-07**
λ111=λ222	**≠**	**λ112≠λ212**	**μ1=μ2**	**4**	**-877.62**	1759.07	**1.33**	**0.189**	**0.189**	**0.082**	**0.038**	**4.13E-07**	**4.13E-07**
λ111=λ222	**≠**	**λ112=λ212**	**μ1≠μ2**	**4**	**-877.96**	1759.74	**2.00**	**0.190**	**0.190**	**0.059**	**0.059**	**8.11E-06**	**6.97E-06**
λ111≠λ222	≠	λ112=λ212	μ1≠μ2	5	-876.99	1759.78	2.07	0.168	0.207	0.060	0.060	1.13E-06	0.003
λ111≠λ222	≠	λ112≠λ212	μ1=μ2	5	-874.92	1759.83	2.09	0.171	0.204	0.068	0.051	1.84E-07	1.84E-07
λ111=λ222	≠	λ112≠λ212	μ1≠μ2	5	-875.52	1761.02	3.26	0.190	0.190	0.084	0.035	0.003	8.37E-07
λ111≠λ222	≠	λ112≠λ212	μ1≠μ2	6	-874.88	1761.75	4.01	0.170	0.205	0.064	0.054	2.65E-06	0.001
λ111=λ222	=	λ112=λ212	μ1=μ2	2	-905.69	1815.37	57.63	0.124	0.124	0.124	0.124	1.97E-06	1.97E-06
λ111=λ222	=	λ112=λ212	μ1≠μ2	3	-905.51	1817.02	59.27	0.170	0.170	0.170	0.170	2.65E-06	0.001

Figure 1. Time-calibrated phylogeny of the tribe Ithomiini. Coloured branches depict the partitions identified by MEDUSA and used for fitting diversification rate models. Red lineages constitute the core-group, green lineages the *Melinaea*-group, blue lineages the backbone. Black and white circles indicate the biogeographic ancestral states reconstructed at the basal nodes of the tree: black = Central Andes, white = Western Amazonia. Question mark and arrows indicate the position of two alternative scenarios for the first colonization of the Andes: BioGeoBEARS, at the root of the Ithomiini, and trait-dependent analyses, at the root of the core-group. Both methods are congruent for Melinaeina and Mechanitina but not for Tithoreina, Methonina and Athesitina. Names and position of the different subtribes are indicated, as well as mean crown age and 95% confidence interval.

Figure 2. Means and 95% confidence intervals of diversification rates through time estimated on 100 posterior trees partitioned into the backbone, the core-group and the *Melinaea*-group. A. Diversification rates estimated using Morlon *et al.* (2011) for the backbone, the core-group and *Melinaea*-group (cropped). B. Diversification rates estimated using TreePar for the backbone and the core-group.

Figure 3. A. Colonization rates and lineage accumulation through time (speciation only) extracted from BioGeoBEARS ancestral state estimation for the core-group. The lines depicted are the median colonization rate after 1000 biogeographic stochastic mapping (Appendix S4). Dots represent the additional contribution to lineage accumulation of local diversification in three regions as reconstructed on the MCC tree. Red dots represent the cumulative number of speciation events through time in Central Andes; orange dots represent the cumulative number of speciation events through time in Central Andes and Northern Andes; blue dots represent the cumulative number of speciation events through time in Central Andes, Northern Andes and Amazonia; Grey dots represent the cumulative number of speciation events through time in the entire Neotropics. B. Confidence intervals of speciation rates through time estimated on seven Amazonian diversification events. All those clades originated during the last 8 My.

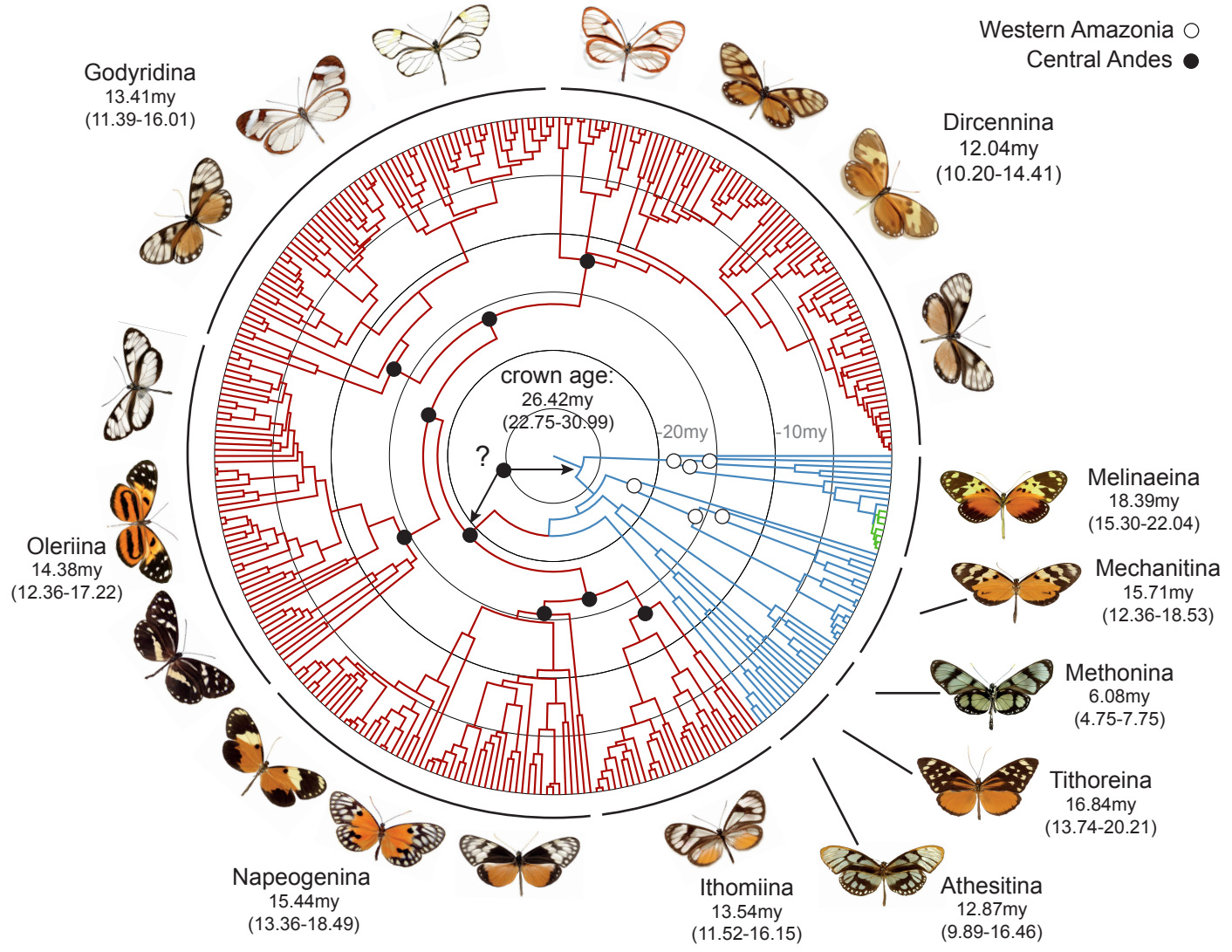
Western Amazonia
Central Andes
Godyridina
13.41my
(11.39-16.01)
Dircennina
12.04my
(10.20-14.41)
crown age:
26.42my
(22.75-30.99)
?
~20my
~10my
Melinaeina
18.39my
(15.30-22.04)
Mechanitina
15.71my
(12.36-18.53)
Methonina
6.08my
(4.75-7.75)
Tithoreina
16.84my
(13.74-20.21)
Athesitina
12.87my
(9.89-16.46)
Ithomiina
13.54my
(11.52-16.15)
Napeogenina
15.44my
(13.36-18.49)
Oleriina
14.38my
(12.36-17.22)

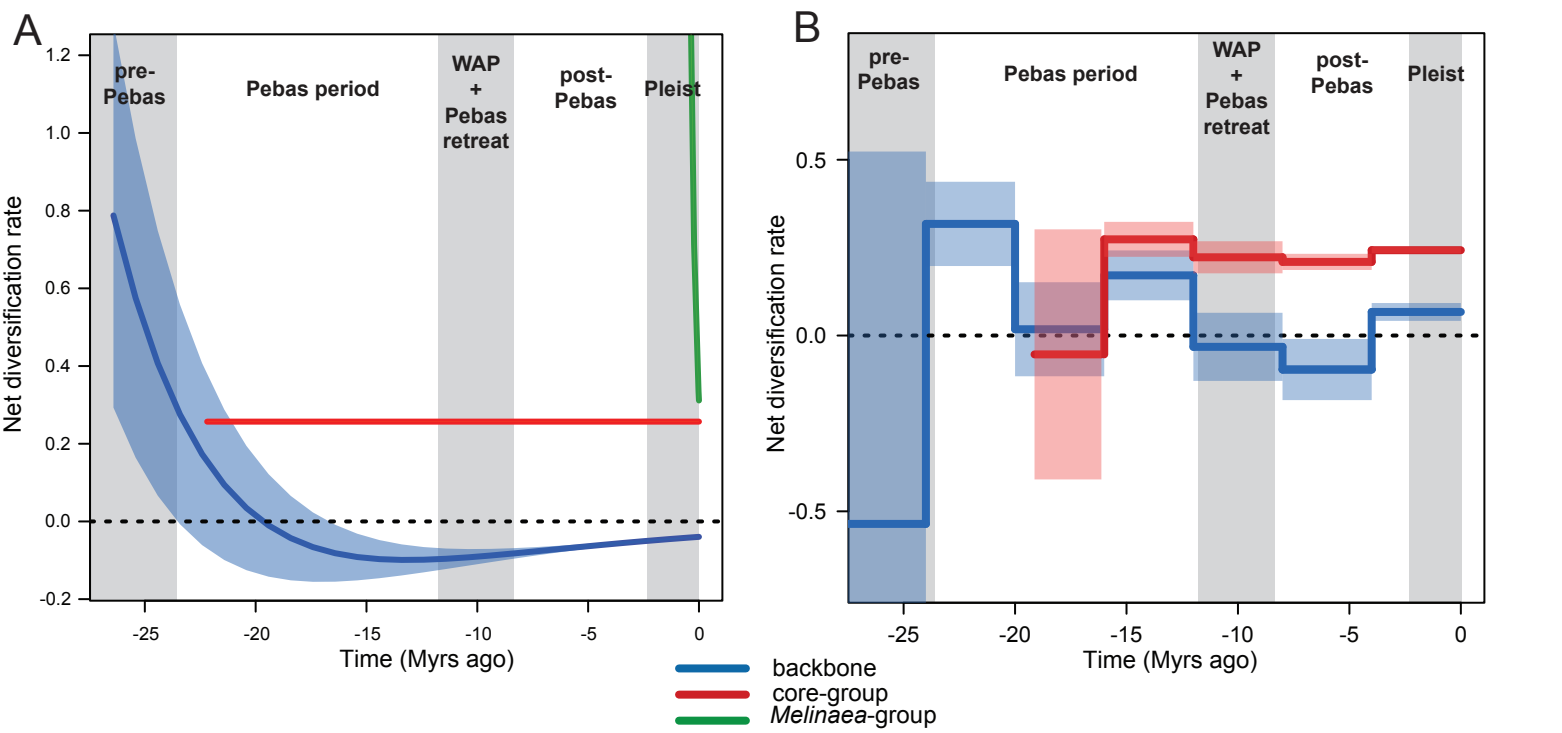
A
B
pre-
Pebas
Pebas period
WAP
+
Pebas
retreat
post-
Pebas
Pleist
Net diversification rate
Time (Myrs ago)
backbone
core-group
Melinaea-group

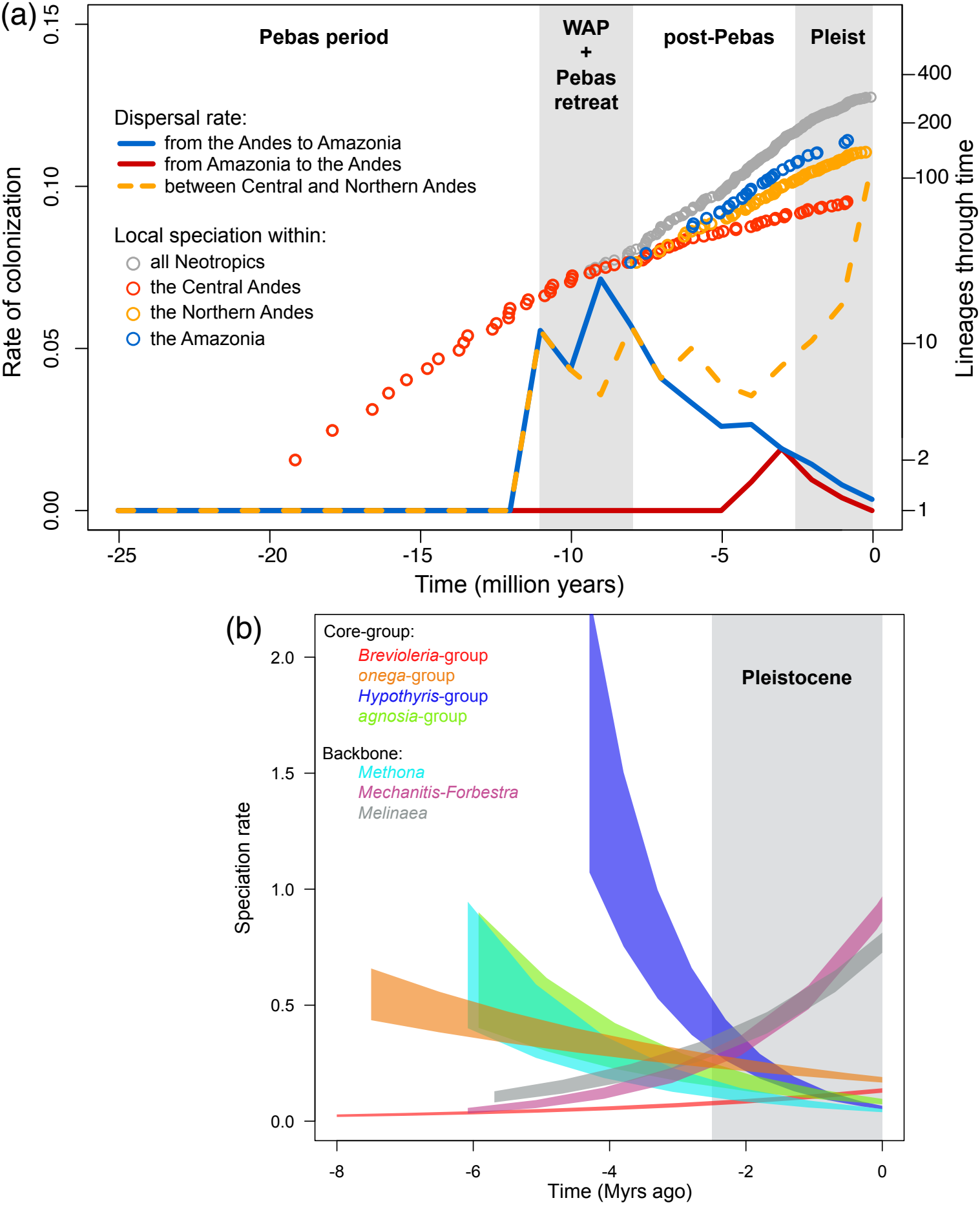
(a)
Pebas period
WAP + Pebas retreat
post-Pebas
Pleist
Dispersal rate:
from the Andes to Amazonia
from Amazonia to the Andes
between Central and Northern Andes
Local speciation within:
all Neotropics
the Central Andes
the Northern Andes
the Amazonia
Rate of colonization
0.00
0.05
0.10
0.15
Lineages through time
400
200
100
10
2
1
-25
-20
-15
-10
-5
0
Time (million years)
(b)
Core-group:
Brevioleria-group
onega-group
Hypothyris-group
agnosia-group
Backbone:
Methona
Mechanitis-Forbestra
Melinaea
Pleistocene
Speciation rate
2.0
1.5
1.0
0.5
0.0
-8
-6
-4
-2
0
Time (Myrs ago)

Appendix S2: Detailed methods and supplementary results for phylogenetic inferences

We generated a phylogeny under maximum likelihood inference (ML). We then enforced this topology to generate a time-calibrated tree under Bayesian inference, using secondary calibrations.

S2.1 Gene partitioning and substitution models

Prior to phylogenetic analyses, gene partitioning and substitution models were estimated using PartitionFinder v.1.1 (Lanfear et al. 2012). We divided all gene fragments into codon positions and allowed all partitions to be tested. Only substitution models available in BEAST were tested. The models of linked partitions had a better fit than unlinked partition schemes, hence the former was used. The best linked partition scheme contained 13 partitions (Table S2.1).

Table S2.1. Gene fragment partitions and substitution models associated obtained by Partition Finder v.1.1.

Gene fragment, codon position	Substitution models
COI codon 2	HKY+I+G
COII codon 3, COI codon 3	GTR+I+G
COII codon 1, COI codon 1, tRNA	GTR+I+G
COII codon 2	GTR+I+G
TKT codon 1, TKT codon 2	TrN+I+G
TKT codon 3	TrN+I+G
EFIα codon 3	SYM+I+G
EFIα codon 1, GAPDH codon 1	TrN+I+G
CAD codon 2, EFIα codon 2, GAPDH codon 2, MDH codon 2	GTR+I+G
CAD codon 3, MDH codon 3	HKY+I+G

CAD codon 1, MDH codon 1, RPS2 codon 1	GTR+I+G
GAPDH codon 3, RPS2 codon 3	GTR+I+G
RPS2 codon 3	K80+I

S2.2 Maximum likelihood inference (IQ-tree)

We generated a phylogeny under maximum likelihood inference (ML), using IQ-Tree software as implemented in the W-ID-TREE server (Trifinopoulos et al. 2016, Nguyen et al. 2014) (Figure S2.1). The dataset was partitioned according to the results above (Table S2.1), and substitution rates modelled using GTR+I+G. We also assessed node support using 1000 bootstrap replicates.

Figure S2.1. Maximum likelihood tree obtained with IQ-tree, with bootstrap support indicated at nodes.

Libythea_celtis_NW71_1
Libytheana_carinenta_NW162
Libytheana_terena
Amnosia_decora_NW101_1
Adelpha_bredowii_NW107_16
Cymothoe_caenis_NW102_16
Heliconius_hecale_NW70_6
Lachnoptera_anticlia_NW103_16
Terinos_atlita_NW134_9
Timelaea_albescens_NW97_8
Hypanartia_paullus
Melitaea_cinxia_NW73_14
Metamorpha_elissa_NW87_2
Cyrestis_thyodamas_NW100_11
Biblis_hyperia
Hamadryas_februa_NW62_3
Charaxes_castor_NW78_3
Consul_fabius_NW109_16
Morpho_peleides_NW66_5
Discophora_necho
Cithaerias_pireta
Melanitis_leda_EU141330
Heteronympha_merope
Lethe_minerva
Pronophila_thelebe
Lymanopoda_rana
Brintesia_circe
Calisto_obscura_DR005
Euptychoides_castrensis
Neonympha_aureolata_DNA96_019
Anetia_briarea_NW152_6
Lycorea_ilione_B_17_37
Lycorea_halia_NW122_19
Euploea_camaralzeman_NW70_8
Idea_leuconoe_NW84_14
Tirumala_limniace_NW156_9
Danaus_plexippus_NW108_21
Amauris_ellioti_NW86_5
Parantica_aspasia_NW112_8
Parantica_luzonensis_NW118_17
Tellervo_zoilus_QL5
Athyrtis_mechanitis
Eutresis_hypereia
Paititia_neglecta
Olyras_crathis
Olyras_insignis
Melinaea_mnasias
Melinaea_ludovica
Melinaea_ethra
Melinaea_marsaeus
Melinaea_idae
Melinaea_isocomma
Melinaea_lilis
Melinaea_mothone
Melinaea_mneme
Melinaea_menophilus
Melinaea_satevis
Thyridia_psidii
Sais_rosalia
Scada_karschina
Scada_reckia
Scada_zibia
Scada_kusa
Scada_zemira
Forbestra_equicola
Forbestra_olivencia
Forbestra_proceris
Mechanitis_menapis
Mechanitis_polymnia
Mechanitis_lysimnia
Mechanitis_messenoides
Mechanitis_mazaeus
Mechanitis_macrinus
Methona_curvifascia
Methona_grandior
Methona_maxima
Methona_singularis
Methona_themisto
Methona_confusa
Aeria_eurimedia
Aeria_olena
Elzunia_pavonii
Elzunia_humboldt
Tithorea_tarricina
Tithorea_harmonia
Tithorea_pacifica
Athesis_clearista
Athesis_acrisione
Patricia_dercyllidas
Patricia_demylus
Patricia_oligyrtis
Placidina_euryanassa
Pagyris_cymothoe
Pagyris_ulla
Pagyris_priscilla
Ithomia_terra_EAST
Ithomia_terra
Ithomia_jucunda
Ithomia_amarilla
Ithomia_arduinna
Ithomia_agnosia
Ithomia_drymo
Ithomia_pseudoagalla
Ithomia_lichyi
Ithomia_adelinda
Ithomia_xenos
Ithomia_avella
Ithomia_hymettia
Ithomia_praeithomia
Ithomia_eleonora
Ithomia_ellara
Ithomia_hyala
Ithomia_celemia
Ithomia_leila
Ithomia_heraldica
Ithomia_patilla
Ithomia_diasia
Ithomia_cleora
Ithomia_salapia
Ithomia_iphianassa
Epityches_eupompe
Aremfoxia_ferra
Napeogenes_larilla
Napeogenes_cranto
Napeogenes_flossina
Napeogenes_benigna
Napeogenes_sulphureophila
Napeogenes_sodalis
Napeogenes_harbona
Napeogenes_nsp3
Napeogenes_lycora
Napeogenes_verticilla
Napeogenes_zurippa
Napeogenes_larina
Napeogenes_aethra
Napeogenes_rhezia
Napeogenes_peridia
Napeogenes_nsp1
Napeogenes_glycera
Napeogenes_pharo
Napeogenes_tolosa
Napeogenes_duessa
Napeogenes_stella
Napeogenes_sylphis
Napeogenes_inachia
Napeogenes_gracilis
Napeogenes_apulia
Napeogenes_nsp2
Hypothyris_cantobrica
Hypothyris_moebiusi
Hyalyris_excelsa
Hyalyris_nsp2
Hypothyris_lycaste
Hypothyris_nsp
Hyalyris_ocna
Hyalyris_nsp1
Hyalyris_oulita
Hyalyris_antea
Hyalyris_juninensis
Hyalyris_coeno
Hyalyris_mestra
Hyalyris_latilimbata
Hyalyris_praxilla
Hypothyris_fluonia
Hyalyris_schlingeri
Hypothyris_daphnis
Hypothyris_semifulva
Hypothyris_thea
Hypothyris_anastasia
Hypothyris_mamercus
Hypothyris_mansuetus
Hypothyris_ninonia
Hypothyris_sp
Hypothyris_euclea
Megoleria_orestilla
Megoleria_susiana
Hyposcada_dujardini
Hyposcada_illinissa
Hyposcada_taliata
Hyposcada_zarepha
Hyposcada_anchiala
Hyposcada_schausi
Hyposcada_kena
Hyposcada_virginiana
Ollantaya_aegineta
Ollantaya_olerioides
Ollantaya_canilla
Oleria_sexmaculata
Oleria_similigena
Oleria_aquata
Oleria_assimilis
Oleria_tigilla
Oleria_antaxis
Oleria_flora
Oleria_agarista
Oleria_enania
Oleria_didymaea
Oleria_ilerdina
Oleria_onega
Oleria_quintina
Oleria_thiemei
Oleria_astrea
Oleria_aegle
Oleria_estella
Oleria_gunilla
Oleria_nsp
Oleria_zelica
Oleria_rubescens
Oleria_amalda
Oleria_paula
Oleria_deronda
Oleria_derondina
Oleria_vicina
Oleria_victorine
Oleria_boyeri
Oleria_quadrata
Oleria_phenomoe
Oleria_santineza
Oleria_fumata
Oleria_baizana
Oleria_radina
Oleria_athalina
Oleria_fasciata
Oleria_bioculata
Oleria_cyrene
Oleria_attalia
Oleria_tremona
Oleria_makrena
Oleria_padilla
Velamysta_peninna
Velamysta_nsp1
Velamysta_pupilla
Velamysta_phengites
Veladyris_pardalis
Veladyris_electrea
Veladyris_cytharista
Genus1_nsp1
Godyris_dircenna
Godyris_kedema
Godyris_nero
Godyris_zavaleta
Godyris_panthyale
Godyris_crinippa
Godyris_hewitsoni
Godyris_lauta
Godyris_duillia
Godyris_sappho
Heterosais_giulia
Heterosais_nephele
Heterosais_edessa
Hypoleria_lavinia
Hypoleria_alema
Hypoleria_xenophis
Hypoleria_sarepta
Mcclungia_cymo
Hypoleria_aureliana
Hypoleria_ocalea
Brevioleria_nsp1
Brevioleria_coenina
Brevioleria_seba
Hypoleria_adasa
Pachacutia_baroni
Pachacutia_mantura
Brevioleria_arzalia
Brevioleria_plisthenes
Brevioleria_aelia
Genus2_annette
Genus2_andromica
Pseudoscada_erruca
Pseudoscada_florula
Pseudoscada_timna_WESTERN
Pseudoscada_timna_COSTARICA
Pseudoscada_acilla
Pseudoscada_timna_EASTERN
Greta_clavijoi
Greta_diaphanus
Greta_morgane
Hypomenitis_libethris
Hypomenitis_theudelinda
Hypomenitis_polissena
Hypomenitis_nspC
Hypomenitis_nspA
Hypomenitis_alphesiboea
Hypomenitis_enigma
Hypomenitis_esula
Hypomenitis_hermana
Hypomenitis_ortygia
Hypomenitis_nspD
Hypomenitis_depauperata
Hypomenitis_lojana
Hypomenitis_gardneri
Hypomenitis_ochretis
Hypomenitis_lydia
Hypomenitis_nspE
Hypomenitis_dercetis
Hypomenitis_nspB
Hypomenitis_oneidodes
Callithomia_hezia
Callithomia_lenea
Callithomia_alexirrhoe
Dircenna_dero
Dircenna_loreta
Dircenna_klugii
Dircenna_olyras
Dircenna_jemina
Dircenna_adina
Hyalenna_paradoxa
Hyalenna_perasippa
Hyalenna_buckleyi
Hyalenna_pascua
Hyalenna_alidella
Hyalenna_sulmona
Haenschia_sidonia
Haenschia_derama
Ceratinia_neso
Episcada_hemixanthe
Episcada_nsp1
Ceratinia_tutia
Ceratinia_iolaia
Episcada_doto
Episcada_philoclea
Episcada_vitrea
Episcada_hymenaea
Episcada_hymen
Episcada_sulphurea
Episcada_nsp2
Episcada_apuleia
Episcada_sicelella
Episcada_trapezula
Episcada_mira
Episcada_polita
Episcada_salvinia
Episcada_sylvo
Episcada_clausina
Episcada_striposis
Pteronymia_obscuratus
Pteronymia_sao
Pteronymia_donella
Pteronymia_forsteri
Pteronymia_hara
Pteronymia_olimba
Pteronymia_artena
Pteronymia_granica
Pteronymia_serrata
Pteronymia_alida
Pteronymia_nsp3
Pteronymia_inania
Pteronymia_thabena
Pteronymia_ionera
Pteronymia_teresita
Pteronymia_dispar
Pteronymia_carlia
Pteronymia_euritea
Pteronymia_nsp1
Pteronymia_medellina
Pteronymia_aletta
Pteronymia_parva
Pteronymia_vestilla
Pteronymia_primula
Pteronymia_cotytto
Pteronymia_rufocincta
Pteronymia_andreas
Pteronymia_sexpunctata
Pteronymia_laura
Pteronymia_alissa
Pteronymia_gertschi
Pteronymia_simplex
Pteronymia_picta
Pteronymia_asopo
Pteronymia_latilla
Pteronymia_tucuna
Pteronymia_ticida
Pteronymia_veia_WEST
Pteronymia_alina
Pteronymia_ozia
Pteronymia_nsp2
Pteronymia_oneida
Pteronymia_fulvimargo
Pteronymia_zerlina
Pteronymia_tamina
Pteronymia_veia_EAST
0.09

S2.3 Bayesian inferences and time-calibration

The tree was time-calibrated using BEAST v.1.8.2 (Drummond et al. 2012) with a birth-death tree prior and an uncorrelated lognormal relaxed clock for each gene partition (using gene partition and substitution models of Table S2.1), and a topology fixed to that of the ML tree. We applied a combination of secondary calibrations and host-plant calibrations (Table S2.2). Four secondary calibration points were retrieved from Wahlberg *et al.* (2009)'s phylogeny of Nymphalidae genera and were placed only outside of Ithomiini. We used uniform distribution priors, corresponding to the 95% HSPD inferred by Wahlberg *et al.* (2009). Host-plant calibrations were used as constraints only within the Ithomiini. Almost all Ithomiini species feed on Solanaceae with a relatively high specificity. A phylogeny of the Solanaceae was published by Särkinen *et al.* (2013), and recalibrated by De-Silva *et al.* (2017). We identified six relevant Solanaceae hostplant clades, which were used as maximum age constraints. Priors for host-plant calibration followed a uniform distribution. The minimum value of the uniform was 0 (present). The maximum value was the upper boundary of the 95% HSPD of the stem age of the host-plant subclade on which the calibrated Ithomiini lineage feeds as estimated in de-Silva et al. (2017). To get a starting tree suitable for time-calibration priors, the ML tree was made ultrametric and rescaled using PATHD8 (Britton et al. 2007) and Mesquite v.3.2 (Maddison & Maddison 2001).

We performed two independent runs of BEAST v.1.8.2 (Drummond et al. 2012) on the CIPRES server (Miller et al. 2010) of 87 million generations, sampling every 10000. Using Tracer v.1.6 we checked that the two runs had converged and the parameter's ESS values. Both runs were combined using Logcombiner v.1.8.3 (Drummond et al. 2012), applying a 15% burn-in for each run. Finally using TreeAnnotator v.1.8.3 (Drummond et al. 2012) we extracted the median branch lengths and credibility interval from the posterior distribution (Figure S2.2). The outgroups were pruned and the remaining tree was used for the following analyses (hereafter, median tree). Phylogenetic analyses with different settings (unconstrained topology in BEAST, Yule tree model or a different number of molecular clocks) produced similar topology and branch lengths (data not shown).

Table S2.2. Node constraints used for time-calibration of the tree. When node constraints were based on host-plant age the corresponding host-plant group is indicated (from de-Silva et al. 2017). The remaining constraints are secondary calibrations from Wahlberg et al. 2009.

node constrained	upper bound	lower bound	host-plant group
Ollantaya + *Oleria*	0	32	*Lycianthes*
Melinaeina	0	37.2	*Schultesianthus*
Methonina	0	41.3	*Brunfelsia*
Athesitina	0	24.8	*Capsicum*
Placidina + *Pagyris*	0	17.3	*Brugmansia*
Ithomiini	0	54.9	Solanaceae
Tellerviini + Ithomiini	39.5	52	
Anetia + *Lycora* + *Ituna*	11	21.5	
Amauris + *Danaus* + *Parantica*	24.5	35	
Danaini	35	48	

Figure S2.2. Bayesian time-calibrated tree obtained with Beast v.1.8.3 (Drummond et al. 2012) with median node ages and 95%HPD indicated at nodes.


Libythea_celtis_NW71_1
Libythea_carinenta_NW162
Libytheana_terena
Amnosia_decora_NW101_1
Adelpha_bredowii_NW107_16
Cymothoe_caenis_NW102_16
Heliconius_hecale_NW70_6
Lachnoptera_anticlia_NW103_16
Terinos_atlita_NW134_9
Timelaea_albescens_NW97_8
Hypanartia_paullus
Melitaea_cinxia_NW73_14
Metamorpha_elissa_NW87_2
Cyrestis_thyodamas_NW100_11
Biblis_hyperia
Hamadryas_februa_NW62_3
Charaxes_castor_NW78_3
Consul_fabius_NW109_16
Morpho_peleides_NW66_5
Discophora_necho
Cithaerias_pireta
Melanitis_leda_EU141330
Heteronympha_merope
Lethe_minerva
Pronophila_thelebe
Lymanopoda_rana
Brintesia_circe
Calisto_obscura_DR005
Euptychoides_castrensis
Neonympha_areolata_DNA96_019
Anetia_briarea_NW152_6
Lycorea_ilione_B_17_37
Lycorea_halia_NW122_19
Euploea_camaralzeman_NW70_8
Idea_leuconoe_NW84_14
Tirumala_limniace_NW156_9
Danaus_plexippus_NW108_21
Amauris_ellioti_NW86_5
Parantica_aspasia_NW112_8
Parantica_luzonensis_NW118_17
Tellervo_zoilus_QL5
Athyrtis_mechanitis
Eutresis_hypereia
Paititia_neglecta
Olyras_crathis
Olyras_insignis
Melinaea_mnasias
Melinaea_ludovica
Melinaea_ethra
Melinaea_marsaeus
Melinaea_idae
Melinaea_isocomma
Melinaea_lilis
Melinaea_mothone
Melinaea_mneme
Melinaea_menophilus
Melinaea_satevis
Thyridia_psidii
Sais_rosalia
Scada_karschina
Scada_reckia
Scada_zibia
Scada_kusa
Scada_zemira
Forbestra_equicola
Forbestra_olivencia
Forbestra_proceris
Mechanitis_menapis
Mechanitis_polymnia
Mechanitis_lysimnia
Mechanitis_messenoides
Mechanitis_mazaeus
Mechanitis_macrinus
Methona_curvifascia
Methona_grandior
Methona_maxima
Methona_singularis
Methona_themisto
Methona_confusa
Aeria_eurimedia
Aeria_olena
Elzunia_pavonii
Elzunia_humboldti
Tithorea_tarricina
Tithorea_harmonia
Tithorea_pacifica
Athesis_clearista
Athesis_acrisione
Patricia_dercyllidas
Patricia_demylus
Patricia_oligyrtis
Placidina_euryanassa
Pagyris_cymothoe
Pagyris_ulla
Pagyris_priscilla
Ithomia_terra_EAST
Ithomia_terra
Ithomia_jucunda
Ithomia_amarilla
Ithomia_arduinna
Ithomia_agnosia
Ithomia_drymo
Ithomia_pseudoagalla
Ithomia_lichyi
Ithomia_adelinda
Ithomia_xenos
Ithomia_avella
Ithomia_hymettia
Ithomia_praeithomia
Ithomia_eleonora
Ithomia_ellara
Ithomia_hyala
Ithomia_celemia
Ithomia_leila
Ithomia_heraldica
Ithomia_patilla
Ithomia_diasia
Ithomia_cleora
Ithomia_salapia
Ithomia_iphianassa
Epityches_eupompe
Aremfoxia_ferra
Napeogenes_larilla
Napeogenes_cranto
Napeogenes_flossina
Napeogenes_benigna
Napeogenes_sulphureophila
Napeogenes_sodalis
Napeogenes_harbona
Napeogenes_nsp3
Napeogenes_lycora
Napeogenes_verticilla
Napeogenes_zurippa
Napeogenes_larina
Napeogenes_aethra
Napeogenes_rhezia
Napeogenes_peridia
Napeogenes_nsp1
Napeogenes_glycera
Napeogenes_pharo
Napeogenes_tolosa
Napeogenes_duessa
Napeogenes_stella
Napeogenes_sylphis
Napeogenes_inachia
Napeogenes_gracilis
Napeogenes_apulia
Napeogenes_nsp2
Hypothyris_cantobrica
Hypothyris_moebiusi
Hyalyris_excelsa
Hyalyris_nsp2
Hypothyris_lycaste
Hypothyris_nsp
Hyalyris_ocna
Hyalyris_nsp1
Hyalyris_oulita
Hyalyris_antea
Hyalyris_juninensis
Hyalyris_coeno
Hyalyris_mestra
Hyalyris_latilimbata
Hyalyris_praxilla
Hypothyris_fluonia
Hyalyris_schlingeri
Hypothyris_daphnis
Hypothyris_semifulva
Hypothyris_thea
Hypothyris_anastasia
Hypothyris_mamercus
Hypothyris_mansuetus
Hypothyris_ninonia
Hypothyris_sp
Hypothyris_euclea
Megoleria_orestilla
Megoleria_susiana
Hyposcada_dujardini
Hyposcada_illinissa
Hyposcada_taliata
Hyposcada_zarepha
Hyposcada_anchiala
Hyposcada_schausi
Hyposcada_kena
Hyposcada_virginiana
Ollantaya_aegineta
Ollantaya_olerioides
Ollantaya_canilla
Oleria_sexmaculata
Oleria_similigena
Oleria_aquata
Oleria_assimilis
Oleria_tigilla
Oleria_antaxis
Oleria_flora
Oleria_agarista
Oleria_enania
Oleria_didymaea
Oleria_ilerdina
Oleria_onega
Oleria_quintina
Oleria_thiemei
Oleria_astrea
Oleria_aegle
Oleria_estella
Oleria_gunilla
Oleria_nsp
Oleria_zelica
Oleria_rubescens
Oleria_amalda
Oleria_paula
Oleria_deronda
Oleria_derondina
Oleria_vicina
Oleria_victorine
Oleria_boyeri
Oleria_quadrata
Oleria_phenomoe
Oleria_santineza
Oleria_fumata
Oleria_baizana
Oleria_radina
Oleria_athalina
Oleria_fasciata
Oleria_bioculata
Oleria_cyrene
Oleria_attalia
Oleria_tremona
Oleria_makrena
Oleria_padilla
Velamysta_peninna
Velamysta_nsp1
Velamysta_pupilla
Velamysta_phengites
Veladyris_pardalis
Veladyris_electrea
Veladyris_cytharista
Genus1_nsp1
Godyris_dircenna
Godyris_kedema
Godyris_nero
Godyris_zavaleta
Godyris_panthyale
Godyris_crinippa
Godyris_hewitsoni
Godyris_lauta
Godyris_duillia
Godyris_sappho
Heterosais_giulia
Heterosais_nephele
Heterosais_edessa
Hypoleria_lavinia
Hypoleria_alema
Hypoleria_xenophis
Hypoleria_sarepta
Mcclungia_cymo
Hypoleria_aureliana
Hypoleria_ocalea
Brevioleria_nsp1
Brevioleria_coenina
Brevioleria_seba
Hypoleria_adasa
Pachacutia_baroni
Pachacutia_mantura
Brevioleria_arzalia
Brevioleria_plisthenes
Brevioleria_aelia
Genus2_annette
Genus2_andromica
Pseudoscada_erruca
Pseudoscada_florula
Pseudoscada_timna_WESTERN
Pseudoscada_timna_COSTARICA
Pseudoscada_acilla
Pseudoscada_timna_EASTERN
Greta_clavijoi
Greta_diaphanus
Greta_morgane
Hypomenitis_libethris
Hypomenitis_theudelinda
Hypomenitis_polyxsena
Hypomenitis_nspC
Hypomenitis_nspA
Hypomenitis_alphesiboea
Hypomenitis_enigma
Hypomenitis_esula
Hypomenitis_hermana
Hypomenitis_ortygia
Hypomenitis_nspD
Hypomenitis_depauperata
Hypomenitis_lojana
Hypomenitis_gardneri
Hypomenitis_ochretis
Hypomenitis_nspE
Hypomenitis_lydia
Hypomenitis_dercetis
Hypomenitis_nspB
Hypomenitis_oneidodes
Callithomia_hezia
Callithomia_lenea
Callithomia_alexirrhoe
Dircenna_dero
Dircenna_loreta
Dircenna_klugii
Dircenna_olyras
Dircenna_jemina
Dircenna_adina
Hyalenna_paradoxa
Hyalenna_perasippa
Hyalenna_buckleyi
Hyalenna_pascua
Hyalenna_alidella
Hyalenna_sulmona
Haenschia_sidonia
Haenschia_derama
Ceratinia_neso
Episcada_hemixanthe
Episcada_nsp1
Ceratinia_tutia
Ceratinia_iolaia
Episcada_doto
Episcada_philoclea
Episcada_vitrea
Episcada_hymenaea
Episcada_hymen
Episcada_sulphurea
Episcada_nsp2
Episcada_apuleia
Episcada_sicidella
Episcada_trapezula
Episcada_mira
Episcada_polita
Episcada_salvinia
Episcada_sylvo
Episcada_clausina
Episcada_striposis
Pteronymia_obscuratus
Pteronymia_sao
Pteronymia_donella
Pteronymia_forsteri
Pteronymia_hara
Pteronymia_olimba
Pteronymia_artena
Pteronymia_granica
Pteronymia_serrata
Pteronymia_alida
Pteronymia_nsp3
Pteronymia_inania
Pteronymia_thabena
Pteronymia_lonera
Pteronymia_teresita
Pteronymia_dispar
Pteronymia_carlia
Pteronymia_euritea
Pteronymia_nsp1
Pteronymia_medellina
Pteronymia_aletta
Pteronymia_parva
Pteronymia_vestilla
Pteronymia_primula
Pteronymia_cotytto
Pteronymia_rufocincta
Pteronymia_andreas
Pteronymia_sexpunctata
Pteronymia_laura
Pteronymia_alissa
Pteronymia_gertschi
Pteronymia_simplex
Pteronymia_picta
Pteronymia_asopo
Pteronymia_latilla
Pteronymia_tucuna
Pteronymia_ticida
Pteronymia_veia_WEST
Pteronymia_alina
Pteronymia_ozia
Pteronymia_nsp2
Pteronymia_oneida
Pteronymia_fulvimargo
Pteronymia_zerlina
Pteronymia_tamina
Pteronymia_veia_EAST
8.0

References

Britton T, Anderson CL, Jacquet D, Lundqvist S, & Bremer K. (2007). Estimating divergence times in large phylogenetic trees. *Systematic Biology*, 56, 741-752.

De-Silva DL, Mota LL, Chazot N, Mallarino R, Silva-Brandão KL, Piñerez LMG, Freitas AVL, Lamas G, Joron M, Mallet J, Giraldo CE, & Elias M. (2017). North Andean origin and diversification of the largest ithomiine butterfly genus. *Scientific Reports*, 7(45966), 1-17.

Drummond AJ, Suchard MA, Xie D, Rambaut A. (2012). Bayesian phylogenetics with BEAUti and the BEAST 1.7. *Molecular biology and evolution* 29, 1969-1973.

Lanfear R, Calcott B, Ho SY, Guindon S. (2012). PartitionFinder: combined selection of partitioning schemes and substitution models for phylogenetic analyses. *Molecular biology and evolution* 29, 1695-1701.

Maddison WP, & Maddison DR. (2001). Mesquite: a modular system for evolutionary analysis.

Miller MA, Pfeiffer W, & Schwartz T. (2010). Creating the CIPRES Science Gateway for inference of large phylogenetic trees. In *Gateway Computing Environments Workshop* (GCE), 2010 (pp. 1-8).

Nguyen L-T, Schmidt HA, von Haeseler A, Minh BQ. (2015). IQ-TREE: a fast and effective stochastic algorithm for estimating maximum-likelihood phylogenies. *Molecular biology and evolution* 32, 268-274.

Särkinen T, Bohs L, Olmstead RG, & Knapp S. (2013). A phylogenetic framework for evolutionary study of the nightshades (Solanaceae): a dated 1000-tip tree. *BMC Evolutionary Biology*, 13, 214.

Trifinopoulos J, Nguyen L-T, von Haeseler A, & Minh BQ. (2016). W-IQ-TREE: a fast online phylogenetic tool for maximum likelihood analysis. *Nucleic Acids Research*, 44(W1):W232-5.

Wahlberg N, Leneveu J, Kodandaramaiah U, Peña C, Nylin S, Freitas AVL, & Brower AV. (2009). Nymphalid butterflies diversify following near demise at the Cretaceous/Tertiary boundary. *Proceedings of the Royal Society of London B: Biological Sciences*, 276(1677), 4295-4302.

Appendix S3: Detailed methods and supplementary results for diversification analyses

Diversification rates

S3.1 Time

S3.1.1 Detection of shifts in diversification process using MEDUSA

We investigated the dynamics of speciation and extinction rates through time and across the phylogeny using two different birth-death models: (1) Morlon et al.'s (2011) method allowing both speciation and extinction rates to vary as a function of time, and allowing extinction to be higher than speciation, (2) TreePar (Stadler 2011) which accommodates models where diversification rates can vary at points in time but are constant between these points. None of these methods however, can automatically detect the number and position of different diversification processes. Hence, we first ran MEDUSA (Alfaro et al. 2009) on the whole median tree in order to partition the tree into different diversification processes. MEDUSA automatically identifies the number and the position of different diversification processes, yet making the strong assumption that speciation and extinction rates are constant through time. MEDUSA detected two shifts from the background diversification rates (Table S3.3): 1) one shift at the root of a large clade hereafter referred to as the core-group, and 2) one shift at the root of a subclade of the genus *Melinaea* that, for simplicity, is referred to as the *Melinaea*-group. The remaining lineages are collectively referred to as the backbone.

Table S3.3 Results of MEDUSA fitted on the whole tree. *r* represents the diversification rates inferred by MEDUSA (not considered in our study).

Steps	position	logL	AICc	Model	r
Step1	root	-863.89	1731.81	bd	0.114
Step2	Core-group	-854.99	1720.08	bd	0.236
Step3	Melinaea-group	-846.45	1709.12	bd	1.245

S3.1.2 Fit of Morlon et al. (2011)'s diversification models

Morlon et al. (2011)'s models were fitted on the core-group, the *Melinaea*-group and the backbone. For each partition, the models were fitted on 100 trees randomly sampled from BEAST's posterior distribution. In each case the stem branch of the shifting clade was included in the subclade, as designed in the method (Morlon et al. 2011), but we excluded the stem branch (root) of the backbone. For each partition we fitted the following models: constant

speciation (no extinction), time-dependent speciation (no extinction), constant speciation and extinction, time-dependent speciation and constant extinction, constant speciation and time-dependent extinction, time-dependent speciation and extinction. In the cases of time-dependent rates we fitted an exponential dependence to time. Sampling fraction was specified for each of the three partitions. All models were compared using AIC scores. The model with the lowest AIC score that was significantly different from the null model of constant speciation rate was used to plot the diversification rate through time. Detailed results are shown in Table S3.4.

Table S3.4 Full results of time-dependent diversification models using Morlon et al (2011)'s method fitted on 100 posterior trees partitioned into the backbone, the coregroup and the *Melinaea*-group, and ranked by increasing mean AIC score. BCST=constant speciation, BVAR=time-dependent speciation, DCST=constant extinction, DVAR time-dependent extinction. λ =speciation rate at present, α=coefficient of time variation of the speciation rate, μ =extinction rate at present, ß =coefficient of time variation of the extinction rate. Models used and discussed in the manuscript are highlighted in bold.

a. Backbone excluding the core-group and the *Melinaea*-group. Mean values from 100 posterior trees.

Model	Parameters	logL	AIC	λ	α	μ	ß
BVARDVAR	**4**	**-129.75**	**267.50**	**0.153**	**0.160**	**0.193**	**0.148**
BVARDCST	3	-131.84	269.68	0.201	0.041	0.264	NA
BCST	1	-134.20	270.40	0.121	NA	NA	NA
BCSTDCST	2	-133.60	271.21	0.162	NA	0.072	NA
BCSTDVAR	3	-132.98	271.95	0.212	NA	0.245	-0.072
BVAR	2	-134.18	272.36	0.124	-0.002	NA	NA

b. Backbone excluding the core-group and the *Melinaea*-group. Standard deviations from 100 posterior trees.

Model	Parameters	logL	AIC	λ	α	μ	ß
BVARDVAR	**4**	**0.30**	**0.61**	**0.0017**	**0.0020**	**0.0023**	**0.0019**
BVARDCST	3	0.30	0.59	0.0020	0.0005	0.0037	NA
BCST	1	0.29	0.58	0.0008	NA	NA	NA
BCSTDCST	2	0.30	0.59	0.0015	NA	0.0016	NA
BCSTDVAR	3	0.30	0.59	0.0024	NA	0.0054	0.0012
BVAR	2	0.29	0.58	0.0010	0.0005	NA	NA

c. Core-group. Mean values from 100 posterior trees.

Model	Parameters	logL	AIC	λ	α	μ	ß
BVAR	2	-700.38	1404.77	0.229	0.030	NA	NA
BCST	**1**	**-702.25**	**1406.50**	**0.257**	**NA**	**NA**	**NA**
BVARDCST	3	-700.38	1406.77	0.229	0.030	1.37E-07	NA
BCSTDCST	2	-702.25	1408.50	0.257	NA	1.80E-07	NA

BVARDVAR	4	-700.38	1408.77	0.229	0.030	8.88E-08	0.036
BCSTDVAR	3	-702.25	1410.50	0.257	NA	8.74E-08	0.015

d. Core-group. Standard deviations from 100 posterior trees.

Model	Parameters	logL	AIC	λ	α	μ	ß
BVAR	2	1.91	3.83	0.0016	0.0006	NA	NA
BCST	**1**	**1.92**	**3.84**	**0.0017**	**NA**	**NA**	**NA**
BVARDCST	3	1.91	3.83	0.0016	0.0006	1.38E-08	NA
BCSTDCST	2	1.92	3.84	0.0017	NA	3.01E-08	NA
BVARDVAR	4	1.91	3.83	0.0016	0.0006	7.06E-09	0.0008
BCSTDVAR	3	1.92	3.84	0.0017	NA	1.13E-08	0.0007

e. *Melinaea*-group. Mean values from 100 posterior trees.

Model	Parameters	logL	AIC	λ	α	μ	ß
BVAR	**2**	**-1.58**	**7.17**	**0.311**	**3.772**	**NA**	**NA**
BVARDCST	3	-1.55	9.10	0.375	3.838	0.488	NA
BCST	1	-4.31	10.62	1.526	NA	NA	NA
BVARDVAR	4	-1.40	10.80	0.301	4.823	1.793	-3.804
BCSTDCST	2	-4.31	12.62	1.527	NA	1.27E-07	NA
BCSTDVAR	3	-4.29	14.58	1.633	NA	12.613	-5.569

f. *Melinaea*-group. Standard deviations from 100 posterior trees.

Model	Parameters	logL	AIC	λ	α	μ	ß
BVAR	**2**	**0.18**	**0.35**	**0.023**	**0.191**	**NA**	**NA**
BVARDCST	3	0.17	0.35	0.037	0.185	0.117	NA
BCST	1	0.10	0.19	0.024	NA	NA	NA
BVARDVAR	4	0.17	0.34	0.030	0.229	1.505	5.366
BCSTDCST	2	0.10	0.19	0.024	NA	2.53E-08	NA
BCSTDVAR	3	0.10	0.19	0.056	NA	12.144	5.296

S3.1.3 Fit of TreePar diversification models

We performed TreePar (Stadler 2011) analyses on the core-group and the backbone. For each case we used 100 trees randomly sampled from BEAST's posterior distribution. For the backbone we included the times of divergence at which the core-group and the *Melinaea*-group diverged from the backbone to keep track of these cladogenetic events. We split time into time bins of four million years, for which diversification rates was estimated. We used these estimates to obtain a second estimate of diversification rate "through time". We did not fit TreePar on the *Melinaea*-group since it is only 1 million years old. We allowed diversification

rate to be negative but we did not allow mass-extinction events. Results are shown in the manuscript (Figure 2).

S3.1.4 Fit of BAMM diversification models

We compared our estimates of diversification dynamics obtained with MEDUSA, Morlon et al. 2011 and TreePar with results obtained from BAMM (Rabosky et al. 2014) We ran BAMM v.2.5.0 on the whole tree of Ithomiini. We did not specify a global sampling fraction. Instead, we used a refined sampling fraction at the genus level. We ran BAMM for 30 million generations sampling every 3000 generations. The results of the MCMC were then analyzed in the R package BAMMTOOLS (Rabosky et al. 2014). First, we checked for MCMC convergence using trace plots and ESS statistics using the R package CODA, after removing 10% of the chain as burnin. Second, we investigated the number and configurations of diversification rate shifts. We report here the set of credible shifts.

The results of BAMM are congruent with our other estimates, supporting a diversification rate shift at the root of the coregroup, pointing at an increasing rate of diversification compared to the background dynamics. The configuration with two shifts of diversification rate corresponding to the partitioning analyzed in the manuscript (i.e. rate shifts at the root of the coregroup and the *Melinaea*-group) was recovered as the third most frequently sampled configuration but with the lowest support (~10%) after a configuration with no rate shift (19%) (Figure S3.3).

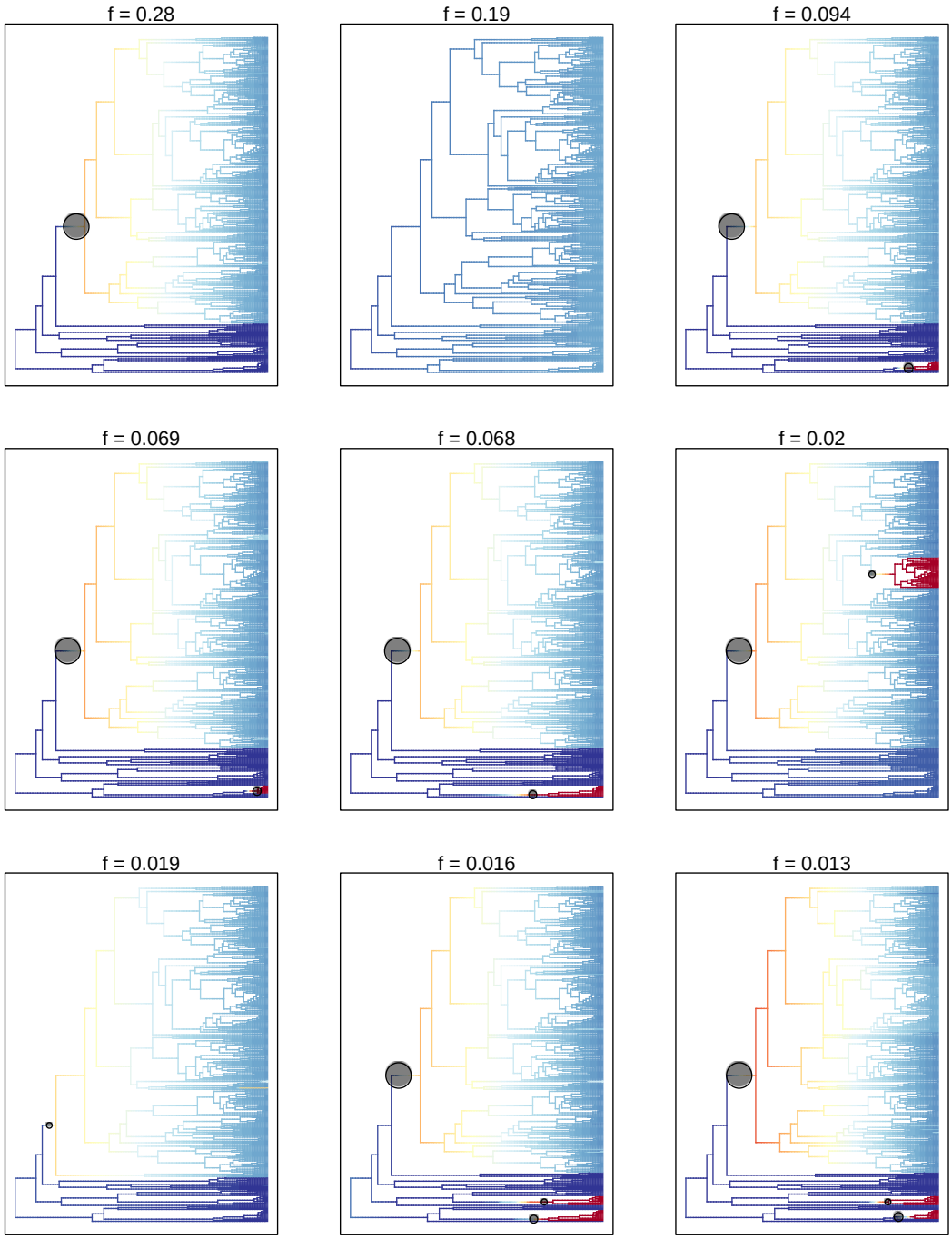

Figure S3.3 Set of credible shift configurations from the analysis performed with BAMM v.2.5.0. Branches are colored according to the diversification rate, the positions of shifts are also indicated and the frequency at which each configuration was recovered across the posterior distribution is indicated above each tree.

S3.1.5 Testing the effect of diversification rate heterogeneity among backbone lineages on diversification rate estimates.

The best fitting time-dependent model of diversification from Morlon et al. (2011) inferred a negative net diversification rate, indicating a declining diversity. We performed further tests to assess the robustness of this inference to (1) the parameters chosen for the initiating the maximum likelihood search and (2) the heterogeneity of diversification rate remaining in the backbone as defined by MEDUSA (Alfaro et al. 2009).

For the time-dependent diversification models (Morlon et al. 2011), maximum likelihood searches consistently converged toward similar parameter estimates over a range of initial parameters (results not shown). The LTT plots of the backbone tree as defined by MEDUSA (i.e excluding the *Melinaea*-group) shows a recent burst of diversification during the last 5 million years. This could be due to a global recent increase of diversification rate but also to specific subclades driven by different diversification processes from that of the remaining backbone. This may influence the selection of the best model and parameter estimations. Thus, we fitted additional models of time-dependent speciation and extinction rates on different backbones for which we removed additional subclades. Time-dependent models were also fitted on these subclades.

First, we sequentially removed the *Melinaea*-group (MEDUSA partition, results discussed in the main document), the genus *Mechanitis*, the genus *Methona* and the genus *Scada* (Figure S3.4 A). We fitted time-dependent diversification models for each of these subclades. Removing these clades reduced the final burst of diversification observed on the LTT plots but the diversification rates inferred for the backbone were only slightly affected (Figure S3.4 A & B). It slightly pushed the extinction signal backward in time and tended to infer an earlier recovery, although the differences are small. Hence, the results described in the paper are not affected by potential rate heterogeneity remaining in the backbone.

Although the timing of the divergence between shifting subclades and the backbone was recorded in the analyses performed on the backbone, the stem branches of those subclades were excluded from the backbone (this is the way the method was designed). Yet, some of those stem branches are long, especially for the *Methona* and *Scada*, and likely bear a signal of association that may have better fitted with the backbone.

Time-dependent diversification models were also fitted on the *Melinaea*-group, and the genera *Mechanitis*, *Methona* and *Scada*, following the procedure described the Method section except that we excluded the stem branches of these subclades. As explained above, some stem branches are very long and should likely be under the background process (but this cannot be

done). Results show that these four subclades all have positive net diversification rate (constant speciation rate model was always the best fitting model, Figure S3.4 C). This strengthens the observation that the lineages in the backbone suffered from high extinction, which was at its maximum around 15 my ago, but have since then started recovering, with a diversification rate generally increasing and several subclades showing positive diversification during the last 5 my.

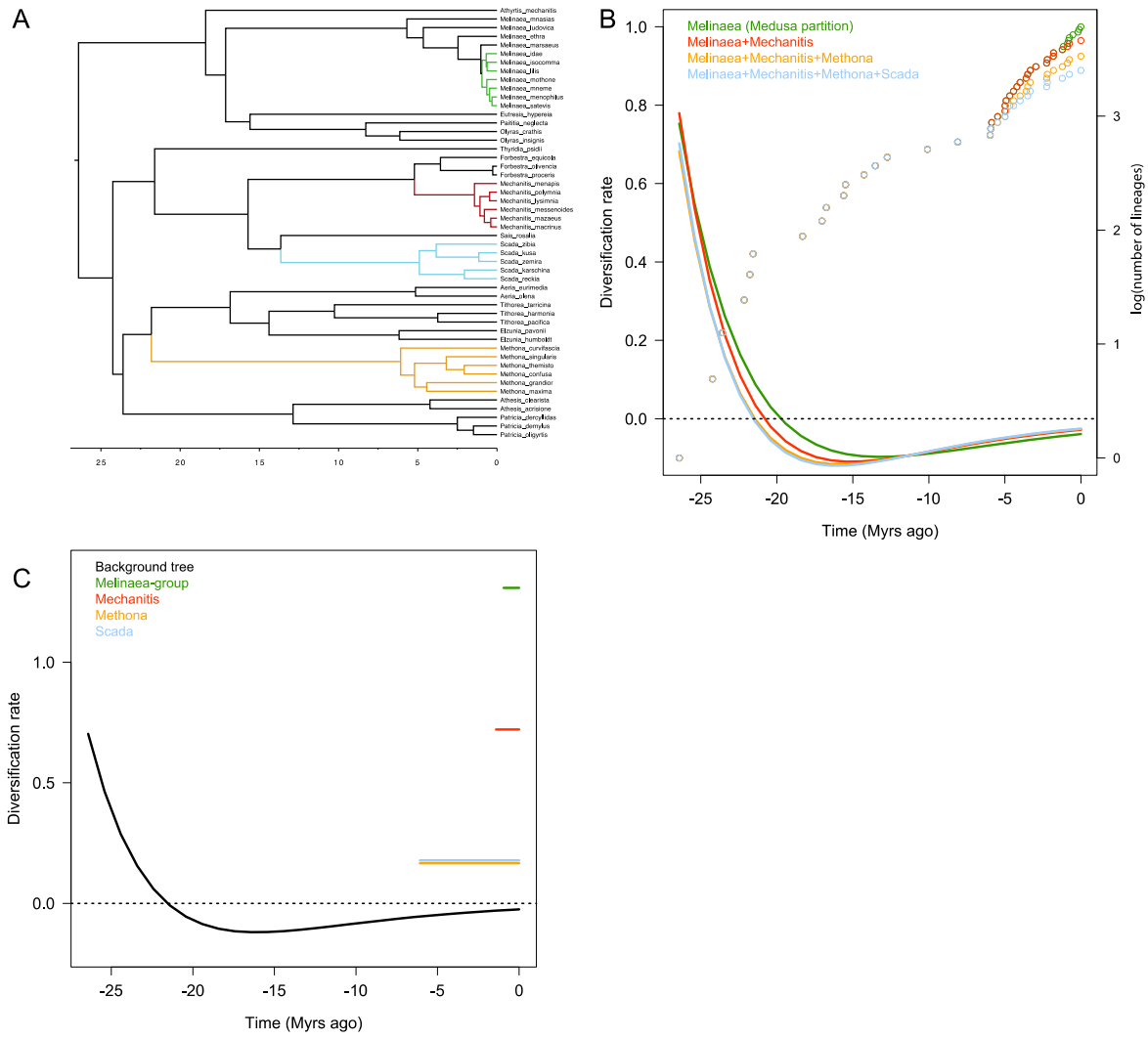

Figure S3.4 The effect of diversification rate heterogeneity among backbone lineages on diversification rate estimates using Morlon et al. (2011) on the median tree. A. the backbone, after the core-group has been removed. Colored subclades indicate the subclades that were sequentially removed from this backbone. B. Diversification rates of the different backbones estimated with Morlon et al. (2011)'s method (solid lines) and corresponding LTT plots (doted lines). Names in the upper left hand corner indicate the subclades that were removed in each case. C. Diversification rate estimated with Morlon et al. (2011)'s method for the four subclades and the remaining backbone when these subclades were removed.

S3.2 Diversification in the Andes

To investigate the pattern of diversification in the Andes with respect to the rest of the Neotropical region, we classified species as Andean or non-Andean, based on a combination of published (Chazot et al. 2016a, Chazot et al. 2016b, De-Silva et al. 2016, Chazot et al. 2014, De-Silva et al. 2010, Elias et al. 2009, Brower et al. 2006, Mallarino et al. 2005, Whinnett et al. 2005) and unpublished (i.e., databases generated from museum collections and our own field collections) georeferenced distribution data and elevation ranges of species (Appendix S1.2). In general species can be unambiguously classified into either of the two categories, because Andean species are never found in the lowlands, whereas species that occur in the lowlands and that sometimes also occur at the Andean foothills never occur above ca. 800m, and are therefore classified as non-Andean. We used trait-dependent models of diversification (Chazot et al. 2016a, Beckman & Witt 2015) to compare the rates of speciation, of extinction and of transition between the Andean area and non-Andean regions. We used the model ClaSSE (Goldberg & Igić 2012), which accounts for up to 10 parameters (2 speciation rates without character state change, 4 cladogenetic transition rates, 2 extinction rates and 2 anagenetic transition rates). However, we constrained parameters that were not biogeographically meaningful to zero (Chazot et al. 2016a). Those include the anagenetic transition rates, considering that transition rates from one region to the other were always accompanied by a speciation event, and the cladogenetic transition rates involving a transition in both descendant lineages, as we considered the scenario unrealistic. We therefore ended up with at most 6 parameters. We tested all models with only one parameter (speciation, extinction, transitions) free to vary, as well as all models combining two or more parameters free to vary. All models were fitted on the 100 trees randomly sampled from BEAST's posterior distribution. Models were compared using mean AIC scores (Table S3.5).

Furthermore, we considered two important sources of potential biases. (1) The major shift of diversification at the root of the core-group could affect our results of trait-dependent diversification models. We therefore repeated the analysis above on the core-group alone. (2) A hidden character may explain the pattern of trait-dependent diversification estimated with ClaSSE. We therefore performed additional analyses with the model HiSSE (Beaulieu & O'Meara 2016) (Box S3.1). All results are presented in Table S3.5.

Box S3.1. Trait-dependent diversification using ClaSSE, BiSSE and HiSSE.

Two papers recently pointed at a number of concerns about the character-state dependent diversification models such as ClaSSE or BiSSE, which we used for testing differences of diversification rates between Andean and non-Andean lineages (Maddison & FitzJohn 2014, Rabosky & Goldberg 2015). The main criticisms are: (1) a high rate of false positive, (2) "pseudoreplication", in particular when diversification rates are not homogeneous across a tree (presence of diversification rate shift) and (3) the existence of "hidden" characters, not measured but influencing the results of character-state dependent models.

We "accounted" for the most important shift of diversification rate in our analysis by testing ClaSSE models both on the whole tree (which included heterogeneous diversification dynamics) and on the core-group only, which appeared as a relatively homogeneous process. While no consensual model emerged from the analyses performed on the whole tree, analyses performed on the core group, which accounts for more than 75% of the current diversity, supports the hypothesis that most of Ithomiini diversification occurred equally in both Andean and non-Andean regions. The high Andean species richness in the core-group results from an early occupation of the Andes and a late colonization of the other regions.

We complemented our ClaSSE analyses and BiSSE ancestral state estimations by testing for the presence of a hidden character that could bias our results, although this is mostly relevant for ruling out misinterpretations of strong signals, which is not our case here. We applied the recently proposed HiSSE model (Beaulieu & O'Meara 2016), which aims at fitting a four-state model, in which each observed character state (in our case Andean *versus* non-Andean) is associated with a hidden state of a character not measured. Because of the large number of parameters associated with this model and the absence of relevance of many potential nested models, we only fitted the most relevant models.

We fitted four models equivalent to BiSSE and seven HiSSE models (Table S3.5). All these models were ranked according to their AIC score and compared to identify the best fitting model. For the whole tree, the HiSSE model was always better than BiSSE. According to AIC scores, the best model corresponded to the "full" one, i.e. allowing all parameters (speciation, extinction and transitions) to be free. According to AICc scores however, the model including equal transition rates, and only differences in speciation and extinction parameters between the observed states and the hidden states was equivalent to the full models, with less parameters. Therefore, there is a significant signal of a hidden character underlying our analyses. The results were similar when performed on the core-group only.

Using the best model with the lowest number of parameters, we performed an ancestral state reconstruction, inferring both the observed states, and the hidden states. The ancestral state reconstruction (Figure S3.5) reveals the presence of a hidden state associated with high diversification rates in both Andean and non-Andean lineages and the presence of a hidden character state with low diversification rates in some poorly diversified Andean lineages. We discuss in the paper the results of previous studies (Chazot et al. 2016a,b) supporting both Andean and non-Andean radiations (and simultaneous increase of diversification rates) within the subtribes Godyridina and Oleriina. The results from the HiSSE model confirm that there is no global association, across all Ithomiini, between the Andes and diversification rate. Instead, we suggest that radiations occurred more specifically in the Northern-Andes and Amazonia following the demise of the Pebas system.

Table S3.5. Results of ClaSSE, BiSSE and HiSSE models fitted on the whole tree and the core-group. A. Full results of the models ClaSSE fitted on 100 posterior trees. B. Comparisons of the models BiSSE and HiSSE fitted on the median tree. Constraints of each model are indicated in the four first columns. 1=non-Andean, 2=Andean, λ111 and λ222 are within-region speciation rates (non-Andean and Andean, respectively), λ112 and λ212 are cladogenetic transition rates (non-Andean towards Andean, and Andean towards non-Andean, respectively), μ = extinction rates, df =number of parameters, logL=log-likelihood, AIC= Akaike information criterion score.

A. a- Whole tree. Mean values from 100 posterior trees.

λ111/λ222		λ112/λ212	μ	df	logL	AIC	λ111	λ222	λ112	λ212	μ1	μ2
λ111≠λ222	**≠**	**λ112=λ212**	**μ1=μ2**	**4**	**-1064.82**	**2137.63**	**0.154**	**0.186**	**0.052**	**0.052**	**0.003**	**0.003**
λ111=λ222	**≠**	**λ112=λ212**	**μ1=μ2**	**3**	**-1065.89**	**2137.79**	**0.171**	**0.171**	**0.052**	**0.052**	**0.004**	**0.004**
λ111≠λ222	**≠**	**λ112≠λ212**	**μ1=μ2**	**5**	**-1064.66**	**2139.31**	**0.151**	**0.188**	**0.046**	**0.058**	**0.002**	**0.002**
λ111=λ222	**≠**	**λ112=λ212**	**μ1≠μ2**	**4**	**-1065.70**	**2139.39**	**0.174**	**0.174**	**0.052**	**0.052**	**0.020**	**0.001**
λ111≠λ222	**≠**	**λ112=λ212**	**μ1≠μ2**	**5**	**-1064.73**	**2139.46**	**0.153**	**0.192**	**0.052**	**0.052**	**0.001**	**0.015**
λ111=λ222	≠	λ112≠λ212	μ1=μ2	4	-1065.88	2139.76	0.172	0.172	0.053	0.051	0.004	0.004
λ111=λ222	≠	λ112≠λ212	μ1≠μ2	5	-1065.65	2141.29	0.175	0.175	0.049	0.056	0.024	7E-05
λ111≠λ222	≠	λ112≠λ212	μ1≠μ2	6	-1064.65	2141.29	0.151	0.190	0.047	0.057	0.001	0.006
λ111=λ222	=	λ112=λ212	μ1=μ2	2	-1102.44	2208.88	0.111	0.111	0.111	0.111	6E-06	6E-06
λ111=λ222	=	λ112=λ212	μ1≠μ2	3	-1102.42	2210.84	0.151	0.151	0.151	0.151	0.001	0.006

A. b- Whole tree. Standard deviations from 100 posterior trees.

λ111/λ222		λ112/λ212	μ	df	logL	AIC	λ111	λ222	λ112	λ212	μ1	μ2
λ111≠λ222	**≠**	**λ112=λ212**	**μ1=μ2**	**4**	**23.20**	**46.40**	**0.011**	**0.004**	**0.004**	**0.013**	**0.005**	**0.005**
λ111=λ222	**≠**	**λ112=λ212**	**μ1=μ2**	**3**	**23.17**	**46.35**	**0.012**	**0.004**	**0.004**	**0.012**	**0.006**	**0.006**
λ111≠λ222	**≠**	**λ112≠λ212**	**μ1=μ2**	**5**	**23.21**	**46.43**	**0.010**	**0.003**	**0.005**	**0.013**	**0.004**	**0.004**
λ111=λ222	**≠**	**λ112=λ212**	**μ1≠μ2**	**4**	**23.17**	**46.34**	**0.012**	**0.012**	**0.004**	**0.004**	**0.005**	**0.002**
λ111≠λ222	**≠**	**λ112=λ212**	**μ1≠μ2**	**5**	**23.21**	**46.41**	**0.010**	**0.004**	**0.004**	**0.015**	**0.002**	**0.009**
λ111=λ222	≠	λ112≠λ212	μ1=μ2	4	23.17	46.34	0.012	0.004	0.004	0.012	0.006	0.006
λ111=λ222	≠	λ112≠λ212	μ1≠μ2	5	23.18	46.35	0.012	0.004	0.005	0.012	0.007	0.000
λ111≠λ222	≠	λ112≠λ212	μ1≠μ2	6	23.21	46.43	0.010	0.004	0.005	0.014	0.002	0.008
λ111=λ222	=	λ112=λ212	μ1=μ2	2	23.17	46.34	0.008	0.008	0.008	0.008	2.15E-05	2.15E-05
λ111=λ222	=	λ112=λ212	μ1≠μ2	3	23.17	46.34	0.010	0.010	0.010	0.010	0.002	0.008

A. c- Core-group. Mean values from 100 posterior trees.

λ111/λ222		λ112/λ212	μ	df	logL	AIC	ΔAIC	λ111	λ222	λ112	λ212	μ1	μ2
λ111=λ222	**≠**	**λ112=λ212**	**μ1=μ2**	**3**	**-877.96**	1757.74	**0.00**	**0.190**	**0.190**	**0.059**	**0.059**	**4.26E-07**	**4.26E-07**
λ111≠λ222	**≠**	**λ112=λ212**	**μ1=μ2**	**4**	**-877.00**	1757.80	**0.08**	**0.168**	**0.205**	**0.060**	**0.060**	**8.15E-07**	**8.15E E-07**
λ111=λ222	**≠**	**λ112≠λ212**	**μ1=μ2**	**4**	**-877.62**	1759.07	**1.33**	**0.189**	**0.189**	**0.082**	**0.038**	**4.13E-07**	**4.13E-07**
λ111=λ222	**≠**	**λ112=λ212**	**μ1≠μ2**	**4**	**-877.96**	1759.74	**2.00**	**0.190**	**0.190**	**0.059**	**0.059**	**8.11E-06**	**6.97E-06**
λ111≠λ222	≠	λ112=λ212	μ1≠μ2	5	-876.99	1759.78	2.07	0.168	0.207	0.060	0.060	1.13E-06	0.003
λ111≠λ222	≠	λ112≠λ212	μ1=μ2	5	-874.92	1759.83	2.09	0.171	0.204	0.068	0.051	1.84E-07	1.84E-07
λ111=λ222	≠	λ112≠λ212	μ1≠μ2	5	-875.52	1761.02	3.26	0.190	0.190	0.084	0.035	0.003	8.37E-07
λ111≠λ222	≠	λ112≠λ212	μ1≠μ2	6	-874.88	1761.75	4.01	0.170	0.205	0.064	0.054	2.65E-06	0.001
λ111=λ222	=	λ112=λ212	μ1=μ2	2	-905.69	1815.37	57.63	0.124	0.124	0.124	0.124	1.97E-06	1.97E-06
λ111=λ222	=	λ112=λ212	μ1≠μ2	3	-905.51	1817.02	59.27	0.170	0.170	0.170	0.170	2.65E-06	0.001

A. d- Core-group. Standard deviations from 100 posterior trees.

λ111/λ222		λ112/λ212	μ	df	logL	AIC	λ111	λ222	λ112	λ212	μ1	μ2
λ111=λ222	**≠**	**λ112=λ212**	**μ1=μ2**	**3**	**25.67**	**51.33**	**0.016**	**0.016**	**0.005**	**0.005**	**1.21E-06**	**1.21E-06**
λ111≠λ222	**≠**	**λ112=λ212**	**μ1=μ2**	**4**	**25.67**	**51.34**	**0.015**	**0.018**	**0.005**	**0.005**	**2.16E-06**	**2.16E-06**
λ111=λ222	**≠**	**λ112≠λ212**	**μ1=μ2**	**4**	**25.62**	**51.23**	**0.016**	**0.016**	**0.011**	**0.010**	**1.06E-06**	**1.06E-06**
λ111=λ222	**≠**	**λ112=λ212**	**μ1≠μ2**	**4**	**25.67**	**51.33**	**0.016**	**0.005**	**0.016**	**0.005**	**1.27E-05**	**1.79E-05**
λ111≠λ222	≠	λ112=λ212	μ1≠μ2	5	25.68	51.35	0.014	0.019	0.005	0.005	3.70E-06	0.005
λ111≠λ222	≠	λ112≠λ212	μ1=μ2	5	25.68	51.36	0.015	0.018	0.015	0.015	3.09E-07	3.09E-07
λ111=λ222	≠	λ112≠λ212	μ1≠μ2	5	25.60	51.20	0.017	0.017	0.008	0.006	0.004	2.48E-06
λ111≠λ222	≠	λ112≠λ212	μ1≠μ2	6	25.70	51.40	0.014	0.019	0.014	0.015	7.04E-06	0.002
λ111=λ222	=	λ112=λ212	μ1=μ2	2	25.66	51.31	0.011	0.011	0.011	0.011	4.14E-06	4.14E-06
λ111=λ222	=	λ112=λ212	μ1≠μ2	3	25.67	51.34	0.014	0.014	0.014	0.014	7.04E-06	0.002

B. a- Whole tree

Model	- logL	AIC
Bisse: null	-1071.379	2148.759
Bisse: λ and μ free	-1069.905	2149.811
Bisse: transitions free	-1071.405	2150.810
Bisse: allfree	-1070.148	2152.295
Hisse: all free	-1043.805	**2119.609**
Hisse: all λ and μ free + transition fixed	-1054.777	2127.555
Hisse: observed λ and μ ≠ hidden λ and μ + transition fixed	-1055.503	2121.007
Hisse: hidden λ and μ free + observed λ and μ fixed + transitions fixed	-1055.465	2124.930
Hisse: observed λ and μ free + hidden λ and μ fixed + transitions fixed	-1055.415	2124.829
Hisse: λ and μ Andes (hidden/observed) free + λ and μ non Andes fixed + transitions fixed	-1060.017	2134.033
Hisse: observed λ and μ ≠ hidden λ and μ + transitions free	-1065.549	2155.098

B. b- Core-group

Model	- logL	AIC
Bisse: null	-879.110	1764.220
Bisse: λ and μ free	-876.968	1763.935

Bisse: transitions free	-877.256	1762.512
Bisse: allfree	-876.280	1764.560
Hisse: all free	-862.671	2119.609
Hisse: all λ and μ free + transition fixed	-869.109	1756.218
Hisse: observed λ and μ ≠ hidden λ and μ + transition fixed	-870.304	1750.608
Hisse: hidden λ and μ free + observed λ and μ fixed + transitions fixed	870.326	**1754.651**
Hisse: observed λ and μ free + hidden λ and μ fixed + transitions fixed	-870.284	**1754.568**
Hisse: λ and μ Andes (hidden/observed) free + λ and μ non Andes fixed + transitions fixed	-872.174	1758.349
Hisse: observed λ and μ ≠ hidden λ and μ + transitions free	-877.021	1778.042

Finally, we also conducted ancestral state estimation based on the models of trait-dependent diversification. Since ancestral state estimation is not available for ClaSSE models we used the model BiSSE (FitzJohn *et al*. 2009) for this purpose. We fitted the model BiSSE corresponding to the best fitting ClaSSE model, and we used these parameters to infer the ancestral states at the nodes of the phylogeny (Figure S3.6). This ancestral state estimation was compared to that obtained using the historical biogeography analyses outlined below. All these analyses were performed on both the whole phylogeny and the core-group only, to account for the diversification rate shift identified by our time-dependent diversification analyses. Ancestral state reconstruction was also performed with the HiSSE model under the best model (Figure S3.6).

Figure S3.5. A. (Next page). Ancestral state estimation performed on the whole tree, using the best HiSSE model. White branches indicate non-Andean lineages, black branches indicate Andean lineages, blue and red branches correspond to the estimations of the hidden character states.

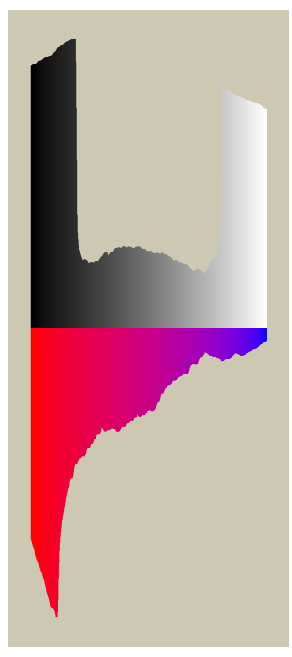
0.12
net.div
0.28
0
State
1

Figure S3.6. B. Ancestral state reconstruction performed using BiSSE diversification models: A. different speciation rates, B. different speciation and colonization rates. Red indicate Andean lineages, blue indicates non-Andean lineages. State probability at each node is represented with pie charts

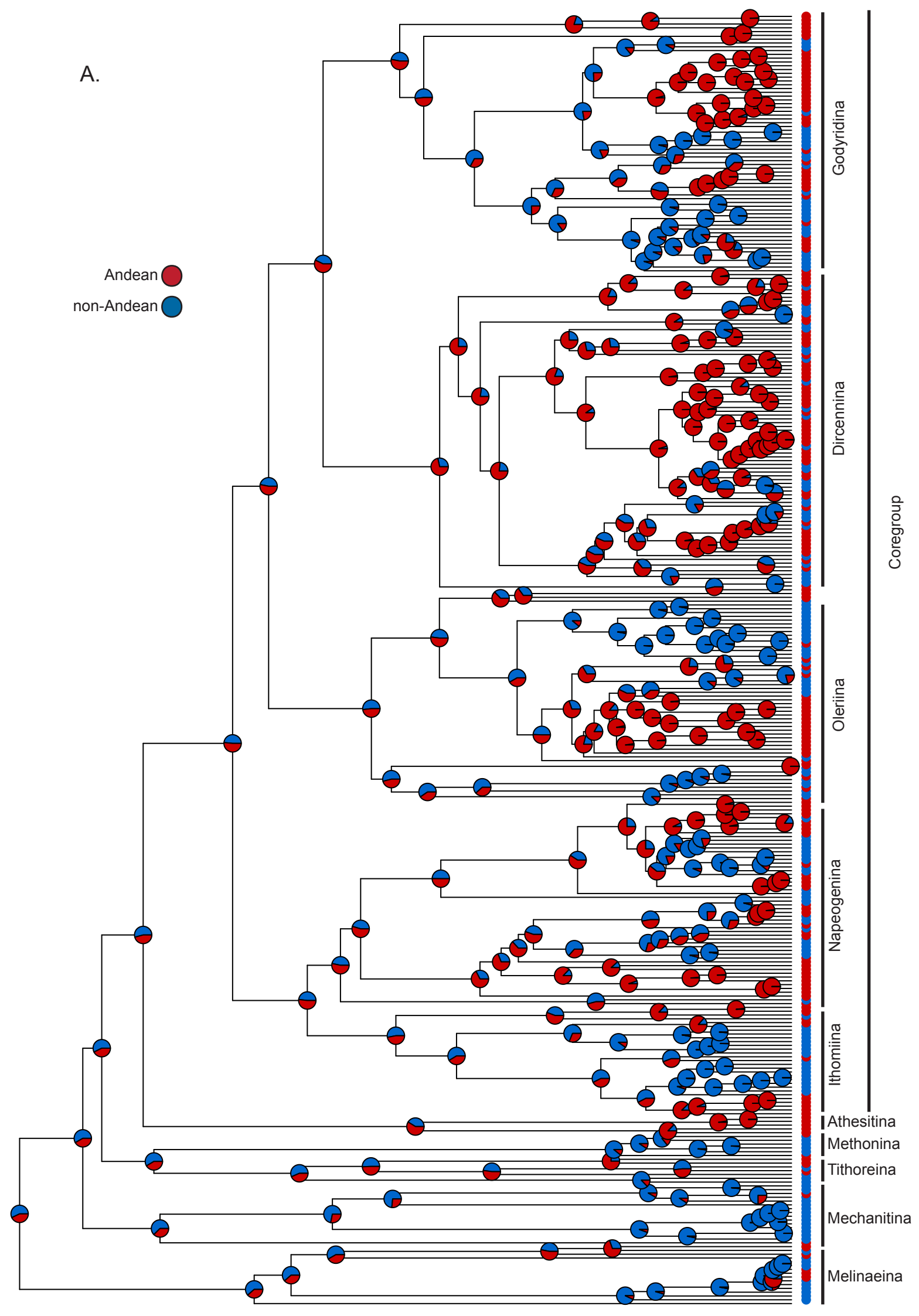
A.
Andean
non-Andean
Godyridina
Dircennina
Oleriina
Napeogenina
Ithomiina
Athesitina
Methonina
Tithoreina
Mechanitina
Melinaeina
Coregroup

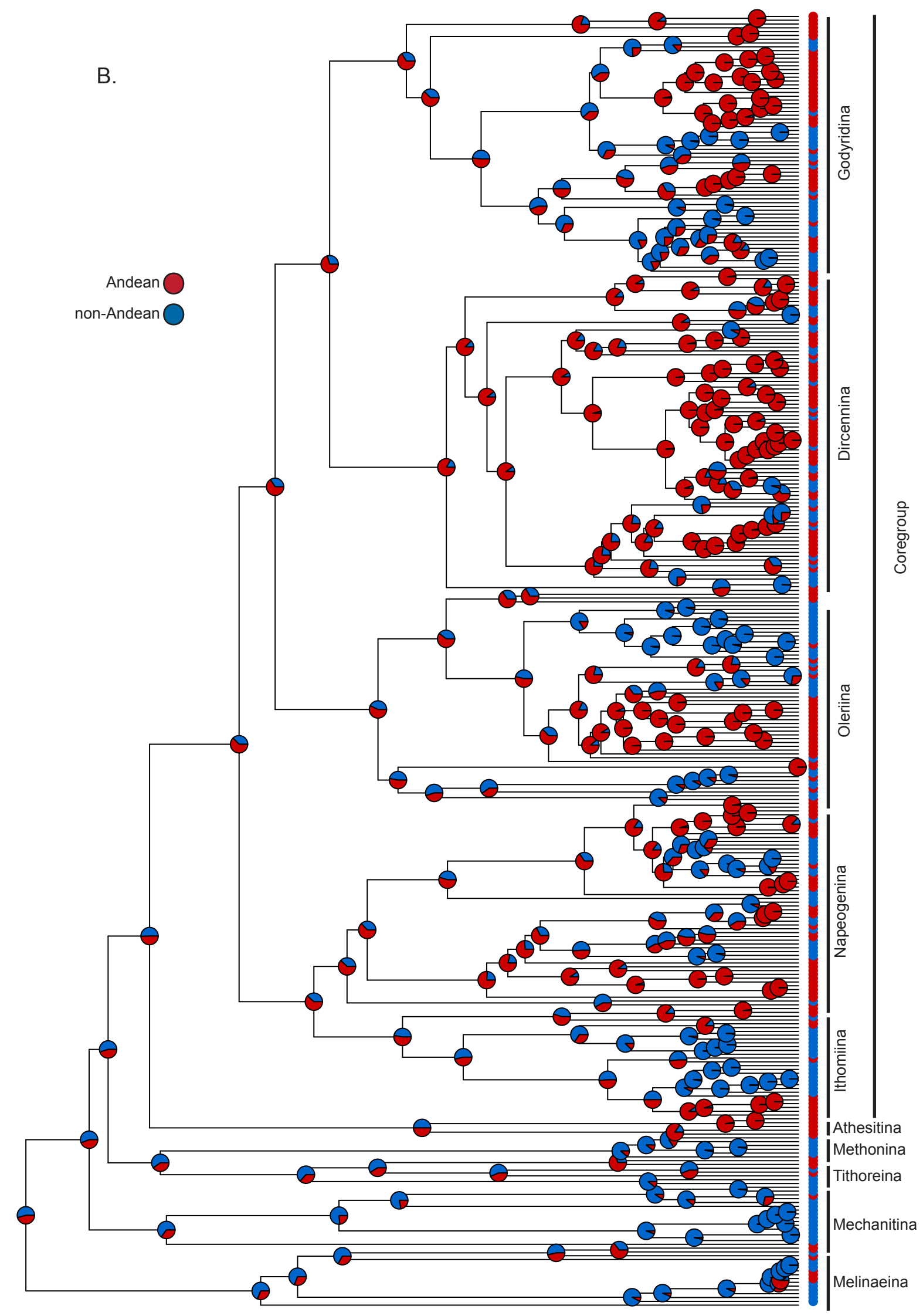
B.
Andean
non-Andean
Godyridina
Dircennina
Oleriina
Napeogenina
Ithomiina
Coregroup
Athesitina
Methonina
Tithoreina
Mechanitina
Melinaeina

S3.3 Diversification in Amazonia

We further investigated the pattern of diversification in Amazonia during the post-Pebas period. The Amazon basin appears to be the second most important place for diversification after the Andes and there is a longstanding hypothesis that speciation in this region has been driven by climatic fluctuations during the Quaternary (Haffer 1969). An interpretation of this scenario is that speciation rate should increase during the last 2.5 million years (Matos-Maraví 2016). To test this hypothesis we identified seven major Amazonian diversification events, i.e. clades which nodes were inferred to be almost all Amazonian from the BioGeoBEARS ancestral state reconstruction. We fitted a model of time-dependent speciation rate (no extinction) to see whether speciation rates increased through time (supporting a recent diversification potentially caused by Pleistocene climatic fluctuations) or decreased through time (supporting radiations accompanying the post-Pebas recolonizations), using Morlon et al.'s (2011) method. Analyses were performed on 100 trees randomly sampled from BEAST's posterior distribution. Results are shown in the manuscript (Figure 3).

References

Alfaro ME, Santini F, Brock C, Alamillo H, Dornburg A, Rabosky DL, Carnevale G, & Harmon LJ. (2009). Nine exceptional radiations plus high turnover explain species diversity in jawed vertebrates. *Proceedings of the National Academy of Sciences*, 106(32), 13410-13414.

Beaulieu JM, & O'Meara BC. (2016). Detecting hidden diversification shifts in models of trait-dependent speciation and extinction. *Systematic Biology*, 65, 583-601.

Beckman EJ, & Witt CC. (2015). Phylogeny and biogeography of the New World siskins and goldfinches: Rapid, recent diversification in the Central Andes. *Molecular Phylogenetics and Evolution*, 87, 28-45.

Brower AV, Freitas AV, Lee MM, Silva-Brandão KL, Whinnett A, & Willmott KR. (2006). Phylogenetic relationships among the Ithomiini (Lepidoptera: Nymphalidae) inferred from one mitochondrial and two nuclear gene regions. *Systematic Entomology(2)*, 31, 288-301.

Chazot N, Willmott KR, Santacruz Endara PG, Toporov A, Hill RI, Jiggins CD, & Elias M. (2014). Mutualistic mimicry and filtering by altitude shape the structure of Andean butterfly communities. *The American Naturalist*, 183(1), 26-39.

Chazot N, Willmott KR, Condamine FL, De-Silva DL, Freitas AV, Lamas G, Morlon H, Giraldo, CE, Jiggins CD, Joron M, Mallet J, & Elias M. (2016a). Into the Andes: multiple independent colonizations drive montane diversity in the Neotropical clearwing butterflies Godyridina. *Molecular Ecology*, 25(22), 5765-5784.

Chazot N, Willmott KR, Freitas AVL, de Silva DL, Pellens R, & Elias M. (2016b). Patterns of Species, Phylogenetic and Mimicry Diversity of Clearwing Butterflies in the Neotropics. *In*: Biodiversity Conservation and Phylogenetic Systematics: Preserving our evolutionary heritage in an extinction crisis (eds Pellens R, Grandcolas P). *Springer International Publishing*.

De-Silva DL, Elias M, Willmott K, Mallet J, & Day JJ. (2016). Diversification of clearwing butterflies with the rise of the Andes. *Journal of Biogeography*, 43(1), 44-58.

De-Silva DL, Day JJ, Elias M, Willmott K, Whinnett A, & Mallet J. (2010). Molecular phylogenetics of the neotropical butterfly subtribe Oleriina (Nymphalidae: Danainae: Ithomiini). *Molecular Phylogenetics and Evolution*, 55(3), 1032-1041.

Elias M, Joron M, Willmott K, Silva-Brandão KL, Kaiser V, Arias CF, Gomez-Piñerez LM, Uribe S, Brower AVZ, Freitas AVL, & Jiggins, CD. (2009). Out of the Andes: patterns of diversification in clearwing butterflies. *Molecular Ecology*, 18(8), 1716-1729.

FitzJohn RG, Maddision WP, Otto SP. (2009). Estimating Trait-Dependent Speciation and Extinction Rates from Incompletely Resolved Phylogenies. *Systematic Biology*, 58(6), 595–611

Goldberg EE, & Igić B. (2012). Tempo and mode in plant breeding system evolution. *Evolution*, 66, 3701-3709.

Haffer J. (1969). Speciation in Amazonian forest birds. *Science*, 165, 131-137.

Maddison WP, FitzJohn RG. (2014). The unsolved challenge to phylogenetic correlation tests for categorical characters. *Systematic biology* **64**, 127-136.

Mallarino R, Bermingham E, Willmott KR, Whinnett A, & Jiggins CD. (2005). Molecular systematics of the butterfly genus *Ithomia* (Lepidoptera: Ithomiinae): a composite phylogenetic hypothesis based on seven genes. *Molecular Phylogenetics and Evolution*, 34(3), 625-644.

Matos-Maraví P. (2016). Investigating the timing of origin and evolutionary processes shaping regional species diversity: Insights from simulated data and neotropical butterfly diversification rates. *Evolution*, 70(7), 1638-1650.

Morlon H, Parsons TL, & Plotkin JB. (2011). Reconciling molecular phylogenies with the fossil record. *Proceedings of the National Academy of Sciences*, 108(39), 16327-16332.

Rabosky DL, Goldberg EE. (2015). Model inadequacy and mistaken inferences of trait-dependent speciation. *Systematic Biology* **64**, 340-355.

Rabosky DL, Grundler M, Anderson C, Title P, Shi JJ, Brown JW, Huang H, & Larson, JG (2014). BAMM tools: an R package for the analysis of evolutionary dynamics on phylogenetic trees. *Methods in Ecology and Evolution*, 5(7), 701-707.

Rabosky DL. (2014). Automatic detection of key innovations, rate shifts, and diversity-dependence on phylogenetic trees. *PloS one*, 9(2), e89543.

Stadler T. (2011). Mammalian phylogeny reveals recent diversification rate shifts. *Proceedings of the National Academy of Sciences*, 108, 6187-6192.

Whinnett A, Brower AV, Lee M-M, Willmott KR, & Mallet J. (2005). Phylogenetic utility of Tektin, a novel region for inferring systematic relationships among Lepidoptera. *Annals of the Entomological Society of America*, 98(6), 873-886.

Appendix S4: Detailed methods and supplementary results for historical biogeography analyses

We proceeded in three steps to reconstruct the historical biogeography of Ithomiini. First, we performed an ancestral state reconstruction using a model with refined area adjacency but uniform dispersal multipliers (null-model). Second, we used the results of this model to compute rates of dispersal between specific regions per million years. This allowed us to test some biogeographic hypotheses but also to identify relevant time frames for which dispersal probabilities might vary. Third, we implemented a time-stratified model designed from the previous information to refine our biogeographic reconstruction. All these models were performed on the median node ages tree from BEAST.

S4.1 Biogeographic null model

We inferred the historical biogeography of Ithomiini using BioGeoBEARS v.0.2.1 (Matzke 2014). We divided the Neotropics into nine distinct biogeographic regions: 1) Central America, 2) Caribbean Islands, 3) lowlands on the Western part of the Andes, including the Magdalena valley, 4) Northern Andes that comprise the Western and eastern Ecuadorian and Colombian cordilleras and the Venezuelan cordillera, 5) Central Andes, 6) Western Amazonia, 7) eastern Amazonia, 8) Guiana Shield and 9) Atlantic Forest (Figure S4.7). In this model, we constrained the combinations of areas to avoid unrealistic distributions (e.g., disjunct distributions) but all dispersal multipliers were set to 1 to avoid biasing the ancestral state reconstruction. We used the best fitting model (DEC) for the following analyses.

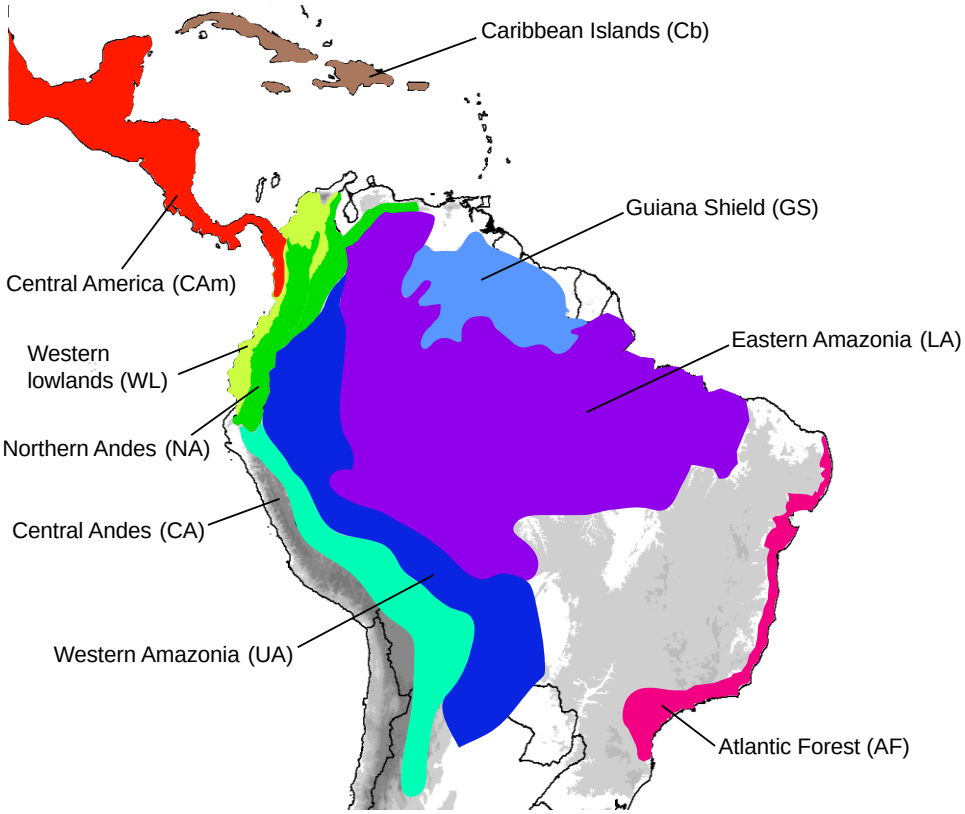

Figure S4.7. Biogeographic areas used in the BioGeoBears analyses

S4.2 Biogeographic interchanges within the core-group

One important hypothesis is that the Pebas influenced the interchanges among biogeographic regions, especially towards or across Western Amazonia. To test this hypothesis, we computed "rates" of colonization from BioGeoBEARS ancestral-state reconstructions performed with the null-model. We ran 1000 biogeographical stochastic mappings as implemented in BioGeoBEARS and extracted the times of dispersal events. Then, for each million-year interval, we computed the proportion of specific dispersal events compared to the maximum number of lineages existing during this interval, which we refer to as "rates" of colonization. We computed rates of dispersal between Andean and non-Andean regions, between the Andes and the Amazonia, between the Central and the Northern Andes, between the Atlantic Forest and the other regions, and between Central America and the rest of the Neotropics. These rates were computed only on the core-group, because (1) this group contains 85% of Ithomiini species, (2) the diversification process is homogeneous throughout the clade and (3) we found high extinction in the backbone, which may falsify the ancestral state reconstruction in these lineages, which were therefore excluded. In the paper we showed the median rates of interchanges between the Andes and Amazonia and between Central and Northern Andes (Figure 3). Below (Figure S4.8) we show the boxplots of rate values per million years for the interchanges between the Andes and Amazonia, Central and Northern Andes, Central America

and the other Neotropical regions, Atlantic Forest and the other Neotropical regions, not only for the total amount of interchanges but also the results when distinguishing one way from the other (*e.g*. from the Northern towards the Central Andes *versus* from the Central towards the Northern Andes).

Figure S4.8. Rates of colonization between different regions computed on the core-group and then used to design a time-stratified biogeographic model (next pages).

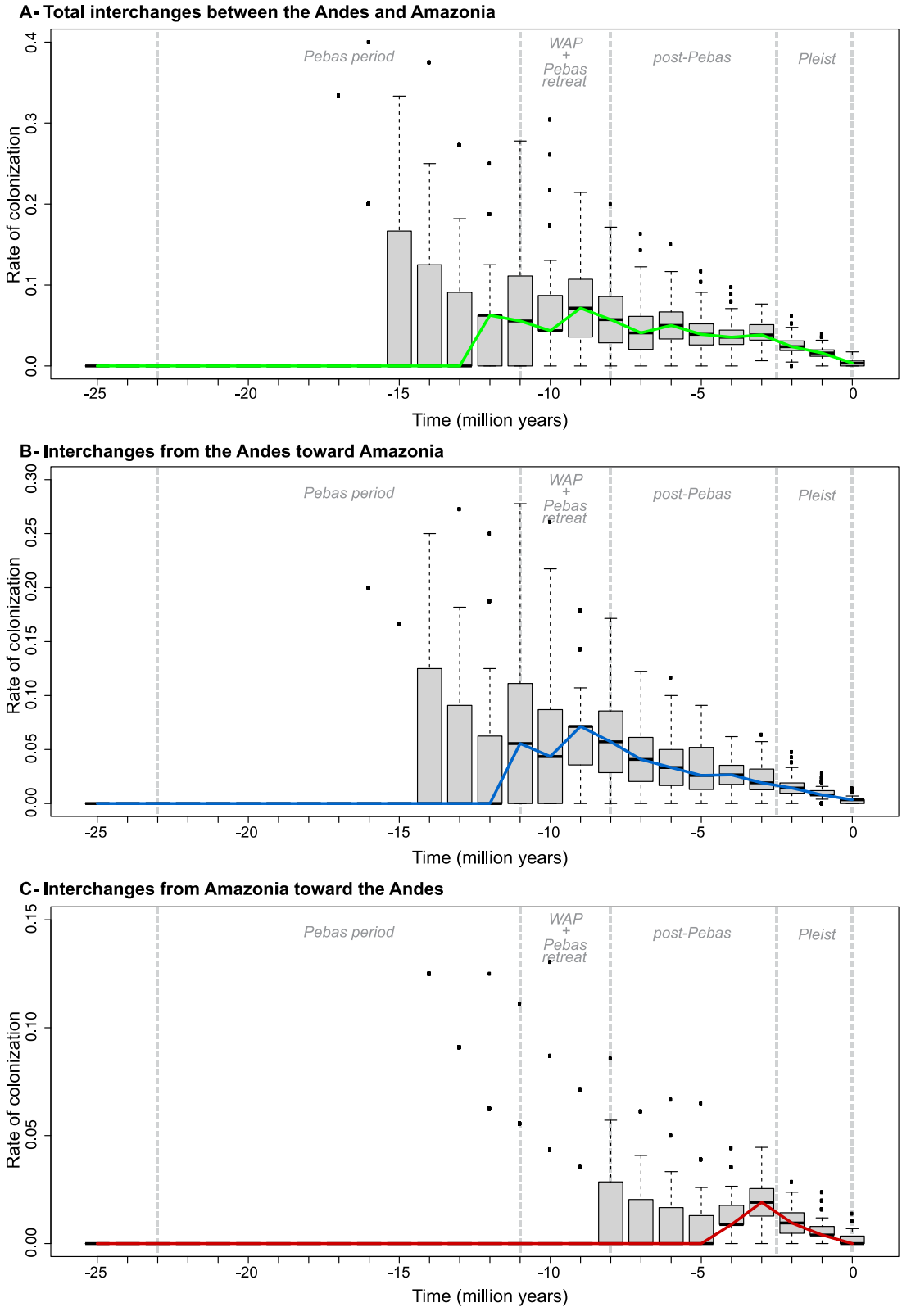

Figure S4.8 A, B & C. Rates of interchanges between all Andes and Amazonia. A: Total number of interchanges. B: Rates of colonization from the Andes toward Amazonia. C: Rates of colonization from Amazonia toward the Andes.

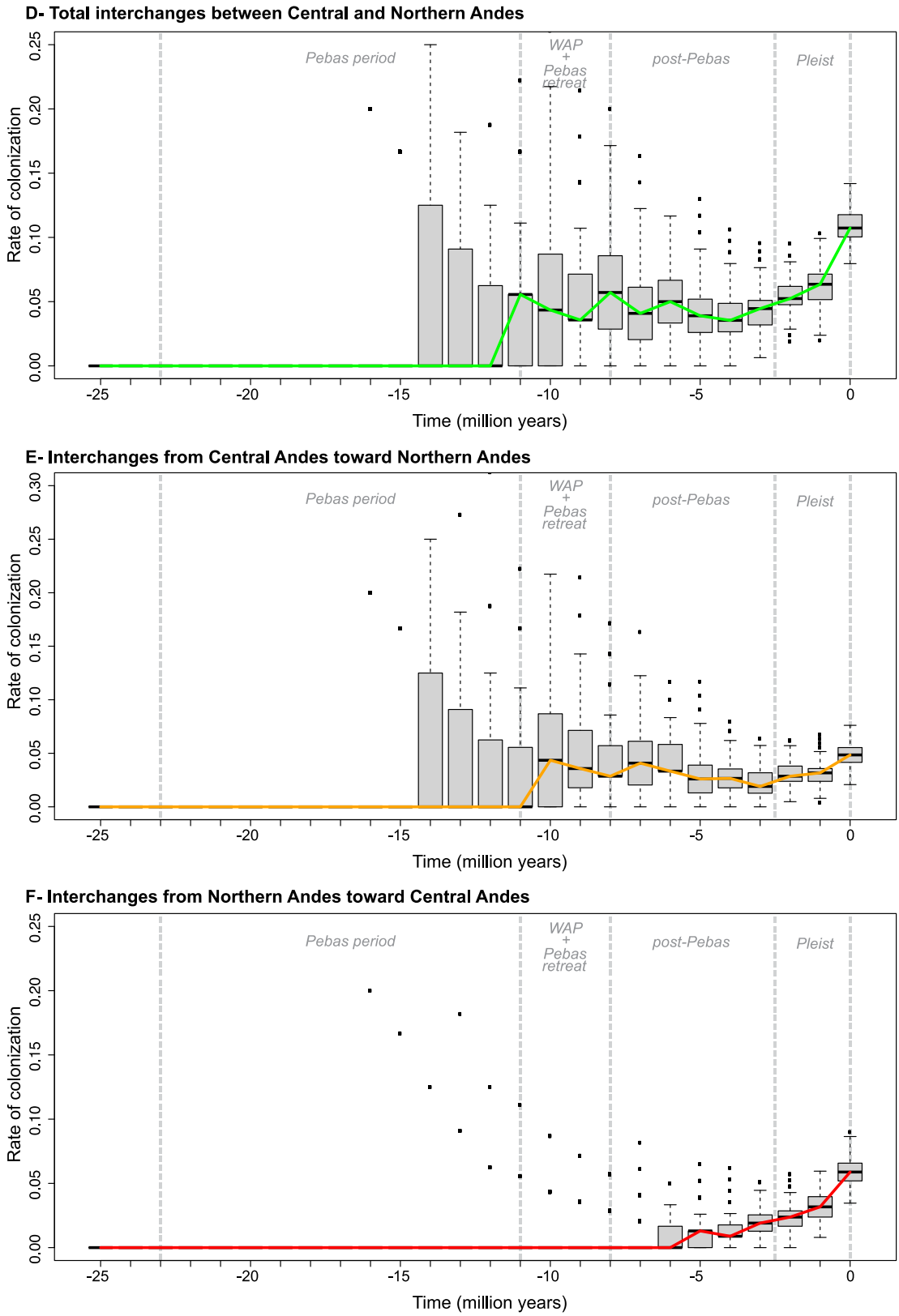

Figure S4.8 D, E & F. Rates of interchanges between Central and Northern Andes. A: Total number of interchanges. B: Rates of colonization from Central toward Northern Andes. C: Rates of colonization from Northern toward Central Andes.

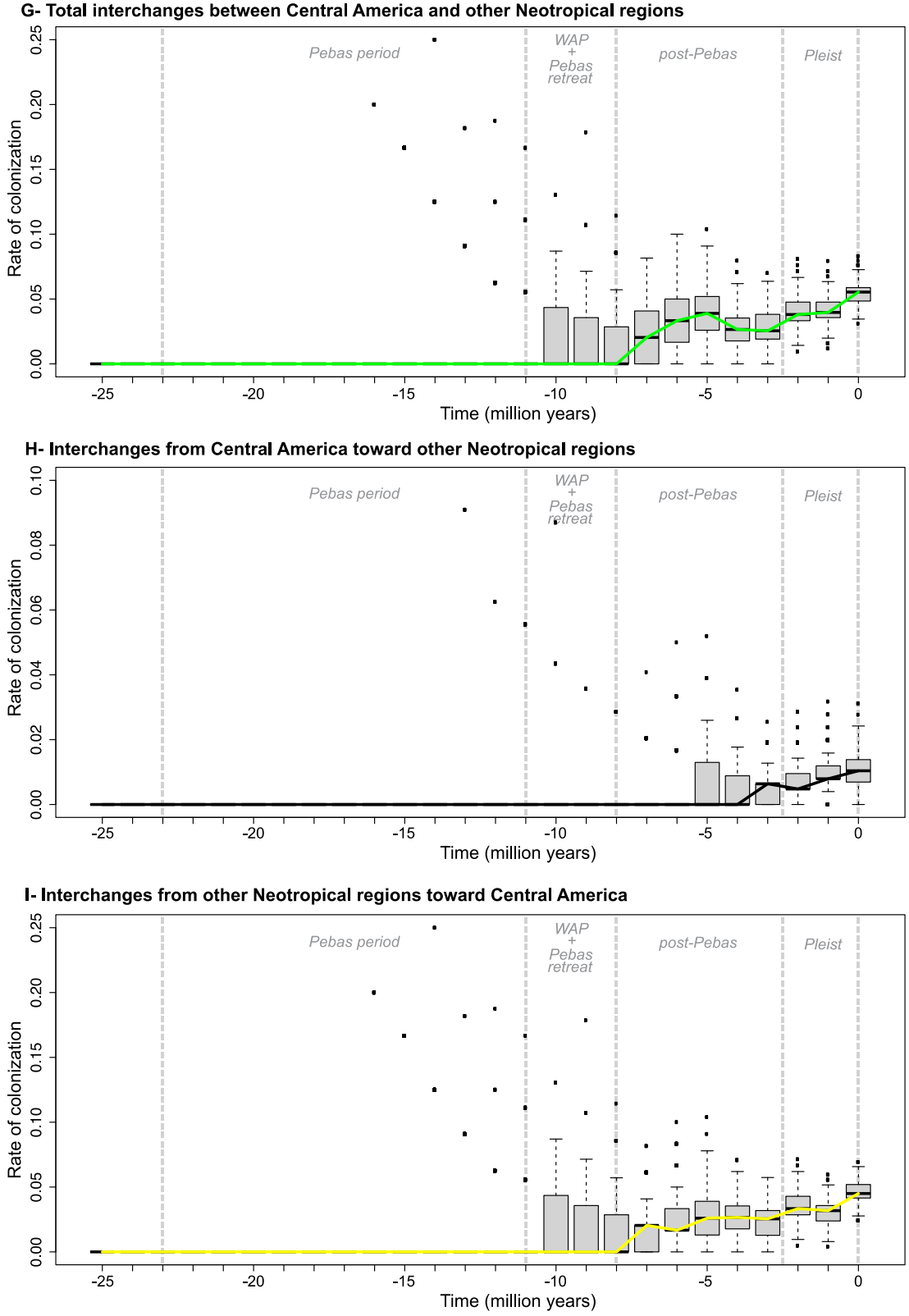

Figure S4.8 G, H & I. Rates of interchanges between Central America and the other Neotropical regions. A: Total number of interchanges. B: Rates of colonization from Central America toward the other regions. C: Rates of colonization from other regions toward Central America.

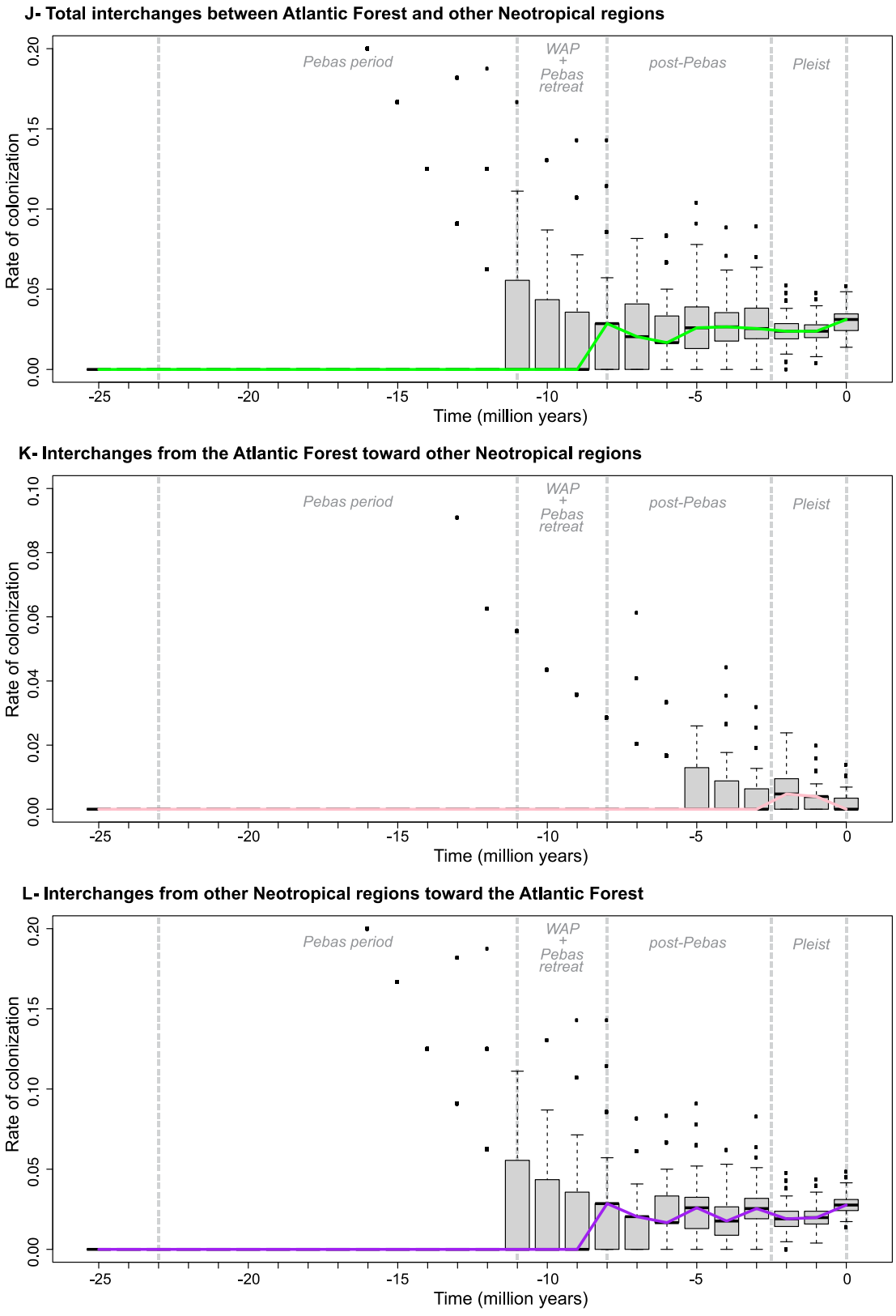

Figure S4.8 J, K & L. Rates of interchanges between Atlantic Forest and the other Neotropical regions. A: Total number of interchanges. B: Rates of colonization from Atlantic Forest toward the other regions. C: Rates of colonization from other regions toward Atlantic Forest.

We used these results of dispersal rates estimated with the null model to design a time-stratified model and improve the resolution of our biogeographic reconstruction. We interpreted the variations of rates of interchanges (including also the interchanges with the Atlantic forest) as indications for time-varying dispersal probabilities to design a time-stratified model (Table S4.6).

Table S4.6. A. Matrix of adjacency and B. stratified dispersal multipliers estimated from the transition rates among regions, and implemented in the time-stratified biogeographic analysis

A. MATRIX OF ADJACENCY

	Cam	Cb	WL	NA	CA	GS	UA	LA	AF
Cam	1	1	1	1	1	0	0	0	0
Cb	1	1	1	0	0	0	1	1	0
WL	1	1	1	1	1	0	1	1	0
NA	1	0	1	1	1	1	1	1	0
CA	1	0	1	1	1	0	1	1	1
GS	0	0	0	1	0	1	1	1	0
UA	0	1	1	1	1	1	1	1	1
LA	0	1	1	1	1	1	1	1	1
AF	0	0	0	0	1	0	1	1	1

B. DISPERSAL MULTIPLIERS

0-4 mya	Cam	Cb	WL	NA	CA	GS	UA	LA	AF
Cam	1.00	0.40	0.30	0.30	0.18	0.18	0.18	0.18	0.00
Cb	0.40	1.00	0.10	0.06	0.00	0.06	0.01	0.10	0.00
WL	0.60	0.10	1.00	0.60	0.60	0.18	0.30	0.30	0.00
NA	0.60	0.06	0.60	1.00	0.60	0.6	0.60	0.60	0.00
CA	0.36	0.00	0.60	0.60	1.00	0.36	0.60	0.60	0.36
GS	0.36	0.06	0.18	0.6	0.36	1	0.6	0.6	0.36
UA	0.18	0.01	0.30	0.60	0.60	0.6	1.00	0.60	0.36

LA	0.18	0.10	0.30	0.60	0.60	0.6	0.60	1.00	0.60
AF	0.00	0.00	0.00	0.00	0.36	0.36	0.36	0.60	1.00

4-8 mya	Cam	Cb	WL	NA	CA	GS	UA	LA	AF
Cam	1.00	0.40	0.30	0.30	0.18	0.18	0.00	0.00	0.00
Cb	0.40	1.00	0.10	0.06	0.00	0.06	0.01	0.10	0.00
WL	0.30	0.10	1.00	0.60	0.60	0.18	0.30	0.30	0.00
NA	0.30	0.06	0.60	1.00	0.40	0.6	0.20	0.20	0.00
CA	0.12	0.00	0.60	0.40	1.00	0.24	0.20	0.20	0.12
GS	0.18	0.06	0.18	0.6	0.24	1	0.6	0.6	0.36
UA	0.00	0.01	0.30	0.20	0.20	0.6	1.00	0.60	0.36
LA	0.00	0.10	0.30	0.20	0.20	0.6	0.60	1.00	0.60
AF	0.00	0.00	0.00	0.00	0.12	0.36	0.36	0.60	1.00

8-13 mya	Cam	Cb	WL	NA	CA	GS	UA	LA	AF
Cam	1.00	0.40	0.30	0.30	0.18	0.18	0.00	0.00	0.00
Cb	0.40	1.00	0.10	0.06	0.00	0.06	0.01	0.10	0.00
WL	0.30	0.10	1.00	0.60	0.60	0.18	0.30	0.30	0.00
NA	0.30	0.06	0.60	1.00	0.40	0.6	0.60	0.60	0.00
CA	0.12	0.00	0.60	0.40	1.00	0.24	0.60	0.60	0.36
GS	0.18	0.06	0.18	0.6	0.24	1	0.6	0.6	0.36
UA	0.00	0.01	0.30	0.60	0.60	0.6	1.00	0.60	0.36
LA	0.00	0.10	0.30	0.60	0.60	0.6	0.60	1.00	0.60
AF	0.00	0.00	0.00	0.00	0.36	0.36	0.36	0.60	1.00

13-30 mya	Cam	Cb	WL	NA	CA	GS	UA	LA	AF
Cam	1.00	0.40	0.00	0.00	0.00	0	0.00	0.00	0.00
Cb	0.40	1.00	0.10	0.06	0.00	0.06	0.01	0.10	0.00

WL	0.00	0.10	1.00	0.60	0.01	0.01	0.01	0.01	0.00
NA	0.00	0.06	0.60	1.00	0.10	0.1	0.10	0.10	0.00
CA	0.00	0.00	0.01	0.10	1.00	0.01	0.10	0.20	0.02
GS	0	0.06	0.01	0.1	0.01	1	0.1	0.6	0.06
UA	0.00	0.01	0.01	0.10	0.10	0.1	1.00	0.10	0.01
LA	0.00	0.10	0.01	0.10	0.20	0.6	0.10	1.00	0.10
AF	0.00	0.00	0.00	0.00	0.02	0.06	0.01	0.10	1.00

Cam: Central-America

Cb: Caribbean Islands

WL: Lowlands west of the Andes, including the Magdalena Valley

NA: Northern Andes

CA: Central Andes

GS: Guiana Shild

UA: Upper Amazon

LA: Lower Amazon

AF: Atlantic Forest

S4.3 Time-stratified biogeographic model

We used our estimations of colonization rates among the major biogeographic regions to design a time-stratified biogeographic model and improve the resolution of our biogeographic reconstruction. We created four time frames: i) 0-4, ii) 4-8, iii) 8-13, and iv) 13-30 My ago, where dispersal multipliers between areas reflected the colonization rate variations identified previously (Table S4.6). This ancestral state reconstruction was compared to the null model as well as to the ancestral state reconstruction obtained from trait-dependent diversification models (Figure S3.6). Ancestral state reconstructions for the null and the time-stratified models are shown in Figure S4.9.

Figure S4.9. Results of biogeographic ancestral state estimation obtained with BiogeoBEARS and using the "null" or time-stratified model.

A. Biogeographic ancestral state estimation obtained from the "null" model using BiogeoBEARS. Pie charts are the probability of each area summed across all possible ranges and standardized.

B. Biogeographic ancestral state estimation obtained from the time-stratified model using BiogeoBEARS. Pie charts are the probability of each area summed across all possible ranges and standardized.

C. Biogeographic ancestral state estimation obtained from the time-stratified model using BiogeoBEARS. Ranges with the highest probability at the nodes are shown. The figure also shows the different sections of the tree that we refer to throughout the paper, including MEDUSA partition (yellow names), the Amazonian radiations (red names) and the North Andean radiation (orange names).

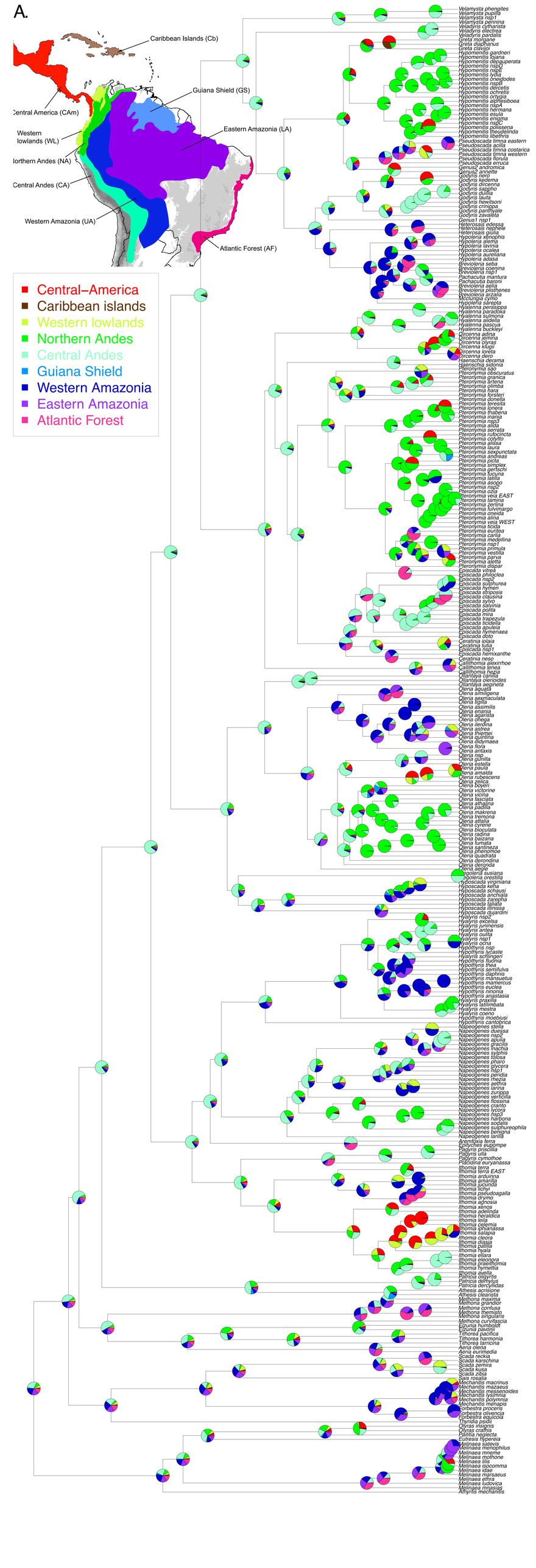
A.
Caribbean Islands (Cb)
Guiana Shield (GS)
Central America (CAm)
Eastern Amazonia (LA)
Western lowlands (WL)
Northern Andes (NA)
Central Andes (CA)
Western Amazonia (UA)
Atlantic Forest (AF)
Central–America
Caribbean islands
Western lowlands
Northern Andes
Central Andes
Guiana Shield
Western Amazonia
Eastern Amazonia
Atlantic Forest
Velamysta phenasites
Velamysta pupilla
Velamysta nsp1
Velamysta pennina
Veladyris cytharista
Veladyris electrea
Veladyris pardalis
Greta morgane
Greta diaphanus
Greta clavijoi
Hypomenitis gardneri
Hypomenitis lojana
Hypomenitis depuperata
Hypomenitis nspD
Hypomenitis nspE
Hypomenitis lydia
Hypomenitis oneigodes
Hypomenitis nspB
Hypomenitis dercetis
Hypomenitis ochretis
Hypomenitis ortygia
Hypomenitis alphesiboea
Hypomenitis nspA
Hypomenitis hermana
Hypomenitis esula
Hypomenitis enigma
Hypomenitis nspC
Hypomenitis poliissena
Hypomenitis theudelinda
Hypomenitis libethris
Pseudoscada timna eastern
Pseudoscada acilia
Pseudoscada timna costarica
Pseudoscada timna western
Pseudoscada florula
Pseudoscada erruca
Genusz andromica
Genusz annette
Godyris nero
Godyris kedema
Godyris dircenna
Godyris sappho
Godyris duilia
Godyris lauta
Godyris hewitsoni
Godyris crinippa
Godyris pantifylale
Godyris zavaleta
Genus1 nsp1
Heterosais edessa
Heterosais nephele
Heterosais giulia
Hypoleria xenophis
Hypoleria alema
Hypoleria lavinia
Hypoleria ocalea
Hypoleria aureliana
Hypoleria adasa
Brevioleria seba
Brevioleria coenina
Brevioleria nsp1
Pachacutia mantura
Pachacutia baroni
Brevioleria aelia
Brevioleria plisthenes
Brevioleria arzalia
Mcclungia cymo
Hypoleria sarepta
Hyalenna perasippa
Hyalenna paradoxa
Hyalenna sulmona
Hyalenna aldella
Hyalenna pascua
Hyalenna buckleyi
Dircenna adina
Dircenna jemina
Dircenna olyras
Dircenna klugii
Dircenna loreta
Dircenna dero
Haenschia derama
Haenschia sidonia
Pteronymia sao
Pteronymia obscuratus
Pteronymia granica
Pteronymia artena
Pteronymia olimba
Pteronymia hara
Pteronymia forsteri
Pteronymia donelia
Pteronymia teresita
Pteronymia lonera
Pteronymia thabena
Pteronymia inania
Pteronymia nsp3
Pteronymia alida
Pteronymia serrata
Pteronymia rubicincta
Pteronymia cotyto
Pteronymia alissa
Pteronymia laura
Pteronymia sexpunctata
Pteronymia andreas
Pteronymia picta
Pteronymia simplex
Pteronymia gertschi
Pteronymia tucuna
Pteronymia latilla
Pteronymia ascipo
Pteronymia nsp2
Pteronymia ozia
Pteronymia veia EAST
Pteronymia tamina
Pteronymia zerlina
Pteronymia fulvimargo
Pteronymia oneida
Pteronymia alina
Pteronymia veia WEST
Pteronymia ticida
Pteronymia eurilea
Pteronymia carila
Pteronymia medeilina
Pteronymia nsp1
Pteronymia primula
Pteronymia vestilla
Pteronymia parva
Pteronymia aletta
Pteronymia dispar
Episcada vitrea
Episcada philoclea
Episcada nsp2
Episcada sulphurea
Episcada hymen
Episcada strigosis
Episcada clausina
Episcada syrvo
Episcada salvinia
Episcada polila
Episcada mira
Episcada trapezula
Episcada hidella
Episcada apulela
Episcada hymenaea
Episcada doto
Ceratinia iolaia
Ceratinia tutia
Episcada nsp1
Episcada hemixanthe
Ceratinia neso
Callithomia alexirrhoe
Callithomia lenea
Callithomia hezia
Oleria aquata
Oleria similigena
Oleria sexmaculata
Oleria figlia
Oleria assimilis
Oleria onega
Oleria agarista
Oleria ohega
Oleria lerdina
Oleria astrea
Oleria thiemei
Oleria quintina
Oleria didymaea
Oleria flora
Oleria antaxis
Oleria nsp
Oleria gunilla
Oleria estella
Oleria paula
Oleria amalda
Oleria rubescens
Oleria zelica
Oleria boveri
Oleria victorina
Oleria vicina
Oleria fascata
Oleria athalina
Oleria padilla
Oleria makrena
Oleria tremona
Oleria attalla
Oleria cyrene
Oleria bioculata
Oleria radina
Oleria baizana
Oleria furnata
Oleria santineza
Oleria phenomoe
Oleria quadrata
Oleria derondina
Oleria deicona
Oleria nsp
Napeogenes susiana
Napeogenes praetilla
Hypoleria virginiana
Hypoleria kefia
Hypoleria schausi
Hypoleria anchiala
Hypoleria zarepha
Hypoleria fallata
Hypoleria illimissa
Hypoleria dujardini
Hyalyris nsp2
Hyalyris excelsa
Hyalyris juninensis
Hyalyris antea
Hyalyris oulita
Hyalyris nsp1
Hyalyris ocina
Hypothyris nsp
Hypothyris lycaste
Hyalyris schlingeri
Hypothyris fuchsia
Hypothyris thea
Hypothyris semifulva
Hypothyris daphnis
Hypothyris mansuetus
Hypothyris mamercus
Hypothyris euclea
Hypothyris ninonia
Hypothyris anastasia
Hyalyris praxilla
Hyalyris latilimbata
Hyalyris mestra
Hyalyris coeno
Hypothyris moebiusi
Hypothyris cantobrica
Napeogenes stella
Napeogenes duessa
Napeogenes nsp2
Napeogenes apulia
Napeogenes gracilis
Napeogenes inachia
Napeogenes sylphis
Napeogenes tolosa
Napeogenes phuro
Napeogenes glycera
Napeogenes nsp1
Napeogenes peridia
Napeogenes rhezia
Napeogenes aethra
Napeogenes larina
Napeogenes zurippa
Napeogenes verticilia
Napeogenes flossina
Napeogenes cranto
Napeogenes lycora
Napeogenes nsp3
Napeogenes harbona
Napeogenes sodalis
Napeogenes sulphureophila
Napeogenes behningia
Napeogenes lanilla
Eremtexia terra
Epityches eupompe
Pteyris priscilla
Pteyris ulla
Pteyris cynothoe
Placidina euryanassa
Ithomia terra
Ithomia terra EAST
Ithomia arduinna
Ithomia amarilla
Ithomia jucunda
Ithomia lichyi
Ithomia pseudoagalla
Ithomia drymo
Ithomia agnosia
Ithomia xenos
Ithomia adelinda
Ithomia heraldica
Ithomia leila
Ithomia celemia
Ithomia iphianassa
Ithomia salapia
Ithomia cleora
Ithomia diasia
Ithomia patilla
Ithomia hyala
Ithomia ellara
Ithomia eleonora
Ithomia praethoma
Ithomia hymettia
Ithomia ayella
Patricia oligyrtis
Patricia dethyllus
Patricia dercylidas
Athesis acrisione
Athesis clearista
Methona maxima
Methona grandior
Methona confusa
Methona thiemisto
Methona sergestes
Methona curvifascia
Ezuma humboldt
Ezuma pavonii
Tithorea pacifica
Tithorea harmonia
Tithorea tarricina
Aeria olena
Aeria eurimedia
Scada reckia
Scada karschina
Scada zemira
Scada kusa
Scada albia
Sais rosalia
Mechanitis macrinus
Mechanitis mazaeus
Mechanitis messenoides
Mechanitis lysimnia
Mechanitis polymnia
Mechanitis menapis
Forbestra proceris
Forbestra olivencia
Forbestra equicola
Thyridia psidii
Olyras itisignis
Olyras crathis
Patitia neglecta
Cutresis flyereia
Melinaea satevis
Melinaea menophilus
Melinaea mneme
Melinaea mothone
Melinaea ilis
Melinaea isocomma
Melinaea idae
Melinaea marsaeus
Melinaea ethra
Melinaea ludovica
Melinaea mnasias
Athyrtis mechanitis

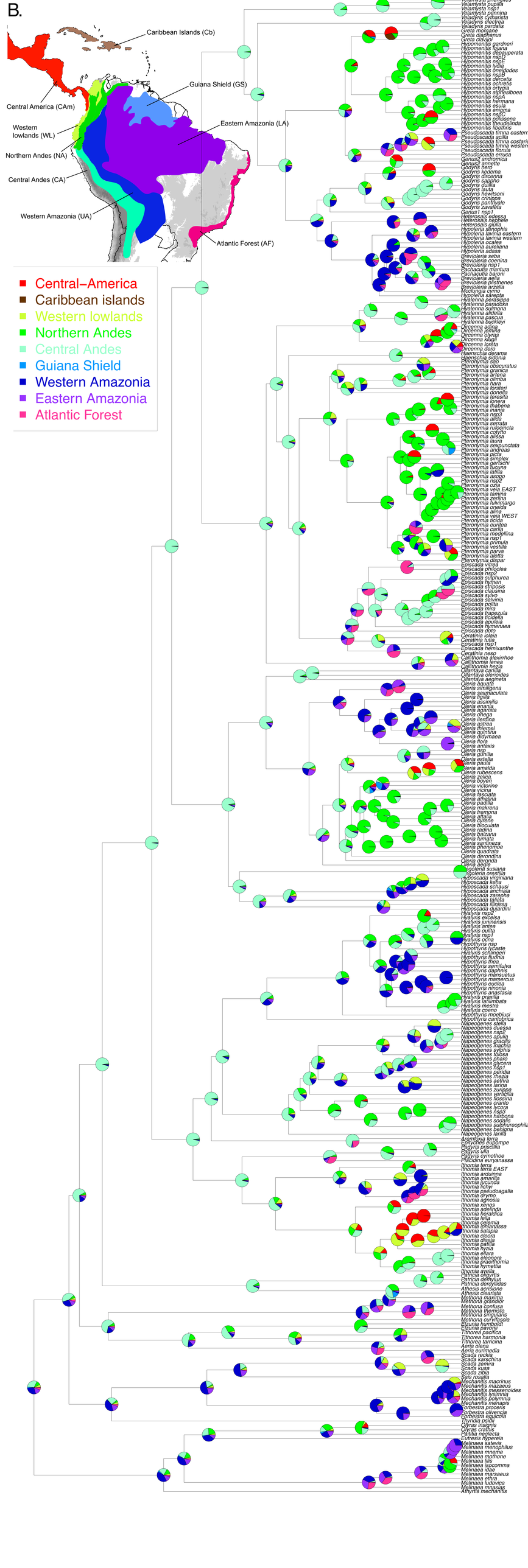
B.
Caribbean Islands (Cb)
Guiana Shield (GS)
Central America (CAm)
Eastern Amazonia (LA)
Western lowlands (WL)
Northern Andes (NA)
Central Andes (CA)
Western Amazonia (UA)
Atlantic Forest (AF)
Central–America
Caribbean islands
Western lowlands
Northern Andes
Central Andes
Guiana Shield
Western Amazonia
Eastern Amazonia
Atlantic Forest

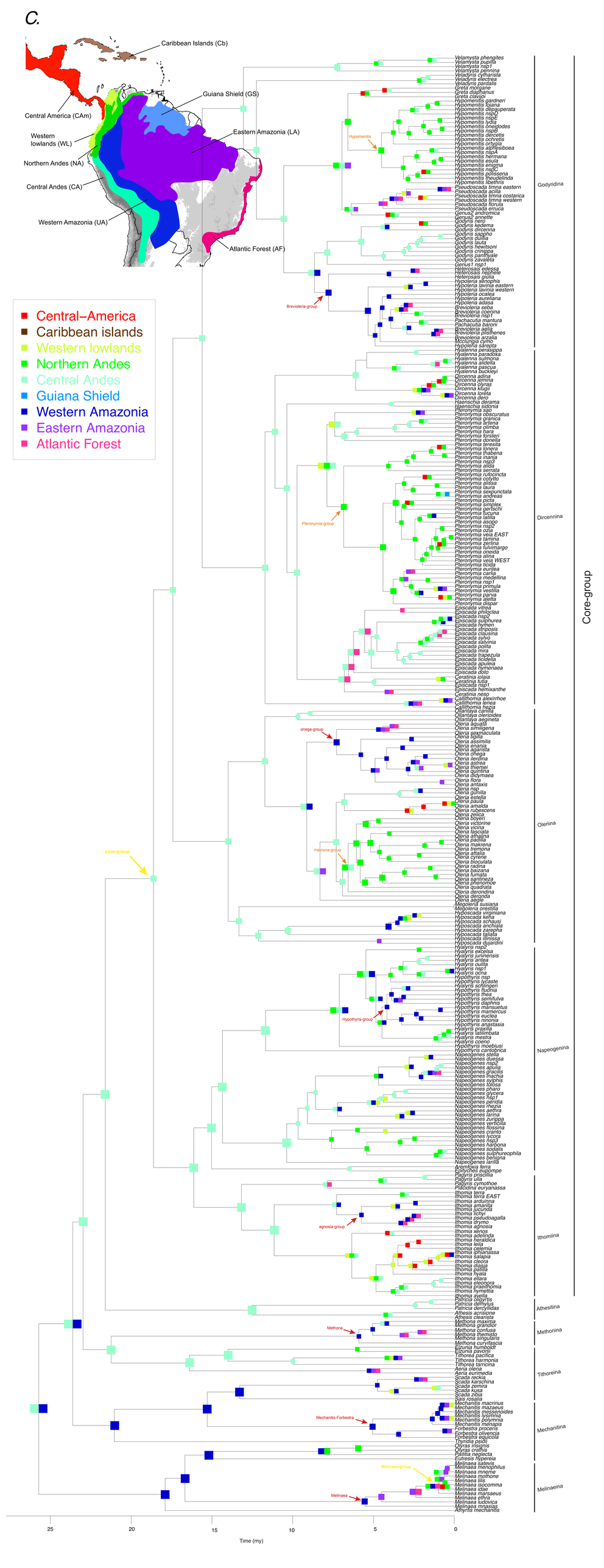
C.
Caribbean Islands (Cb)
Guiana Shield (GS)
Central America (CAm)
Eastern Amazonia (LA)
Western lowlands (WL)
Northern Andes (NA)
Central Andes (CA)
Western Amazonia (UA)
Atlantic Forest (AF)
Central–America
Caribbean islands
Western lowlands
Northern Andes
Central Andes
Guiana Shield
Western Amazonia
Eastern Amazonia
Atlantic Forest
Hypomenitis
Brevioleria-group
Pteronymia-group
onega-group
makrena-group
core-group
Hypothyris-group
agnosia-group
Methona
Mechanitis-Forbestra
Melinaea-group
Melinaea
Godyridina
Dircennina
Oleriina
Napeogenina
Ithomiina
Athesitina
Methonina
Tithoreina
Mechanitina
Melinaeina
Core-group
25
20
15
10
5
0
Time (my)

References

Matzke NJ. (2014). Model selection in historical biogeography reveals that founder-event speciation is a crucial process in island clades. *Systematic Biology*, 63(6), 951-970.